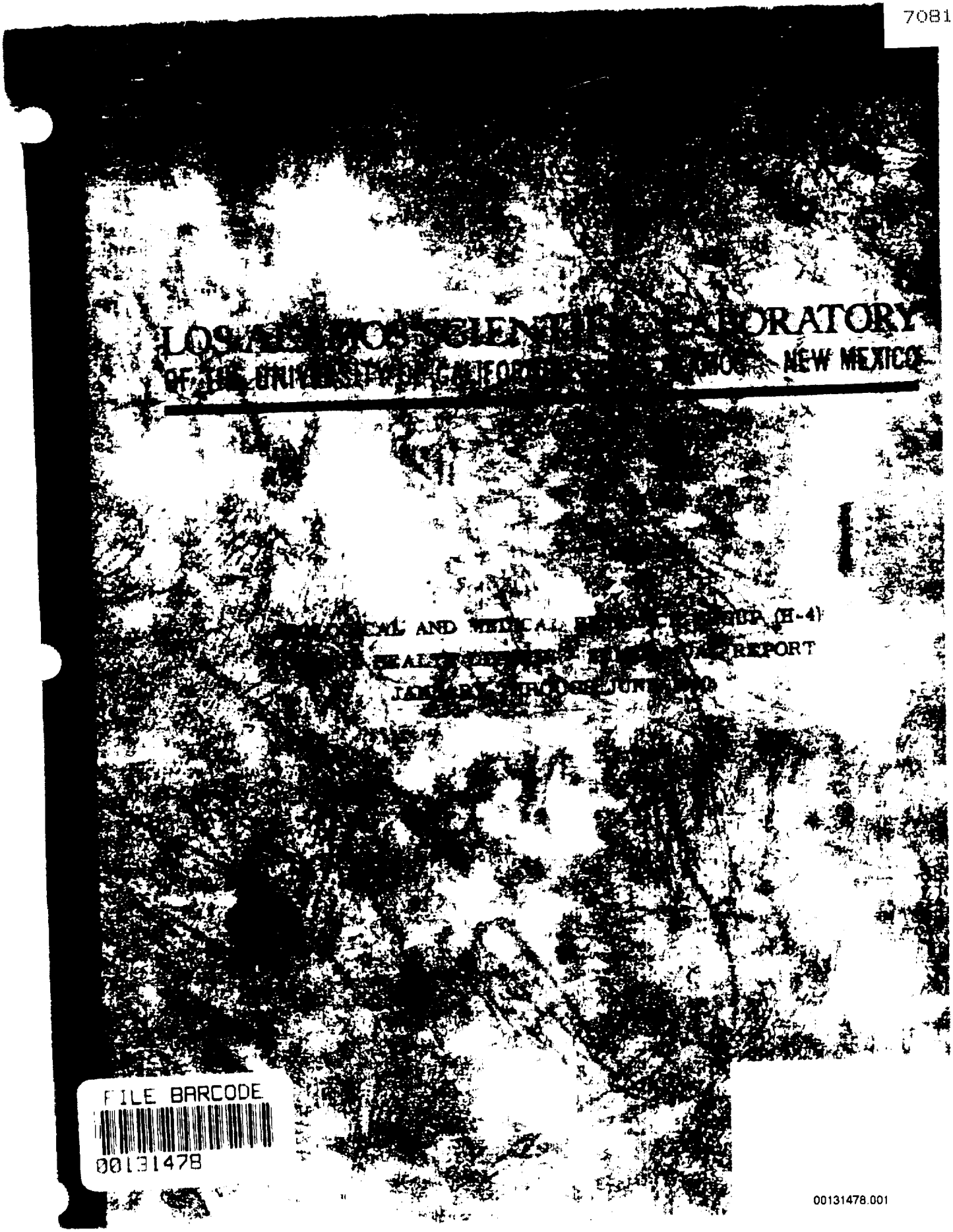

00131478.001

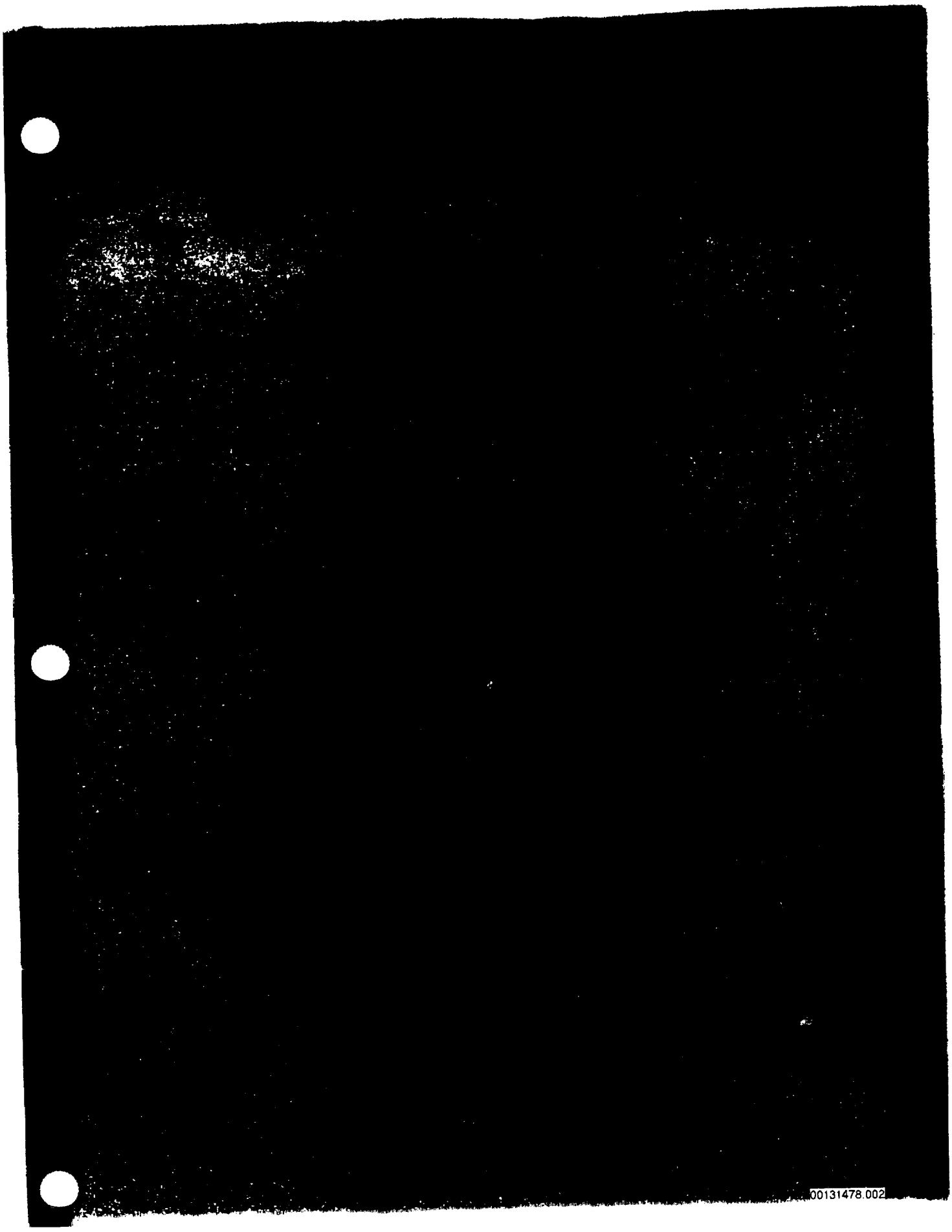

1046604

LANL

2

LAMS-2455
UC-48, BIOLOGY AND MEDICINE
(TID-4500, 15th Ed.)

LOS ALAMOS SCIENTIFIC LABORATORY
OF THE UNIVERSITY OF CALIFORNIA LOS ALAMOS NEW MEXICO

REPORT WRITTEN: July 1960

REPORT DISTRIBUTED: October 21, 1960

BIOLOGICAL AND MEDICAL RESEARCH GROUP (H-4) OF THE HEALTH DIVISION - SEMIANNUAL REPORT JANUARY THROUGH JUNE 1960

Group Leader, W. Langham
Division Leader, T. L. Shipman

Contract W-7405-ENG. 36 with the U. S. Atomic Energy Commission

CONTENTS

CHAPTER 1

INTRODUCTION

This document is the second semiannual report of the research activities of the Biological and Medical Research Group of the Los Alamos Scientific Laboratory's Health Division, and covers the period from January 1 through June 30, 1960. The report covering the previous period was issued as Los Alamos Scientific Laboratory Report LAMS-2445 (February 1960).

During the present period, the Group expended considerable effort on preparations for field experiments in connection with Project Rover, which is LASL's program of developing and testing nuclear propulsion reactors for rockets. The Group's participation will consist of measurement of neutron and gamma ray dose rates and integral doses, under shielded and free air conditions, from Kiwi-A Prime and Kiwi-A III. Participation also will include helping Group H-5 with studies of fission product release and fallout contamination. No

attempt is made in the Group's semiannual reports to cover completely the progress on these projects. This omission is deliberate, because occasionally classified information is involved and the projects are budgeted through the Rover program and not through the Division of Biology and Medicine. As the studies are completed, the information will be made available through appropriate interim and final reports.

Administratively, the most important development during the present report period was the occupancy of the new $325,000 addition to the experimental animal quarters (see Chapter 7).

As in the previous report, the Group's activities have been divided into six broad categories: biochemistry, low-level counting, organic chemistry, radiobiology, radiopathology, and veterinary services. The activities of each of these sections constitute a chapter of this report.

The personnel of the Group, as of the end of the present report period, their qualifications, classification, and Group and Section affiliation are shown by the following table of organization.

GROUP H-4
BIOMEDICAL RESEARCH

W. H. Langham, Ph.D., Leader
P. S. Harris, M.D., Alternate Leader
O. S. Johnson, Alt. Ldr. for Administration

MILITARY
Lt. Col. E. R. Ballinger (MC)

SWITCHBOARD
J. Gardell

SECRETARIES
E. M. Sullivan
T. R. Williams

BIOCHEMISTRY

(Vacancy), Leader

Staff Members

H. Foreman, M.D., Ph.D.
J. E. Furchner, Ph.D.
D. F. Petersen, Ph.D.
C. R. Richmond, Ph.D.

Research Assistants

L. B. Cole, M.S.
E. H. Lilly, B.S.
G. A. Trafton, B.S.

Technical Staff

M. Magee
V. E. Mitchell

LOW-LEVEL COUNTING

E. C. Anderson, Ph.D., Leader

Staff Members

*J. H. Larkins, B.S.
J. D. Perrings
R. L. Schuch
M. A. Van Dilla, Ph.D.

Research Assistant

M. W. Rowe, B.S.

Technical Staff

*J. M. Allen
B. E. Clinton

ORGANIC CHEMISTRY

F. N. Hayes, Ph.D., Leader

Staff Members

V. N. Kerr, M.A.
A. Murray, M.S.
D. G. Ott, Ph.D.
D. L. Williams, M.S.

Research Assistant

E. Hansbury, M.A.

*Casual employees.

TABLE OF ORGANIZATION GROUP H-4 AS OF JUNE 30, 1960.

GROUP H-4 (continued)

RADIOBIOLOGY

P. S. Harris, M.D., Leader

Staff Members

I. U. Boone, M.D.
J. A. Sayeg, Ph.D.
J. F. Spalding, Ph.D.
T. T. Trujillo, B.S.
F. C. V. Worman, M.S.

Research Assistant

P. C. Sanders, M.S.

Technical Staff

L. M. Conklin, B.S.
E. F. Montoya
V. G. Strang

RADIOPATHOLOGY

C. C. Lushbaugh, M.D., Leader

Research Assistants

D. B. Hale, B.S.
G. L. Humason, M.S.
J. M. Wellnitz, A.B.

Technical Staff

N. J. Basmann

VETERINARY MEDICINE

O. S. Johnson, B.S., Leader

Animal Caretakers

J. M. Alire
F. Archuleta
J. Lovato
R. Martinez
L. Ortiz
A. Trujillo
D. Valdez
F. Valdez

CHAPTER 2

BIOCHEMISTRY SECTION

Retention and Excretion of Cesium^{137} by Mice during Chronic Oral Administration. I. Prediction of Equilibrium Level from Acute Exposure Parameters (J. E. Furchner, C. R. Richmond, and G. A. Trafton)

INTRODUCTION

Retention of Cs^{137} by mice following acute oral intubation can be expressed by

$$R_t = 39.09\ e^{-1.5260t} + 43.27\ e^{-0.3360t} + 17.69\ e^{-0.1474t}$$

where R_t is the whole body retention at any time t, e is the base of natural logarithms, and the coefficient and exponent of each term are the intercept and rate constant. Integration of this function from t_o to t_n should predict the amount retained at any time (t_n) during chronic exposure. Such a prediction should be of importance in determining maximum permissible body burden (MPBB) and maximum permissible

concentration (MPC) values for conditions of chronic exposure. These values are almost invariably based on parameters obtained from small animals following acute exposure. Conceptually, however, conditions of chronic exposure are inherent to the calculations.

METHODS AND RESULTS

Female RF mice (average weight 20.8 g) 89 days old at t_o were used in both the chronic and acute exposures. The mice were maintained in plastic cages, each containing 2 mice. The 12 mice in each group had free access to water and Purina laboratory chow during the course of the experiment. The acute exposures were made by oral administration of 0.89 μc of Cs^{137} as the chloride in a solution of pH 5. The chronic exposures were administered by contaminating the animals' drinking water with 0.012 μc Cs^{137} per ml.

Figure 1 shows the retention of Cs^{137} following an acute exposure. An iterative least square computer analysis resolved the data into 3 components. Figure 2 shows the predicted equilibrium levels derived from an integration of each component and the whole body equilibrium level obtained by summing the integrated components. The points represent the actual measurements obtained by whole body counting.

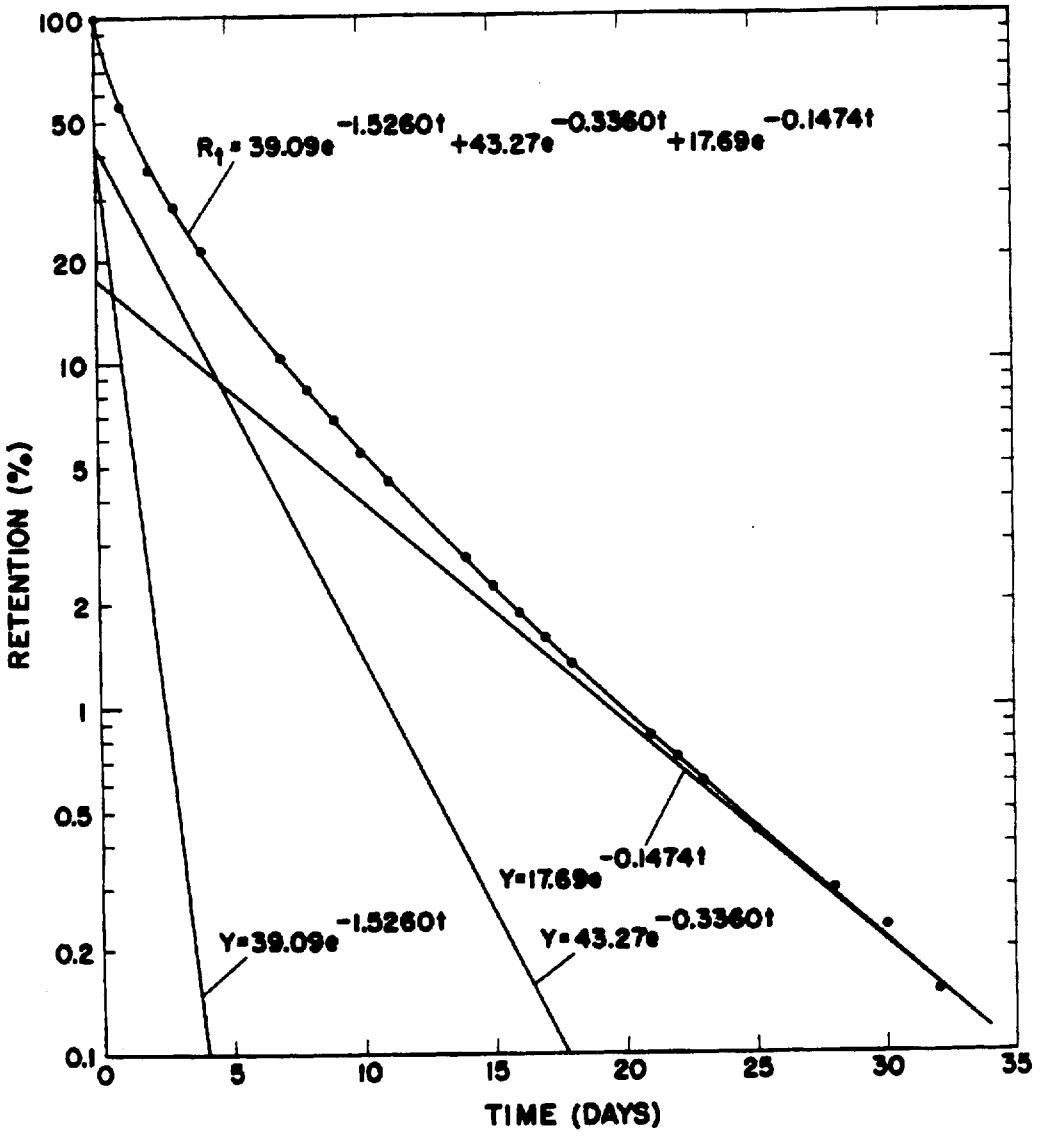

Fig. 1. Retention of Cs^{137} in mice after single acute oral administration.

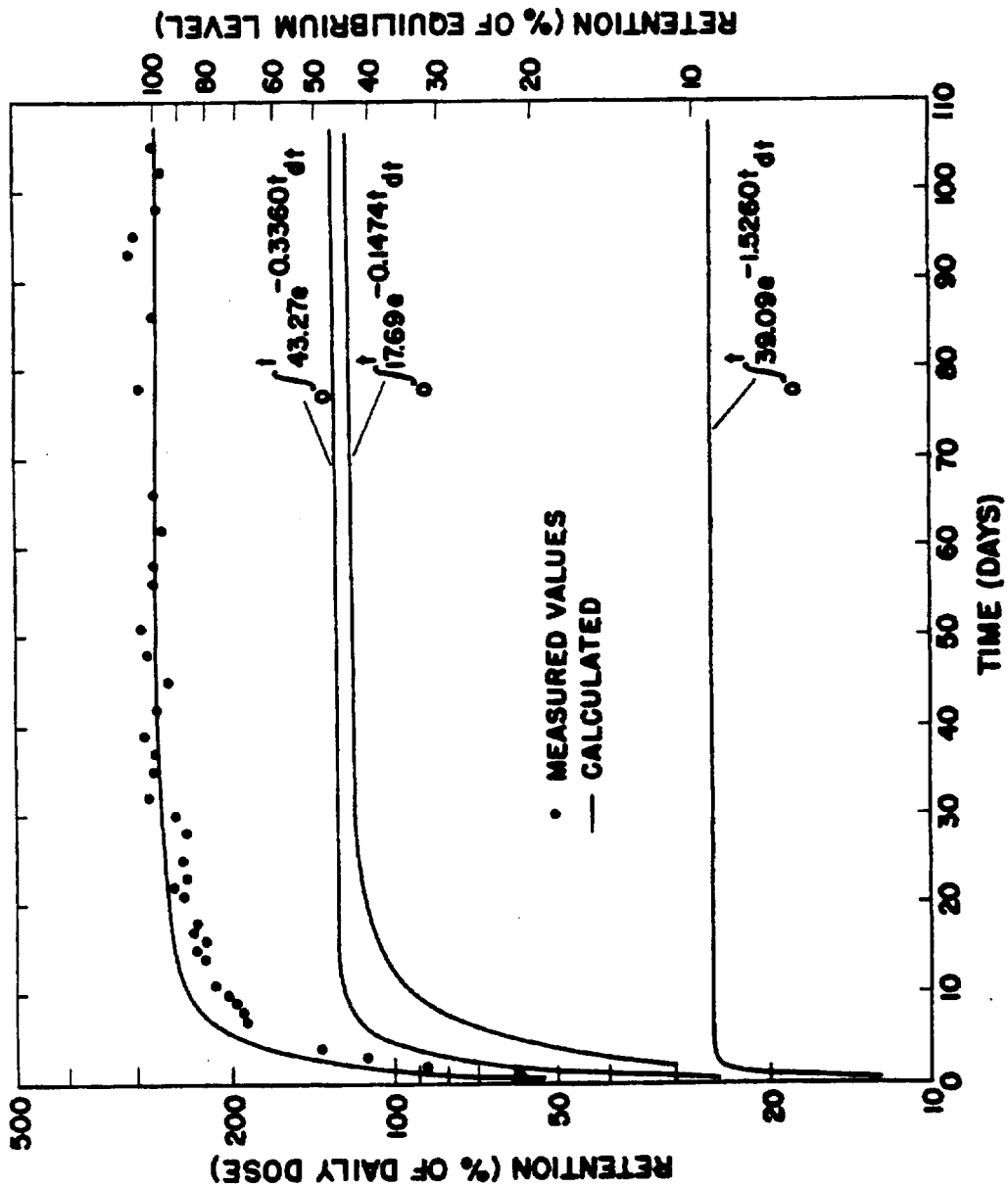

Fig. 2. Cesium^{137} retention in mice during chronic oral administration.

00131478.012

DISCUSSION

A comparison of the measured points and the line representing the summed integrals (Fig. 2) shows that the equilibrium retention level was accurately predicted from the acute exposure data given in Fig. 1. The approach to equilibrium, however, appeared to be at a slightly slower rate than predicted. The right hand ordinate of Fig. 2 is constructed such that the equilibrium level is equated to 100 per cent (for example if, after equilibrium is reached and chronic feeding is stopped, the predicted intercept values of the retention function are 9.3, 43.7, and 47.0 per cent, respectively, as compared with those shown in Fig. 1).

The decrease in whole body activity after withdrawal from chronic exposure to Cs^{137} is being observed for comparison of the predicted to the actual change in retention with time. Similar studies of predicted and actual equilibrium levels with "bone-seeking" isotopes are planned.

Excretion of Cesium^{137} as a Function of Age in Mice (J. E. Furchner, C. R. Richmond, and G. A. Trafton)

INTRODUCTION

The concentration of potassium per unit weight in humans and in rats has been reported to vary with age (1). It may be reasonable to expect these variations to be due to metabolic fluctuations concomitant with age. If this assumption is correct, other univalent cations may be excreted at age-dependent rates.

These implications, in addition to offering a possibility of a measure of physiological age, may also necessitate a more thorough consideration of age factors when determining maximum permissible concentration (MPC) and maximum permissible body burden (MPBB) values. In order to accumulate relevant quantitative data, an experiment was set up to determine whether excretion of Cs^{137} by mice was influenced by their age at the time of administration.

MATERIALS AND METHODS

Groups of 12 RF female mice were injected intraperitoneally with 0.89 μc of carrier-free Cs^{137} chloride in a solution adjusted to a pH of 5. The ages of the animals are given in Table 1. All animals were injected on the same day, and all

TABLE 1. AGE, WEIGHT, AND RETENTION PARAMETERS* IN FEMALE RF MICE GIVEN CESIUM^{137} INTRAPERITONEALLY

Group and Age**	Weight (g) t_o	Weight (g) t_{30}	a_1	k_1	a_2	k_2	Area (per cent days)
A (4)	19.3	24.5	54.44	0.4914	44.38	0.1611	386
B (12)	22.0	23.3	57.97	0.6303	40.88	0.1423	379
C (20)	24.6	25.1	53.62	0.7763	45.86	0.1295	423
D (32)	31.3	32.2	53.27	0.7128	46.45	0.1206	460
E (51)	29.4	28.5	48.38	0.6743	51.15	0.1195	500
F (74)	31.5	29.9	48.00	0.7227	51.77	0.1289	468
G (88)	30.6	30.8	49.32	0.7541	50.17	0.1240	470

*From $R_t = a_1 e^{-k_1 t} + a_2 e^{-k_2 t}$.

**Age at t_o in weeks shown in parentheses.

groups were subjected to whole body counting for retained Cs^{137} at regular intervals. The animals were maintained under normal laboratory conditions before and during the experiment.

RESULTS AND DISCUSSION

The data were analyzed by a 704 computer, and the resolved parameters of the retention functions are given in Table 1, which shows the rate constant of the second component (k_2) decreases between the ages of 4 and 51 weeks and increases and may plateau thereafter. These changes are reflected in the areas $\left(\Sigma \frac{a_i}{k_i} \right)$, which increase to a maximum at 51 weeks and then decrease at greater ages. Body weight increases with age until 32 weeks and is relatively constant thereafter. If the area is an accurate index of the equilibrium level, then a 30 per cent difference in equilibrium levels may be anticipated when animals 3 months of age are compared with animals 1 year old. Under conditions of chronic exposure and when chronic exposures are maintained over long periods of time, slow changes in equilibrium levels may occur.

It is immediately apparent that studies of retention and excretion should take into consideration the age and weight of the experimental animals. The differences in retention described in this report may be due more to growth, rather

than to aging phenomena (unless one chooses to consider a declining growth rate as an index of aging). In order to explore these questions further, a single group of mice will be tested repeatedly at suitable intervals for changes in excretion rates as a function of age.

REFERENCE

(1) C. R. Richmond, J. E. Furchner, and M. A. Van Dilla, Potassium Concentration as a Function of Age in Rats (this report).

Effect of a Carbonic Anhydrase Inhibitor (Diamox) on Cesium^{137} Excretion in Rats (C. R. Richmond, J. E. Furchner, and G. A. Trafton)

INTRODUCTION

2-Acetylamino-1,3,4-thiadiazole-5-sulfonamide (Diamox) is a nonmercurial diuretic and acid-base regulator of low toxicity, which acts specifically to inhibit the carbonic anhydrase enzyme system. Diuresis is due to the effect on the reversible hydration of carbon dioxide and dehydration of carbonic acid in the kidneys. The net result is a renal loss of HCO_3^- ion and, subsequently, increased loss of water, sodium, and potassium. One might also reasonably expect this compound to accelerate the excretion of other monovalent metal cations such as rubidium and cesium. The purpose of this study was to investigate the effect of Diamox on the excretion of Cs^{137} in rats.

METHODS AND RESULTS

Twenty-four adult male Sprague-Dawley rats were used. These animals were 64 days old at the time of administration and weighed 273.9 $\pm$ 7.1 g ($\bar{x} \pm \sigma$). Each animal was injected intraperitoneally with 0.1 ml of carrier-free $Cs^{137}Cl_3$ (0.75 μc) at a pH of 5. At 30 minutes following administration, the animals were divided into 4 equal groups, and the

Cs^{137} activity in each animal was determined by whole body counting with a 4 π liquid scintillation detector (1). Activity measurements were also made at subsequent intervals over a 76 day period.

Immediately after administration, all animals were placed on a dietary regimen which consisted of Purina chow and tap water ad libitum. For a period of 20 days, Diamox was added to the drinking water of 3 groups to give concentrations of 0.045, 0.090, and 0.180 mg/ml, respectively. The average Diamox intake per g of body weight was calculated from measurements of body weight and volume of fluid intake. These values are given in Table 1.

At the completion of the experiment, the retention function was calculated for each group by an iterative least square 704 computer analysis. Each retention function contained 3 terms (i.e., 3 exponential components). The integrated area under each retention function from t_o to t_n was then calculated and used for assessing the effectiveness of various Diamox intake levels on Cs^{137} retention. The derivative of the retention function is the excretion rate.

Table 1 gives the values for the intercept (a) and rate (k) parameters, which describe each component of the retention function for all 4 groups of animals. The area under each component is given and also expressed as a per

TABLE 1. PARAMETERS AND AREAS OF CESIUM^{137} RETENTION FUNCTIONS FOR RATS GIVEN DIAMOX

Treatment (mg/kg)	Component	a (per cent)	k (fraction per day)	T_b (days)	Area (per cent days)	Area (per cent of total)
0	1	17.20	0.7650	0.91	22.5	1.7
	2	31.78	0.1020	6.79	311.5	23.7
	3	50.94	0.0520	13.32	979.2	74.6
	Total				1313.2	
6.5	1	20.91	1.6581	0.42	12.6	1.2
	2	47.64	0.1198	5.78	397.6	37.0
	3	31.44	0.0474	14.61	662.8	61.8
	Total				1073.0	
12.8	1	17.99	1.2817	0.54	14.0	1.2
	2	46.53	0.1211	5.72	384.1	34.9
	3	35.46	0.0504	13.75	703.4	63.9
	Total				1101.5	
27.0	1	17.86	1.0446	0.66	17.1	1.7
	2	48.34	0.1233	5.62	392.0	38.2
	3	33.83	0.0549	12.63	616.9	60.1
	Total				1026.0	

cent of the total area under each of the retention functions. The areas under the retention functions of the animals receiving Diamox treatment averaged ~81 per cent of that of rats receiving no Diamox. All 3 dose levels increased Cs^{137} excretion to about the same degree. The most noticeable effects of Diamox on the retention functions are reflected in the intercept values of the third component and in the values of the rate constants of the first and second components. Figure 1 illustrates these changes by comparing the averages of the second and third components of the treated animals with that of the controls. Apparently the Cs^{137} atoms associated with the first and second components are excreted at an increased rate from animals receiving Diamox. This leaves a smaller fraction of the administered dose available for deposition at sites which lose the Cs^{137} at the slowest rate. The scale of Fig. 1 is too small to show the differences in the first component.

DISCUSSION

Oral administration of Diamox for 20 days at levels of 6.5, 12.8, and 27.0 mg/kg elicits similar responses in accelerating the renal excretion of intraperitoneally administered Cs^{137} in rats. The primary effect is an increased rate of loss from the components (i.e., compartments) with

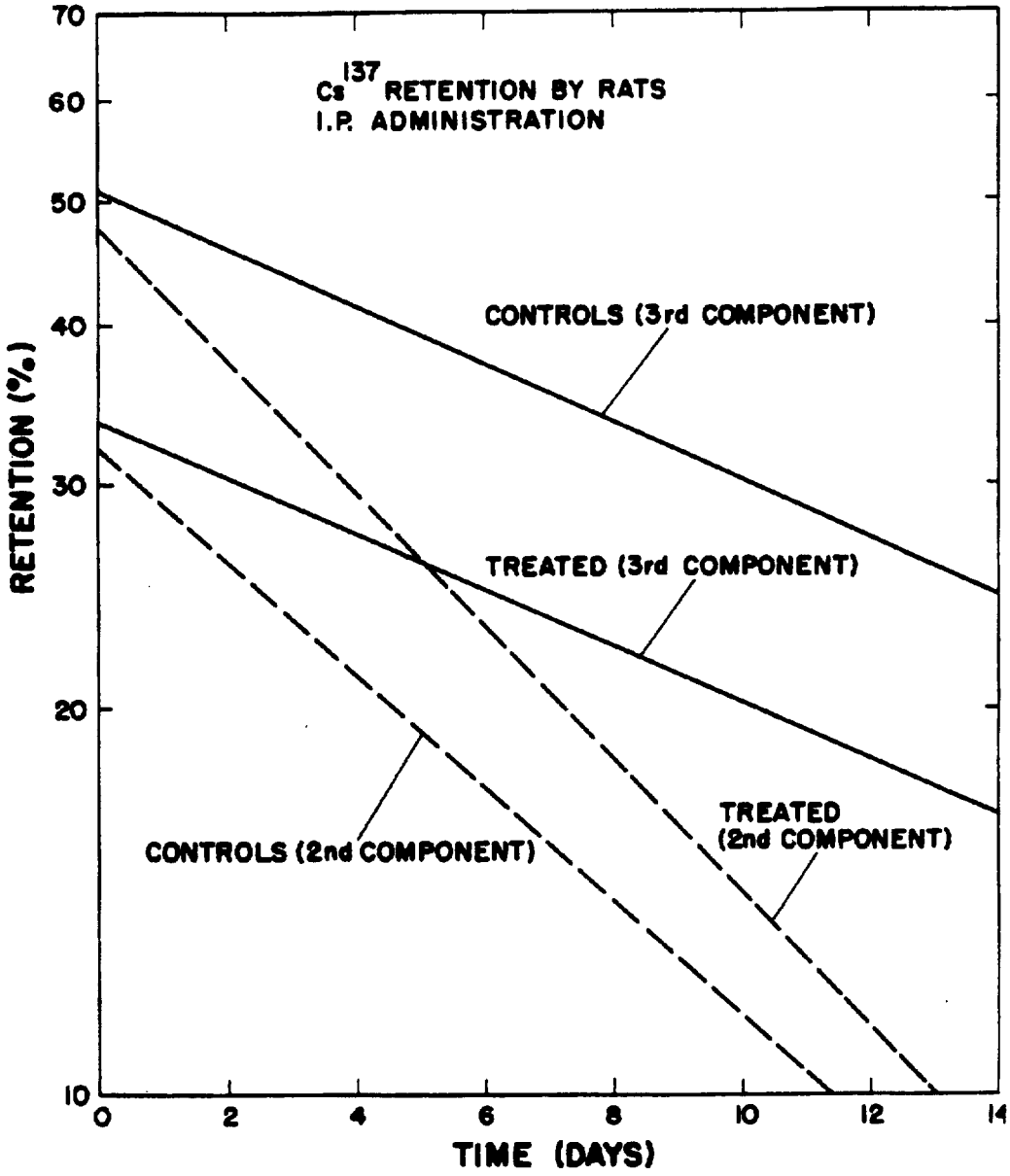

Fig. 1. Effect of Diamox on retention of Cs^{137} in rats.

the largest and intermediate rate constants. The most firmly bound Cs^{137} (smallest rate constant) is not lost at an accelerated rate, as its rate of loss from the body is apparently not governed by renal function. However, relatively less of the administered dose is available for binding by sites which lose Cs^{137} at the slowest rate. This is of some practical value, since the major fraction of the radiation dose is directly related to the component with the longest half-time. The increase in effective excretion, however, is only ~20 per cent.

REFERENCE

(1) C. R. Richmond, Los Alamos Scientific Laboratory Report LA-2207 (1958).

Retention of Barium^{133} in Mice, Rats, and Dogs (C. R. Richmond, J. E. Furchner, and G. A. Trafton)

INTRODUCTION

As a part of the program of studying interspecies correlations in metabolism of gamma ray emitting isotopes, Ba^{133} was administered by various routes to mice, rats, and dogs. Although Ba^{133} has only a series of weak gamma rays (0.3 to 0.4 Mev), it has a half-life of ~8 years and is, therefore, preferable to other barium isotopes for retention studies which may extend over long time periods.

The only isotope of strontium with a relatively long half-life is Sr^{90}, which is a pure beta emitter. It is, therefore, difficult to study radiostrontium retention and excretion by whole body counting techniques. Bauer et al. (1) have reported that calcium and strontium are metabolized in exactly the same way and that barium and calcium are metabolized in much the same way. Hamilton (2) also reports that the behavior of barium and strontium is similar. It is reasonable, then, that whole body retention data derived from barium studies may be used to approximate the retention pattern of strontium.

METHODS AND RESULTS

Twelve LAF_1 female mice, weighing 18.7 g at the age of 2 months, were given intravenous injections of 0.3 μc of Ba^{133}

as the carrier-free chloride. Six Sprague-Dawley male rats, about 3 months old and weighing 250 g, were given intravenous injections of 0.6 μc of the same $Ba^{133}Cl_2$ solution. Four male beagle hounds (weighing ~30 lb) were given ~13.0 μc of $Ba^{133}Cl_2$ orally by means of gelatin capsules. The intravenous route of administration to rats and mice was necessary to ensure enough uptake of radioactivity to permit its detection over a long retention period.

All animals were kept under standard laboratory conditions. Radioisotope measurements were made by whole body counting techniques described elsewhere (3). The retention data were analyzed by a 704 computer, and the derived parameters are given in Table 1. Figure 1 shows the experimental data and the best fit lines derived by computer analysis. Expressions for the retention functions are as follows:

Rats - Intravenous Administration

$$R_t = 25.91e^{-1.4561t} + 23.34e^{-0.0375t} + 50.66e^{-0.00122t}$$

Mice - Intravenous Administration

$$R_t = 50.00e^{-1.8578t} + 20.45e^{-0.0518t} + 25.47e^{-0.00257t}$$

Dogs - Oral Administration

$$R_t = 75.37e^{-1.3368t} + 16.74e^{-0.01060t} + 8.17e^{-0.000433t}$$

TABLE 1. PARAMETERS AND AREAS OF BARIUM^{133} RETENTION FUNCTIONS IN MICE, RATS, AND DOGS

Species and Route of Administration	Component	a (per cent)	k (fraction/day)	T_b (days)	Area (per cent days)	Area (per cent of total)
Mice, I. V.	1	54.00	1.8578	0.37	29.1	0.28
	2	20.45	0.0518	13.38	394.8	3.82
	3	25.47	0.00257	269.65	9912.1	95.90
	Σ				10,336.0	100.00
Rats, I. V.	1	25.91	1.4561	0.48	17.8	0.04
	2	23.34	0.0375	18.48	622.4	1.48
	3	50.66	0.00122	565.71	41,353.9	98.47
	Σ				41,994.1	99.99
Dogs, Oral	1	75.37	1.3368	0.52	56.4	0.27
	2	16.34	0.1060	65.40	1579.5	7.70
	3	8.17	0.000433	1600.64	18,877.6	92.03
	Σ				20,513.5	100.00

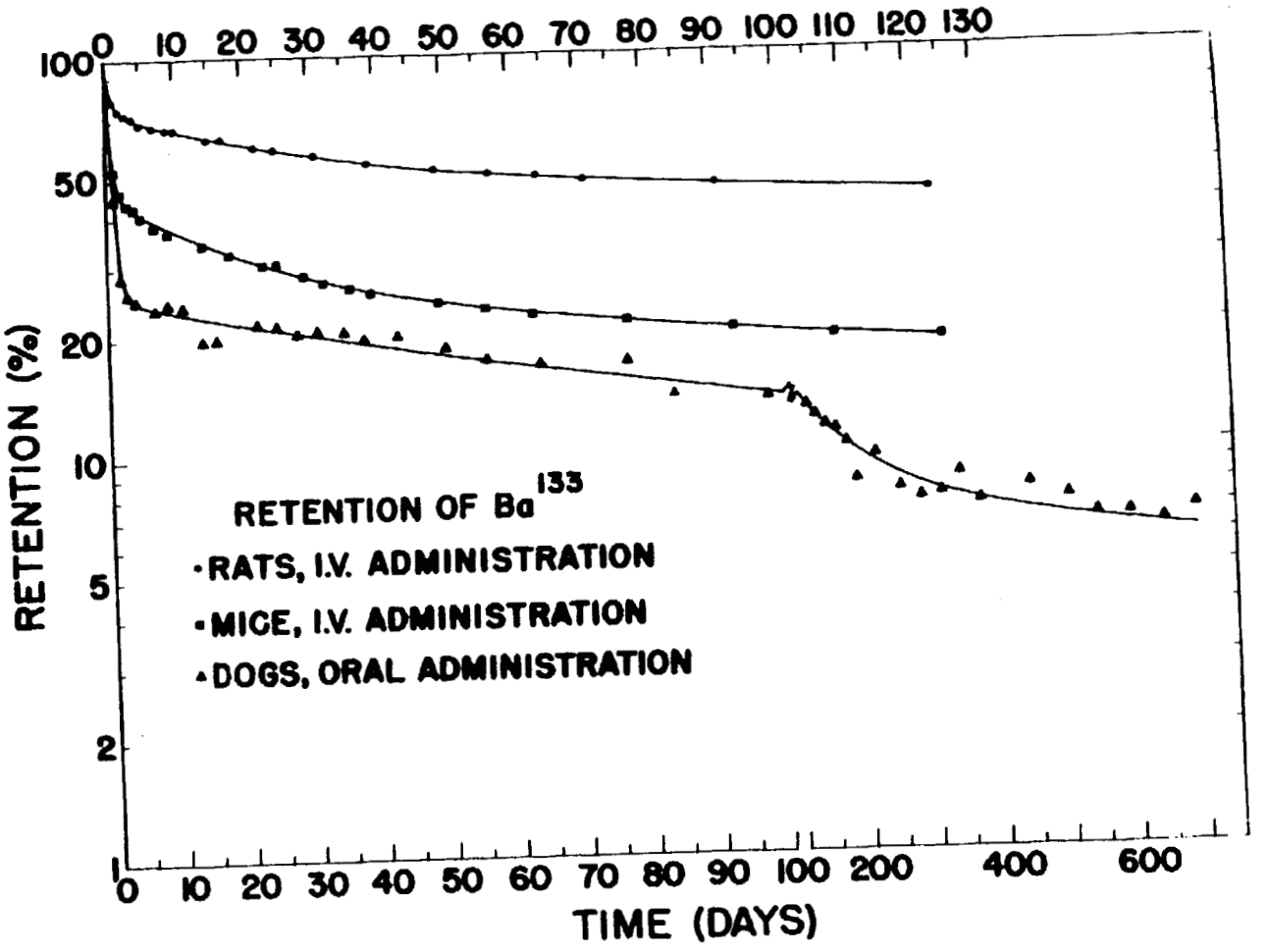

Fig. 1. Retention of Ba^{133} by mice, rats, and dogs.

The data show that rats excreted proportionally less Ba^{133} than mice and that both rats and mice excreted less than dogs. The scatter of the points about the calculated line summarizing the retention of Ba^{133} by dogs is thought to be due to the limited capability of the Humco I detector in low energy ranges. The mouse and rat data were collected by means of the Los Alamos Small-Animal Counter, which has somewhat better accuracy in this range.

Dogs excreted 75 per cent of the orally administered dose with a half-time of 0.52 day, whereas 54 per cent and 26 per cent of the intravenous doses were excreted with a half-time of $\sim$0.5 day by the mice and rats, respectively. The large and rapid initial loss by the dogs was due to the route of administration. The half-times of the long and intermediate components indicate that the dogs would retain more were the barium to be given intravenously.

Figure 2 shows a comparison of the measured total urinary and fecal excretion of Ba^{133} by rats with the derivative of the whole body retention equation. The derivative of the retention equation closely approximates both the total excretion pattern and the individual urinary plus fecal values.

Studies on the distribution of Ba^{133} in the tissues of rats at various times after acute administration indicated

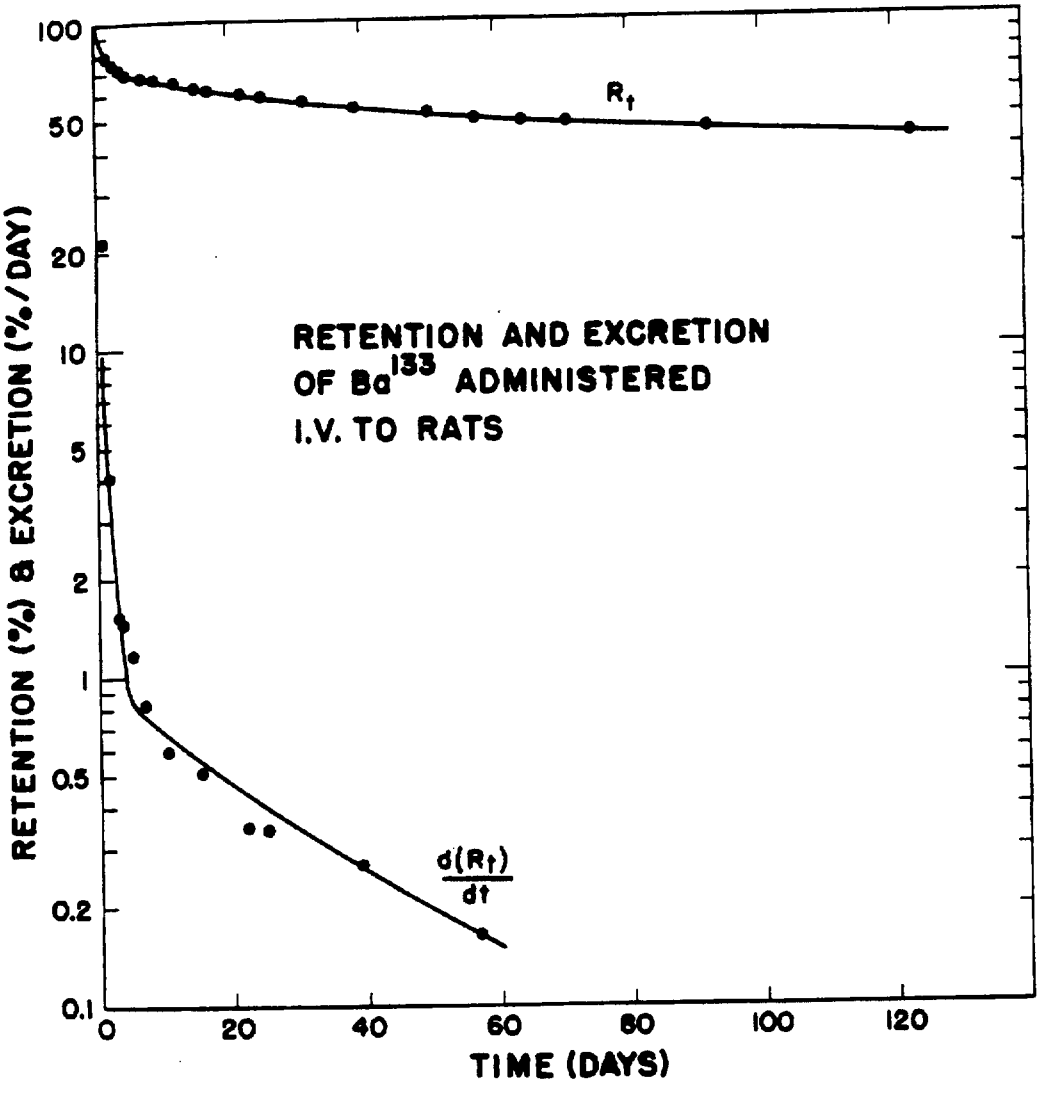

Fig. 2. Retention and excretion of intravenously administered Ba^{133} by the rat.

that practically all (~95 per cent) of the body burden at the time of sacrifice was localized in the skeleton. It seems reasonable, therefore, that the component with the longest T_b represents Ba^{133} which is bound in the skeleton (Table 1).

DISCUSSION

The sum of three exponential expressions adequately describes the retention of $Ba^{133}Cl_2$ measured by whole body counting techniques in three species of animals. Measurements were made on the dogs for ~700 days. Although the intercept of the longest component was only 8 per cent of the administered dose, the area under this component was 92 per cent of the area under all components. The per cent of total area contributed by the long component was ~92 per cent for all species, even though the T_b's of these components were ~270, 566, and 1600 days for the mouse, rat, and dog, respectively. In man, one might reasonably expect the T_b of the long component to be greater than the 1600 days found for the dog. The relatively large T_b values for the long components are reasonable because of the metabolic similarity of barium and calcium.

Data presented in Fig. 2 show that the total excretion pattern for Ba^{133} can be quite accurately predicted from

whole body retention measurements. Additional data are being collected from mice and rats following acute oral administration so that correlations can be made among the three species and predictions made for human beings.

REFERENCES

(1) G. C. H. Bauer, A. Carlson, and B. Lindquist, Biochem. J. 63, 535 (1956).

(2) J. G. Hamilton, Radiology 49, 325 (1947).

(3) C. R. Richmond, Los Alamos Scientific Laboratory Report LA-2207 (1958).

Metabolism of Ruthenium^{106} Chloride in Mammals Studied with the Aid of Whole Body Gamma Ray Assay Techniques. I. Mice and Rats (C. R. Richmond, J. E. Furchner, and G. A. Trafton)

INTRODUCTION

Ruthenium^{103} and Ru^{106}/Rh^{106} are fission products of high yield and contribute significantly to that portion of the fallout radiation dose caused by radionuclides of short or intermediate half-lives. Little information is available on the metabolism of ruthenium radionuclides in mammals, particularly at relatively long periods after administration. Recent work (1) has pointed out the need for such information. It is very possible that bone, rather than kidney, should be considered as the critical organ following oral or parenteral administration.

METHODS AND RESULTS

Twelve adult RF female mice, whose average weight was 21.0 g, and 6 male Sprague-Dawley rats, whose average weight was 290.0 g, were injected intraperitoneally with $Ru^{106}Cl_3$ adjusted to a pH of 2.9. All animals were 63 days old at the time of injection. Each mouse received 1.02 μc Ru^{106}, and each rat received 2.52 μc Ru^{106}.

The whole body gamma ray activity of each animal was measured after injection and at subsequent intervals by

standardized methods which have been presented in detail elsewhere (2). All assay data were corrected for coincidence loss and physical decay of the Ru^{106}. An iterative least square 704 computer method was used to determine the retention function which best described the experimental data. Figure 1 shows the calculated retention functions drawn as solid lines, together with the actual measured retention data. Three components describe the function for each species. Parameters which describe these components and the biological half-times (T_b) are as follows:

Mice

$$R_t = 39.70\ e^{-1.7939t} + 40.30\ e^{-0.0994t} + 19.96\ e^{-0.0020t}$$

T_b = 0.4 day 7.0 days 345 days

Rats

$$R_t = 26.51\ e^{-0.8084t} + 51.03\ e^{-0.0574t} + 21.38\ e^{-0.0019t}$$

T_b = 0.9 day 12.1 days 370 days

Although the 370-day T_b value of the last component of the retention function for rats agrees with the value of 340 days which others have reported for rat bone (3), a value of 16 days is given in the most recent report of the International Commission on Radiological Protection (4). It is

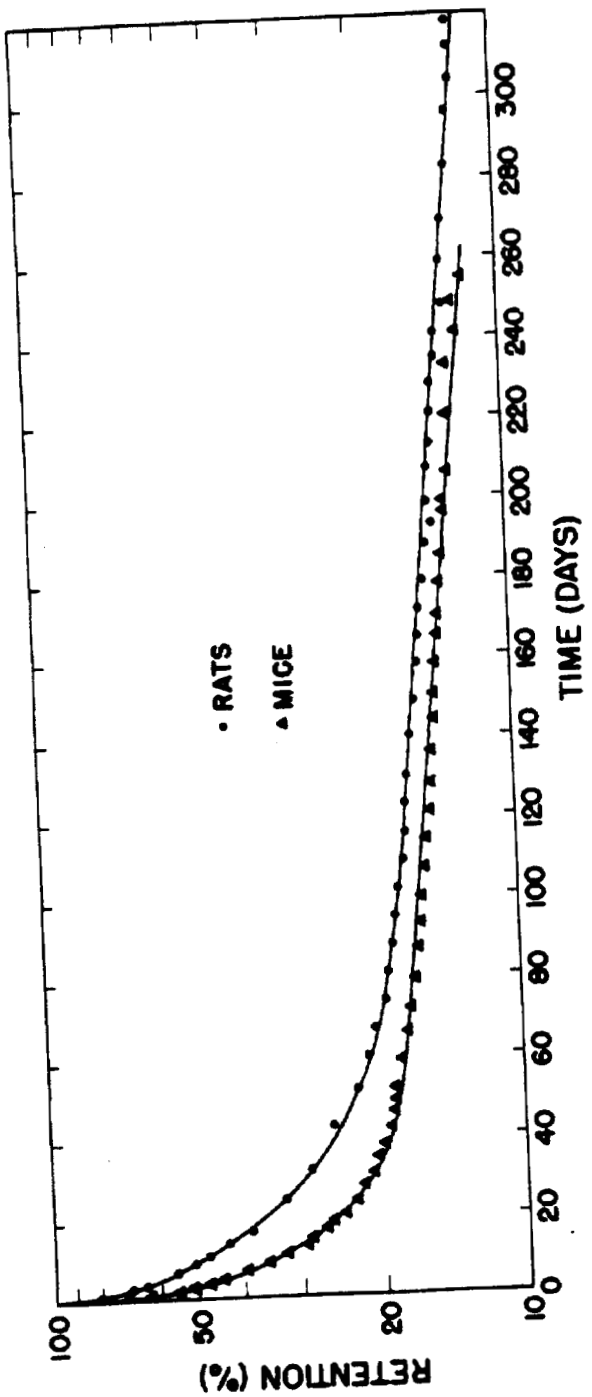

Fig. 1. Retention of Ru^{106} by mice and rats following intraperitoneal injection.

not possible at the present time to estimate for our studies what fraction of the activity in each component of the retention function is associated with bone. It is interesting to note that the T_b value for each component is larger for rats than for mice.

Table 1 gives the total integrated area from t_o to t_n under the biological and effective retention functions and the per cent of the total under each component. Most of the area under the retention function of both species is contributed by the component of longest biological or effective half-life. Table 1 also shows that the total area under the retention function for rats is ~16 per cent greater than that for mice. Future reports will summarize retention and excretion data for Ru^{106} following different routes of administration in these and other species. These data will be used for interspecies comparisons.

DISCUSSION

Whole body retention of Ru^{106}/Rh^{106} following intraperitoneal injection in both mice and rats can be adequately described by the sum of 3 exponential components. The component with longest half-life represents activity deposited in bone or in bone plus other tissues, and represents 86 to 92 per cent of the total area under the effective retention

TABLE 1. INTEGRATED AREA (t_o to t_n) REPRESENTING VARIOUS COMPONENTS OF THE BIOLOGICAL AND EFFECTIVE RETENTION FUNCTIONS FOR RUTHENIUM^{106}

Retention Function	Area under Total Curve (% days)	Components		
		First (% total area)	Second (% total area)	Third (% total area)
Mice				
Biological	10,391*	0.2	4.5	95.3
Effective	5,520**	0.4	7.2	92.4
Rats				
Biological	12,335	0.3	7.2	92.5
Effective	6,561	0.5	13.1	86.4

*Area $= \frac{a_1}{k_1} + \frac{a_2}{k_2} + \frac{a_3}{k_3}$.

**Area $= \frac{a_1}{k_1+\lambda} + \frac{a_2}{k_2+\lambda} + \frac{a_3}{k_3+\lambda}$, where $\lambda = \frac{0.693}{T_r}$ for Ru^{106}.

functions for mice and rats, respectively. It is very possible that bone, rather than kidney, should be considered as the critical organ when evaluating the possible hazard from Ru^{106} following oral or parenteral administration. It is known that Ru^{106} is lost from kidney tissue at a relatively rapid rate even though the initial kidney concentration (activity per g) is higher than that for other tissues. The long-term experiments of Burykin (5) showed that the concentration of Ru^{106} was greater in bone than in other tissues. Additional studies should clarify these points and also supply data needed for assessing possible interspecific correlations in the metabolic patterns of Ru^{106}. Calculations of maximum permissible body burden (MPBB) and maximum permissible concentration (MPC) values (food and water) can then be made with reasonable confidence.

REFERENCES

(1) E. Spode and F. Gensicke, Strahlentherapie 111, 266 (1960).

(2) C. R. Richmond, Los Alamos Scientific Laboratory Report LA-2207 (1958).

(3) R. C. Thompson, Hanford Atomic Operations Report HW-41422 (1956).

(4) Report of the International Commission on Radiological Protection, Committee II, On Permissible Dose for Radiation (1959), with Bibliography for Biological, Mathematical, and Physical Data, Vol. 3, 182 (1960).

(5) L. N. Burykin, In: Experimental Results on the Toxicology of Radioactive Substances, p. 61 (Russian), Moscow (1957).

Retention of Iridium^{192} in Mice and Rats following Oral Administration (J. E. Furchner, C. R. Richmond, and G. A. Trafton)

INTRODUCTION

This study was initiated by a specific need to know the amount of Ir^{192} remaining in the body after oral ingestion. Although it was obvious within a few days that less than 10 per cent of the ingested dose was absorbed, the retention-excretion pattern was determined until the activity of the animals reached the limits of the detection system.

METHODS AND RESULTS

To 6 male Sprague-Dawley rats, 78 days old and weighing 312 g, 1.1 μc of Ir^{192} as Na_2IrCl_6 (pH 0.7) was administered by gastric tube. A dose of 0.46 μc of Ir^{192} in the same chemical state was administered by the same route to 12 female RF mice (average weight 22 g) 63 days of age. The animals were maintained under standard laboratory conditions during the experiment. Whole body counting techniques, described elsewhere, were used to determine residual activities. The per cent retention as a function of time after administration is shown in Fig. 1. Expressions for the retention functions are not given as results of computer analysis are not available at present.

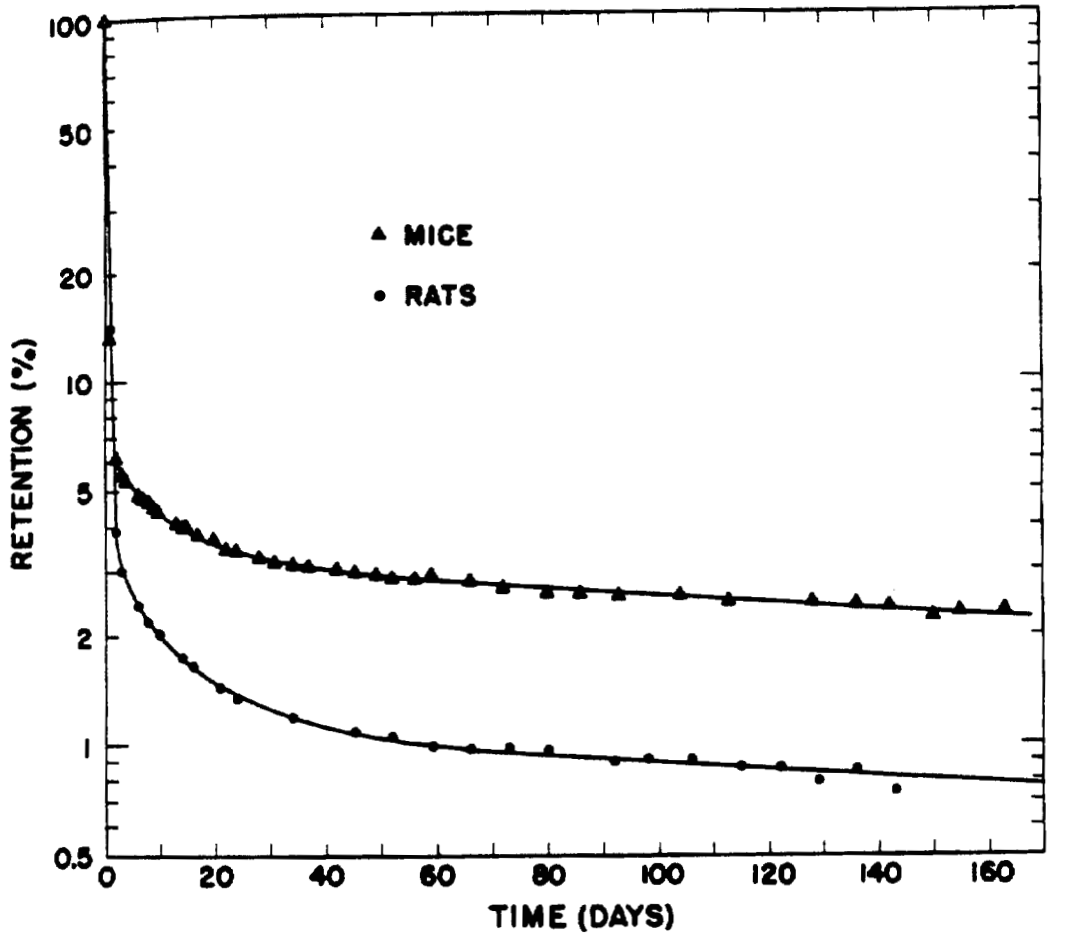

Fig. 1. Retention of orally administered Ir^{192} by mice and rats.

DISCUSSION

Within 2 days after oral administration, the retention of Ir^{192} by both rats and mice dropped to about 5 per cent of the administered dose. Retention continued to drop until, at about 60 days, it was approximately 3 and 1 per cent for mice and rats, respectively. The long components of the retention curves were approximately parallel for the two species and showed a biological half-time of about 300 days. For comparison, if the whole body is considered to be the critical organ, the most recent report of the International Commission on Radiological Protection (ICRP) gives a T_b value of 20 days for Ir^{192} (1).

It is disconcerting but interesting that the present data on Ir^{192} indicate for the first time a failure of the log of gastrointestinal uptake to be directly proportional to the log of body weight of the species.

REFERENCE

(1) Report of the International Commission on Radiological Protection, Committee II, on Permissible Dose for Radiation (1959), with Bibliography for Biological, Mathematical, and Physical Data, Vol. 3, 212 (1960).

Potassium Content of Dogs, Calculated from Natural Potassium^{40} Levels (C. R. Richmond and J. E. Furchner)

INTRODUCTION

Measurements of the inherent gamma ray activity of the human body have been reported by several groups of workers using large ionization chambers, NaI (Tl) crystals, and large liquid scintillation counters. Photopeaks at 0.66 and 1.46 Mev were the major activities detected in the scintillation spectra (1). These energies correspond to Cs^{137} and the naturally occurring K^{40}.

A large number of people measured in the Los Alamos Human Counter (Humco I) showed a natural K^{40} gamma ray activity of ~5.7 d/s/kg of gross body weight (2) with a standard deviation equal to 18 per cent of the mean. Whole body potassium content can readily be calculated from the activity measurements, as the gamma ray emission rate of ordinary potassium is essentially 3 γ/s/g. Consequently, the K^{40} activity of a 70 kg man corresponds to about 133 g of potassium. When expressed as a percentage of the gross body weight, the total body potassium content is known to vary with factors such as age, sex, and the relative amounts of fat, muscle, and water in the body. The effect of age on body potassium concentration is particularly hard to assess because of the large variations observed in the data. One

might reasonably expect to find less variation in the body potassium content among members of the same species of laboratory animal because of the relatively standardized dietary and environmental regimens and a more homogeneous genetic composition. Quantitative relations between body potassium and age, if they do exist, could be applied to many radiobiological studies which deal with aging phenomena.

METHODS AND RESULTS

Thirty-one beagle hounds were whole body radioassayed in Humco I for naturally occurring K^{40}. Each animal was thoroughly washed and dried prior to assay to remove surface contamination. Counting times were of sufficient duration to ensure a statistical precision of ~5 per cent. The K^{40} activities were then corrected for background depression and relative counting efficiency and converted to d/s of K^{40} per kg gross body weight.

Table 1 shows the individual values for the calculated body potassium concentration (g/kg) for 22 male and 9 female hounds. The average potassium concentration (61.86 mEq/kg gross body weight) is somewhat higher than the value of ~49 mEq/kg usually given for human beings. This difference is probably related to the fat-to-muscle ratio for each species, as the body potassium content is thought to be a proportionate

TABLE 1. POTASSIUM CONCENTRATION IN BEAGLE HOUNDS

Sex	Age (months)	Potassium Concentration (mEq/kg)	Deviation from Average ($x - \bar{x}/\sigma$)
Male	38	53.48	-1.74
Male	17	60.12	-0.40
Male	19	59.74	-0.48
Male	19	54.24	-1.59
Male	22	66.76	+0.94
Male	22	69.79	+1.55
Male	16	56.24	-1.18
Male	22	66.76	+0.94
Male	10	55.38	-1.36
Male	11	64.10	+0.40
Male	11	57.84	-0.86
Male	11	60.88	-0.25
Male	11	70.36	+1.66
Male	11	61.07	-0.21
Male	11	62.58	+0.09
Male	20	62.12	+0.01
Male	20	62.92	+0.16
Male	20	60.19	-0.39
Male	35	62.78	+0.14
Male	35	64.75	+0.53
Male	35	66.87	+0.96
Male	35	58.38	-0.77
Female	22	61.26	+0.03
Female	19	69.98	+1.76
Female	22	52.72	-1.88
Female	16	61.26	+0.02
Female	84	60.31	-0.18
Female	70	63.34	+0.49
Female	11	61.82	+0.15
Female	55	60.50	-0.14
Female	57	59.98	-0.26
$\bar{x} \pm \sigma$		61.86 ± 4.68 (all)	
$\bar{x} \pm \sigma$		62.11 ± 4.86 (males)	
$\bar{x} \pm \sigma$		61.13 ± 4.47 (females)	

function of the lean body mass. The value for σ (7.5 per cent of the mean) indicates the relatively small dispersion of values about the mean. A small but probably insignificant difference was found between the mean potassium concentrations for males and females. No obvious decrease in potassium concentration with respect to age was apparent; however, only 4 animals were more than 38 months of age (Fig. 1). An additional 21 animals, most of which are ~50 months of age, will be measured in the future.

DISCUSSION

Body potassium concentration for 31 beagle hounds was found to be 61.86 ± 4.68 ($\bar{x}$ ± σ) mEq/kg body weight. This value is ~20 per cent greater than the mean potassium concentration usually reported for human beings. Variations in the potassium concentration or relative variations in the body fat concentration among species could explain the difference. Regardless, as potassium concentration is an index of an animal's lean oxidizing protoplasmic mass, beagle hounds appear to have more "lean tissue" (or less fat) than human beings. Additional data are being collected so that possible age-dependent changes in potassium concentration can be observed.

REFERENCES

(1) C. E. Miller and L. D. Marinelli, Science 124, 122 (1956).

(2) E. C. Anderson, R. L. Schuch, W. R. Fisher, and W. Langham, Science 125, 1273 (1957).

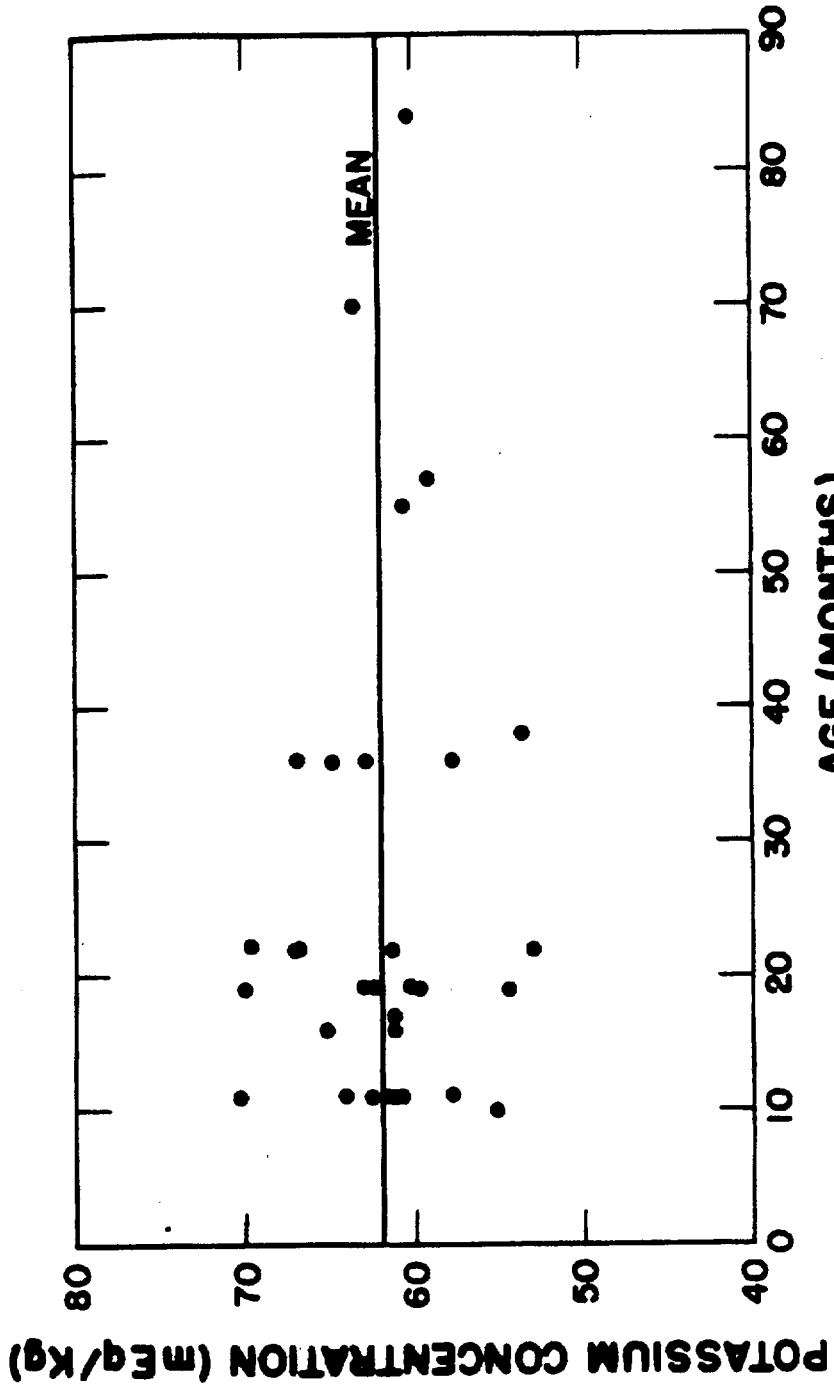

Fig. 1. Potassium concentration as a function of age in beagle hounds.

Potassium Concentration as a Function of Age in Rats (C. R. Richmond, J. E. Furchner, and M. A. Van Dilla)

INTRODUCTION

Previous studies have indicated that potassium concentration in man decreases as a function of age (1,2). This observation may be of importance in assessing physiological age. If this phenomenon also applies to small animals, it may be used to assess the effect of various physical and chemical stresses on physiological age. Such a method of measuring physiological age would be preferable to the usual criterion of aging (death rate), especially in problems dealing with precocious aging.

METHODS AND RESULTS

An 8 x 4 in. NaI (Tl) crystal and 100 channel analyzer were used to measure the natural K^{40} activity in male Sprague-Dawley rats of different ages. Two to 6 animals were used for each determination. The animals were weighed and compressed in a 2 gallon tin can (8 in. diameter) immediately after sacrifice. Plastic plates and rods were used to hold the sample in a fixed position in the can during the overnight (about 15 hours) activity measurement. Corrections for relative geometry and efficiency changes were made. Replicate measurements on the same sample agreed within 1 per cent.

Figure 1 shows the potassium concentration (g/kg) as a function of age for rats and man. Although the curves for man show considerable structure, the change in potassium concentration from 20 years on is about 9 mg/kg/yr. To detect such relatively small changes, many measurements must be made. The curves for man represent average values for ~1600 individuals.

The potassium concentration in rats appears to decrease rapidly between 2 and 4 months and then slowly between 4 and 24 months. This decrease is a change in potassium concentration of about 16 per cent between 2 and 4 months, and only about 6 per cent over the next 20 months. The rate of change from 4 months on is ~100 mg/kg/yr. Too much confidence should not be placed on these estimates, which are based on the small number of measurements shown in Fig. 1.

DISCUSSION

The data presented represent 11 groups of ~4 animals per point. Considerably more determinations should be made in order to determine quantitatively the possible changes in potassium concentration as a function of age. Measurements will also be made on animals younger than 2 and older than 24 months of age. In view of the small number of animals and small differences in potassium concentrations, no reliable

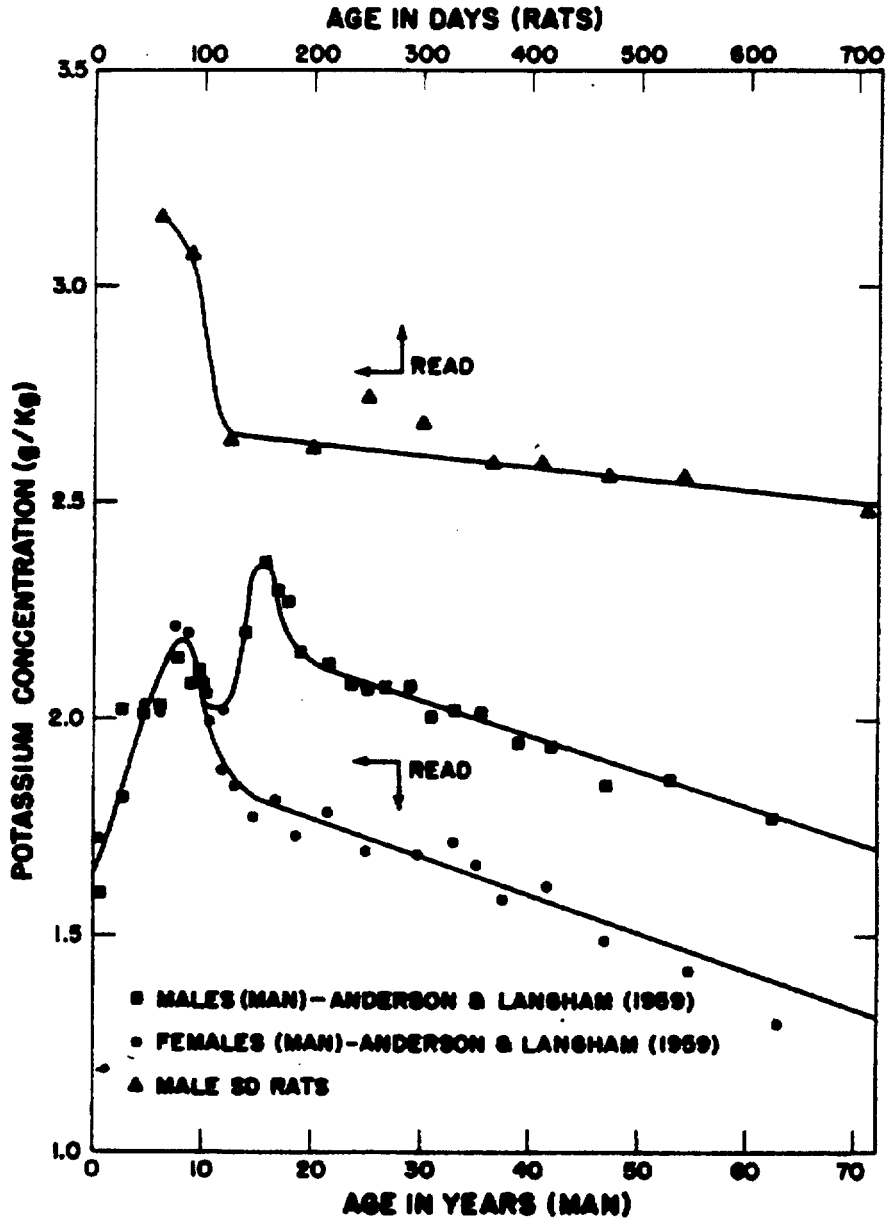

Fig. 1. Potassium concentration in rats and man as a function of age.

estimate of the change in potassium concentration as a function of age (or its statistical precision) can be made until more data are collected. It would be extremely difficult to predict age-dependent changes in potassium concentrations in rats, on the basis of data obtained from man, because of the large differences in the growth pattern and life span for each species.

REFERENCES

(1) U. Sagild, Scand. J. Invest. 8, 44 (1956).

(2) E. C. Anderson and W. H. Langham, Science 130, 713 (1959).

Radiochemical Neutron Dosimetry by Induced P^{32} Activity in Sulfur-Rich Biological Materials (D. F. Petersen, V. E. Mitchell, and W. H. Langham)

INTRODUCTION

In a preliminary report (1), data were presented indicating the possibility of utilizing neutron capture by sulfur-rich tissues for the estimation of incident fast neutron doses. The method was successfully employed in a recent nuclear critical accident (2) and a systematic study was, therefore, undertaken to improve analytical techniques and define the limits of applicability of the procedure. Results of these studies have demonstrated that incident neutron doses, based on determination of the P^{32} arising from the $S^{32}(n,p)P^{32}$ reaction in hair sulfur, are consistently in good agreement with a variety of other methods of neutron dosimetry. Improved analytical techniques have increased the sensitivity of the method approximately 10 fold. Thus, 1 rad of sulfur neutrons can be detected in a hair sample weighing from 0.5 to 1.0 g. The use of smaller samples has made it possible to assess dose distribution and deduce orientation by performing separate analyses on hair samples obtained from various parts of the body.

METHODS AND RESULTS

Hair obtained from the head, chest, abdomen, pubis, and

legs was appropriately positioned on plastic mannequins and exposed to the fission spectrum of the Godiva III critical assembly. Following recovery, 0.5 to 1.0 g samples were accurately weighed and digested in 10 ml of a mixture of equal volumes of concentrated nitric and perchloric acid for 2 hours at 200°C. The samples were cooled, diluted to 50 ml, and two 2.0 ml aliquots were removed for the determination of sulfur (3) and phosphorus (4). The remainder of the digest was adjusted to pH 3.5, 2 mg of carrier phosphate was added, and the P^{32} precipitated by the addition of excess 5 per cent ammonium molybdate. Wherever possible, duplicate determinations were performed with the addition of a P^{32} internal standard. The P^{32} precipitates were filtered on Whatman No. 42 paper to which had been added a small pad of Johns-Manville filter aid. The precipitates were sucked dry and immediately counted with a thin window Geiger-Müller tube for 30 minutes or to 10,000 counts. Counts were taken at subsequent intervals of 7 and 14 days to establish the identity of the radioactive material in the sample.

Beta counts were corrected for self-absorption, counter efficiency, and physical decay, and were expressed as disintegrations per minute per g of hair at T = 0. The incident flux of sulfur-level neutrons was computed from the following equation:

$$F = \frac{A \cdot W}{\sigma \cdot \omega \cdot N \cdot \lambda}$$

Where F = fast neutron flux detected by sulfur (n/cm^2)

A = activity per g of hair (d/m/g)

W = atomic weight of sulfur (32)

σ = activation cross section (225×10^{-27} cm^2/atom)

ω = sulfur content per g of hair

N = Avogadro's number (6.02×10^{23} atoms)

λ = decay constant (3.37×10^{-5}/min)

The factor for converting flux to dose for neutrons with energies in excess of 2.5 Mev is 3.83×10^{-9} rads/n/cm^2 (5). In the case of fission spectra where the extent of degradation is unknown, only the dose contributed by sulfur-level neutrons can be computed. However, the fission spectrum of the Godiva assembly has been well defined (5), and it has been established that neutrons above the sulfur threshold contribute approximately 30 per cent of the total neutron dose. Thus, in these experiments, it was possible to compute total doses as well as the incident sulfur threshold component.

To facilitate further the application of this procedure, a large number of sulfur analyses was performed to establish

whether the sulfur content of human hair varied sufficiently between individuals and with body distribution to necessitate separate elemental analysis of exposed samples. Phosphorus measurements were performed to determine whether the normal abundance of phosphorus was great enough to permit significant phosphorus activation by the $P^{31}(n,\gamma)P^{32}$ reaction.

Results shown in Table 1 indicate that the sulfur content of hair is remarkably constant without regard for color, consistency, or body distribution. Phosphorus concentration varied somewhat more than did sulfur, presumably due to contamination of the samples with varying amounts of epidermal cells. However, no cases were observed where phosphorus exceeded 1 per cent of the sulfur concentration, and it was concluded that except in extreme cases of spectrum degradation, phosphorus activation could be disregarded. Measurements of the sulfur and phosphorus content of hair from various anatomical locations of 1 individual are summarized in Table 2. These data provide additional evidence for the constancy of chemical composition regardless of distribution.

Table 3 summarizes the results of a number of neutron experiments in which doses computed from hair beta activity were compared with dose estimates based on data obtained from (a) Pu^{239}, Np^{237}, U^{238}, and S^{32} threshold detectors, (b) the Hurst proportional counter, and (c) tissue-equivalent

TABLE 1. RELATIVE SULFUR AND PHOSPHORUS CONTENT OF HUMAN HAIR

Distribution	Samples Analyzed (No.)	Sulfur* (mg/g)	Phosphorus* (mg/g)	Phosphorus-to-Sulfur (per cent)
Head	64	47.1 ± 5.1	0.155 ± 0.042	0.33
Pubis	68	47.3 ± 5.6	0.251 ± 0.065	0.53
All samples (head, chest, abdomen, pubis, legs)	168	47.7 ± 5.5	---	--

*Mean ± standard deviation.

TABLE 2. SULFUR AND PHOSPHORUS CONTENT OF HAIR FROM VARIOUS ANATOMICAL LOCATIONS OF THE SAME INDIVIDUAL

Location	Sulfur (mg/g)	Phosphorus (mg/g)	Phosphorus-to-Sulfur (per cent)
Head	43.2	0.162	0.38
Beard	39.5	0.143	0.36
Chest	43.8	0.185	0.42
Abdomen	46.3	0.158	0.34
Pubis	45.6	0.194	0.43
Leg	46.6	0.153	0.33
Arm	48.7	0.129	0.26
Mean ± Standard Deviation	44.8 ± 3.0	0.161 ± 0.026	0.36

TABLE 3. COMPARISON OF NEUTRON DOSE ESTIMATES BASED ON HAIR SULFUR ACTIVATION MEASUREMENTS WITH OTHER PHYSICAL DOSIMETRY

Experiment No.	Sulfur Threshold Neutrons - Hair (rads)	Total Neutrons - Hair (rads)	Total Neutrons - Other (rads)	Estimated Dose (per cent)
1	6.9	23.0	26.2	87.8
2	45.6	152.0	165.0	92.1
3	41.8	139.4	165.0	84.5
4	9.4	31.4	28.9	108.7
5	4.9	16.4	28.9	56.7
6	81.6	272.0	311.4	87.5
7	82.8	276.1	311.4	88.7
8	142.8	456.0	526.0	86.7
9	109.2	364.0	404.0	90.1

and graphite-CO_2 ionization chambers (5,6). The data show that in most instances estimates based on hair activation analyses agree with the other methods of physical dosimetry within 20 per cent or less.

The possibility of determining dose distribution and orientation at the time of exposure was investigated by placing coded hair samples on the head and at 90° intervals around the pelvis of a mannequin prior to irradiation. Subsequently the analyst was required to indicate the position of each sample as well as estimate the incident dose. Results in Table 4 show that it was possible not only to estimate the incident dose but also to position successfully each sample on the mannequin.

DISCUSSION

It should be emphasized that although these measurements are subject to somewhat greater uncertainties than the referee dosimetry, the largest discrepancies tend to occur with very low doses. The method appears to be reliable for exposures covering a range from sublethal to supralethal doses, assuming a gamma-to-neutron ratio of 3 and an RBE for neutrons of 2. Moreover, information obtained after larger doses would be quite useful in rapidly assessing the severity of exposure, and the data lend support to our earlier conclusions based on

TABLE 4. DOSE DISTRIBUTION AND ORIENTATION OF PLASTIC MANNEQUIN DEDUCED FROM HEAD AND PUBIC HAIR ACTIVATION

Sample No.	Position of Sample	Incident Dose Hair Activation (rads)	Incident Dose Fission Counter (rads)
1	Pelvic posterior	4.36	---
2	Pelvic lateral	159.00	---
3	Pelvic lateral	150.00	---
4	Pelvic anterior	199.00	186
5	Head	183.00	186
6	Head	170.00	186

hair activation analyses in the recent fatal Los Alamos nuclear critical accident (2). The relatively constant sulfur content of hair indicates that an average value could be substituted in place of direct sulfur analysis, materially shortening the procedure without appreciably affecting the result.

Chemical separation of the beta activity provides a significant advantage over our previous ashing technique. Losses due to volatilization are eliminated by the low digestion temperature, and separation from other activated materials is accomplished without extraction of phosphorus into an organic solvent. Preliminary data from a recent Nevada reactor test indicate that induced P^{32} activity in neutron-irradiated hair can be successfully separated from local fallout associated with operation of the reactor.

The simplicity of the analytical method, together with the almost universal availability of hair, suggest that this procedure as an additional biological parameter for determining first approximations of the neutron dose sustained by potential nuclear critical accident victims is feasible.

ACKNOWLEDGMENT

The cooperation of Drs. J. A. Sayeg and E. R. Ballinger in exposing samples and providing referee dosimetry is gratefully acknowledged.

REFERENCES

(1) D. F. Petersen and W. H. Langham, Biological and Medical Research Group (H-4) of the Health Division - Semiannual Report July through December 1959, Los Alamos Scientific Laboratory Report LAMS-2445 (February 1960).

(2) P. S. Harris, Report on the Nuclear Criticality Accident at the Los Alamos Scientific Laboratory, submitted to J. Occup. Med. (1960).

(3) I. Lysyj and J. E. Zarembo, Microchem. J. 3, 173 (1959).

(4) C. H. Fiske and Y. Subbarow, J. Biol. Chem. 66, 375 (1925).

(5) J. A. Sayeg, Los Alamos Scientific Laboratory Report LA-2432, in press (1960).

(6) J. A. Sayeg, Los Alamos Scientific Laboratory Report LA-2310 (September 28, 1959).

Determination of Strontium^{90} in Bone (H. Foreman and M. B. Roberts)

INTRODUCTION

In the course of a study of the accumulation of fallout isotopes in deer antlers, a procedure was developed for the determination of Sr^{90} in bone. Since this procedure presents a unique approach to the problem of low-level Sr^{90} assay and has procedural advantages over presently used methods, it is worth reporting separately for its own merits.

In brief, the procedure involves extraction of Y^{90} into a solution of 2.5 per cent dibutyl phosphate in scintillation solution (consisting of terphenyl and POPOP in toluene) from a dilute nitric acid solution containing Sr^{90} concentrated from bone ash by the standard fuming nitric acid procedure. The radioactive yttrium is assayed by counting in a liquid scintillation counter.

DETAILED PROCEDURE

1. Prepare 100 gm of bone ash by grinding with a mortar and pestle to a coarse powder, weigh into a 400 ml beaker, and add 50 ml of strontium carrier solution (10 mg Sr^{++}/ml distilled H_2O).

2. Add 50 ml strontium carrier solution and 30 ml distilled water. Add 225 ml fuming HNO_3 slowly. Stir for 1 hour.

3. Filter while still warm through a medium sintered glass filter, and discard the filtrate.

4. Dissolve the preparation with hot distilled H_2O and evaporate to 50 ml.

5. Adjust the solution to pH 1.0 with a concentrated NaOH solution, added dropwise.

6. Store sample for 14 days to allow the Y^{90} to grow in.

7. Transfer the sample to a 125 ml separatory funnel and shake for 5 minutes with an equal volume of di-n-butyl orthophosphoric acid (DBP) dissolved in a scintillation solution consisting of 0.05 per cent POPOP and 0.5 per cent p-terphenyl in toluene (0.3 to 0.4 N in DBP), noting the time.

8. Discard the aqueous phase and dry the organic portion with silica gel for approximately 15 minutes.

9. Draw off 30 ml of the organic portion, place in a 10 dram counting vial, and count in a standard liquid scintillation counting setup (10,000 counts). Note the counting time.

10. Correct for decay of Y^{90}.

11. Strontium^{90} values can be calculated from the Y^{90} count, since there is 1 d/m of Sr^{90} for each d/m of Y^{90}.

RESULTS AND DISCUSSION

To evaluate the procedure and judge its merits, the following procedures and measurements have been carried out.

(a) Counting and Extraction Efficiency.--Known amounts of Sr^{90} in tenth normal nitric acid solution were extracted and counted by the method presented above. This procedure was performed each day a "run" was done on a series of unknowns to check the reagents and the counter. Results of 18 different determinations are shown in Table 1. When the nitric acid solution was extracted again immediately after the first extraction, less than 1 per cent of Y^{90} was found, indicating essentially complete extraction initially. The 10 per cent or so diminution from the expected values un-

TABLE 1. COUNTING AND EXTRACTION EFFICIENCY

Yttrium^{90} Added (d/m)	Yttrium^{90} Recovered (d/m)	Per Cent
36,102	31,855	88.93
4,430	3,820	86.63
106,660	9,785	92.20
8,533	7,904	92.63
17,558	16,050	91.41
15,918	14,276	89.68
45,128	40,505	89.76
24,421	22,300	91.21
34,789	31,428	90.37
43,158	38,658	89.57
49,467	46,729	93.99
48,410	43,702	90.27
46,933	42,619	90.81
45,784	40,793	89.80
57,435	52,690	91.70
58,420	53,588	91.72
49,066	44,127	88.93
44,635	40,532	90.76
	Average	90.58
	Standard Deviation σ	$\pm$ 1.73

TABLE 2. RECOVERY OF STRONTIUM^{90}

Strontium^{90} Added (d/m)	Strontium^{90} Recovered (d/m)	Efficiency (per cent
35,774	32,898	91.96
39,384	35,032	88.95
76,799	67,506	87.90
41,025	33,673	82.08
13,128	9,900	75.41
16,410	11,983	73.02
147,149	119,529	80.90
97,147	79,048	81.37
	Average	82.70
	Standard Deviation $\sigma \pm$	6.70

(c) Reproducibility.--Replicate samples were run on all antler samples to the extent allowed by the amount of sample available. Where a large quantity of sample was available, replicates were run by two different individuals. Table 3 shows the results of samples run in triplicate.

(d) Sensitivity.--To a large extent, interest in Sr^{90} determinations lies in situations wherein the isotope content is at very low levels. In our procedure, the use of large samples (100 grams) allows the assay of low-level samples without recourse to complicated counting equipment and very prolonged counting times. Table 4 shows the counting time necessary to obtain a given accuracy for samples containing given levels of activity. These calculations are based upon the following considerations:

(1) Background = 70 c/m.

(2) A 100-gram bone sample contains 35 per cent calcium; therefore, at 1 Sunshine Unit (SU) the sample yields 70 c/m, assuming 90 per cent counting efficiency.

(3) Per cent standard deviation =

$$100 \frac{\sqrt{\frac{R_{(S+B)}}{t_{(S+B)}} + \frac{R_B}{t_B}}}{R_S}$$

and

TABLE 3. REPRODUCIBILITY OF RESULTS

Type of Sample	Year and Place		Strontium^{90} (d/m/gm)
Reindeer antler	1958	Alaska	85.32; 86.38; 93.28
Elk antler	1956	Missouri	23.25; 23.24; 22.17; 23.37; 23.46
Deer antler	1958	New Mexico	12.61; 12.36; 12.06
Deer antler	1955	New Mexico	5.35; 6.37; 6.80
Deer long bone	1957	New Mexico	8.31; 9.80; 9.40; 10.08
Elk antler	1957	Colorado	12.84; 12.13; 13.47
Elk skull	1957	Colorado	17.07; 17.88; 18.13
Elk antler	1956	New Mexico	8.47; 8.16; 8.45
Moose antler	1953	Yukon	2.21; 2.17; 2.30
Caribou antler	1953	Yukon	4.11; 5.35; 4.99

TABLE 4. COUNTING TIMES REQUIRED TO OBTAIN GIVEN ACCURACY

Strontium ^{90} Content (S. U.)	Standard Deviation (per cent)	Counting Time (minutes)
1.0	10	3.4
1.0	5	13.6
1.0	2	85.2
0.5	10	12.7
0.5	5	51.8
0.1	10	291.0
0.1	5	1170.0

$$\frac{t_{(S+B)}}{t_B} = \sqrt{\frac{R_{(S+B)}}{R_B}}$$

where $R_{(S+B)}$ = counting rate of sample plus background

R_B = counting rate of background

$t_{(S+B)}$ = time for counting sample plus background

t_B = time for counting background

(e) Other Studies.--A comparison (Table 5) of the times required to perform various parts of the procedure is made with one other widely used Sr^{90} assay method, namely the Harwell procedure (1).

REFERENCE

(1) F. J. Bryant, A. Morgan, and G. S. Spicer, Atomic Energy Research Establishment Report AERE-R-30 (1959).

TABLE 5. TIME FOR PERFORMANCE OF VARIOUS STEPS IN STRONTIUM^{90} PROCEDURE

	LASL Procedure	Harwell Procedure[a]
Size of sample	100 gm	5 gm
Ashing	4 hr	4 hr
Weighing and dissolving sample	1 hr	0.5 hr
Separation of strontium from bulk of calcium	1.5 hr	5 hr
Yttrium^{90} growth period	14 days	14 days
Separation of Yttrium^{90} and preparation of sample for counting	5 min	2 hr
Counting time (see Table 4)	less than 2 hr	Not less than 24 hr[b]

[a] Times for Harwell procedure are estimated.

[b] Using calculations in Table 4 to obtain a 10 per cent standard deviation at the 1 S. U. level, Harwell procedure counting time is 300 min.

Effect of Diethyltriamine Pentaacetic Acid (DTPA) on Elimination of Americium^{241} Administered Intratracheally to Rats

(H. Foreman and M. B. Roberts)

INTRODUCTION

As reported previously, diethyltriamine pentaacetic acid (DTPA) is a superior chelating agent for hastening the excretion of heavy and radioactive metal ions from the body. The present study was set up to determine the extent to which this drug could hasten the excretion of an actinide element when deposited in the lungs. This is a situation of considerable interest, because inhalation is a most likely mode for accumulation of radioisotopes internally.

METHODS

Two groups of animals, each consisting of 5 Sprague-Dawley adult rats weighing 350 g, were injected into the trachea with 0.2 cc of a neutral solution of Am^{241} nitrate in 0.5 per cent sodium citrate. Each animal received about 4×10^5 d/m. Twenty-four hours following the injection, each animal in 1 group was given 1 cc of a solution containing 100 mg of DTPA, intraperitoneally. The injections were continued daily for 5 days, then stopped for 2 days. This regimen was continued for 1 month. The animals were counted daily in a whole body counter described previously. There was no attempt made to collect the excreta.

RESULTS

The results presented in Fig. 1 show that the drug was considerably effective in hastening the removal of the isotope when the route of entry was the respiratory tract. At the end of 1 month, the controls had retained 70 per cent of the original dose, whereas the treated animals had a body content of only 16 per cent. By the end of the treatment period, treatment had become less effective as evidenced by the flattening of the retention curve wherein the slope of the experimental group rapidly approached that of the control group. It may be that after a period of rest, resumption of treatment would bring forth increased excretion, as was seen in studies where the isotope had been given intravenously.

It must be pointed out that this is an unusual type of inhalation exposure in that the material consisted entirely of soluble material, which remained largely in the body. If the isotope had been in a particulate form, then a large quantity of it would have been removed by mucous formation and ciliary action. Since samples of urine and feces were not counted, it was not possible to determine whether excretion had occurred through the urine or whether the isotope had been transferred in a retrograde manner back into the upper respiratory tract and swallowed and passed out through the gastrointestinal tract. Nonetheless, these results are encouraging in the net effect of ridding the body of the isoto

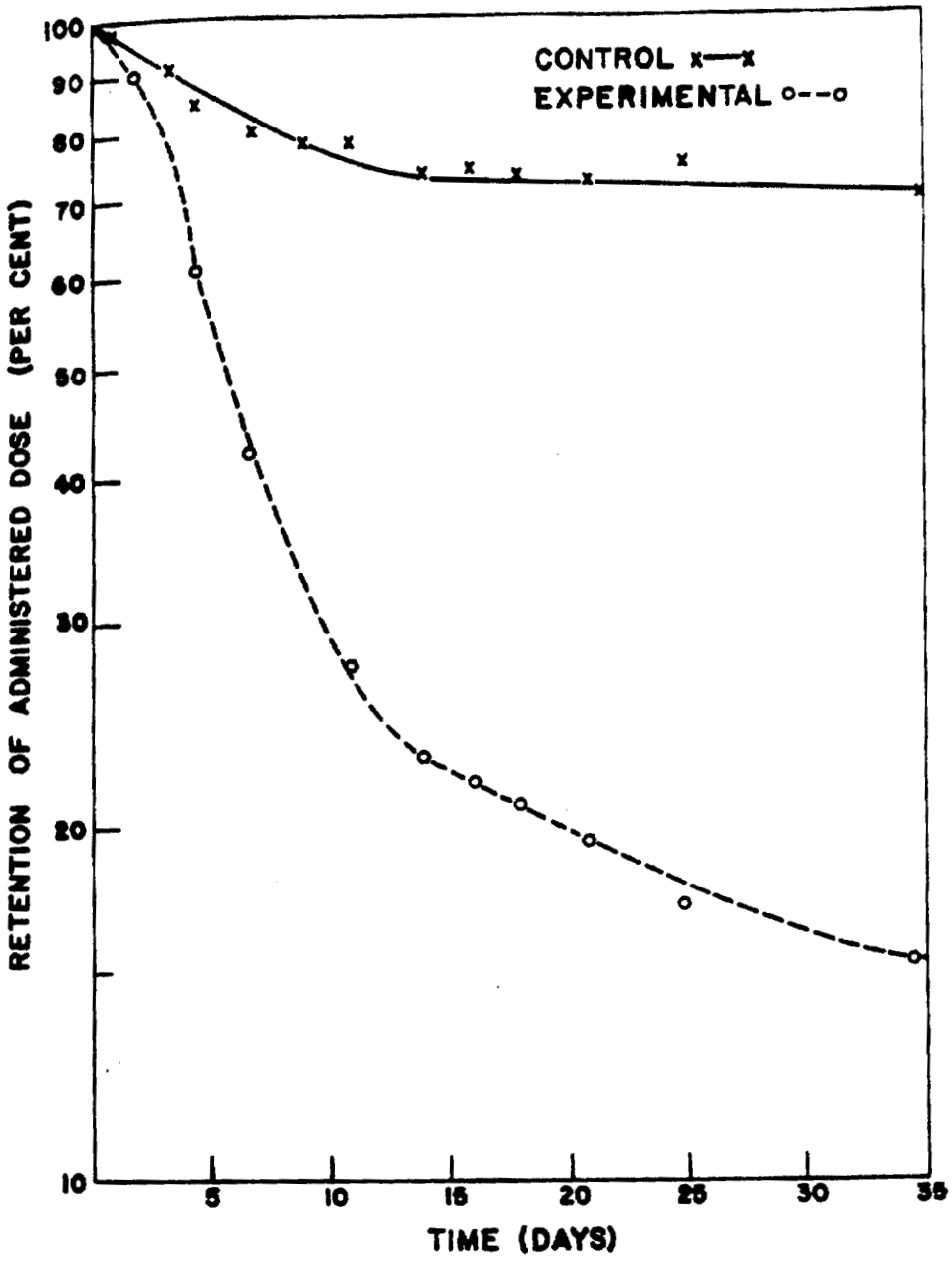

Fig. 1. Effect of DTPA on excretion of Am^{241} given into the respiratory tract of rats.

Nephrotoxicity of Chelating Agents - A Continuing Study

(H. Foreman, C. C. Lushbaugh, M. B. Roberts, and G. L. Humason)

INTRODUCTION

Studies reported earlier (1) showed that the administration of diethyltriamine pentaacetic acid (DTPA) to rats produced a kidney lesion which was demonstrated histologically by the use of the periodic acid Schiff stain. The lesion is a "hyaline droplet" degeneration of the proximal tubules (Fig. 1). Similar studies showed that the renal lesion produced by ethylenediamine tetraacetic acid (EDTA) under similar conditions was a "vacuolar" type of tubular degeneration (Fig. 2), but only hematoxylin and eosin were used. It would be of considerable practical and theoretical interest to determine whether these are in fact two separate lesions or whether one is dealing with different manifestations of the same lesion, which have become apparent because of different procedures of demonstration.

The delineation of the lesion is of practical interest in establishing a safe dosage schedule for DTPA. If the relative nephrotoxicity of the two drugs could be established, the dosage schedule for DTPA perhaps could be set from the large clinical experience that has been obtained with the use of EDTA. The present study was designed to determine

Fig. 1. "Hyaline droplet" renal tubular lesion (magnification X300).

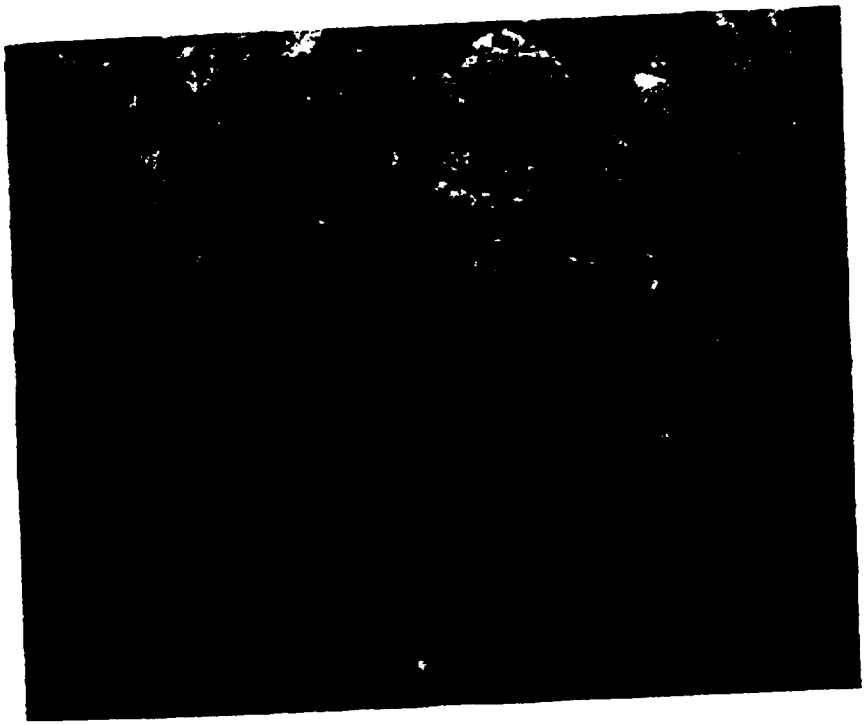

Fig. 2. "Vacuolar" renal tubular lesion (magnification X480).

definitively whether two different tubular lesions are produced. From a theoretical viewpoint, it is desirable to know if it is possible that two so closely similar chemical agents could produce different kidney lesions. This would be surprising indeed and worthy of considerable investigation in itself.

The second part of the study was set up to determine the mechanism by which the lesions were produced. The "vacuolar" lesion is seen after the administration of many types of substances, i.e., sucrose, urea, creatine, acacia, etc. The current theory (2) postulates that the passage of these substances across the cells of the proximal tubules (either in the resorptive or secretory process) results in the formation of hypertonic solutions in the cytoplasm of the cell. This leads to the imbibition of water into the cells, and during the staining process the water-containing spaces show up as vacuoles. There are many things which this hypothesis does not adequately explain, among which are the persistence of vacuoles for several days whereas the offending materials are eliminated in hours, phloridzin does not prevent the formation of the lesion, and the lesion does not occur in the distal tubule region where the tubular fluids are persistently hypertonic.

The lesion seemingly is produced by a wide variety of

materials, including aspirin. Generally speaking, these materials are not altered in the body but pass through it unchanged and are excreted by both glomerular filtration and tubular secretion. The following postulates, if true, may explain the course of events resulting in the formation of the lesion:

(a) The droplet lesion seen with PAS is an early stage of the vacuolar lesion.

(b) The droplets are morphologic manifestation of the tubule at work and may represent an agglomeration of the mitochondria.

(c) The droplets are always formed during tubule secretion and restitute to normal at rest. However, when the tubule cell is overworked, then the droplets persist long enough so that they can be seen in a microscopic preparation.

(d) When the tubule is markedly overworked, then the droplets accumulate in agglomerations large enough to drop out and leave a vacuole.

In other words, the lesions are merely representations of the overload of the kidneys as they attempt to rid the body of an excessive burden of foreign substance. As the tubule cells restitute at rest, so does the extreme manifestation restitute, hence the recoverable nature of the lesion. To test this hypothesis, the following experiments were set up.

MATERIALS AND METHODS

Para-amino-hippuric acid, a material for which the tubul maximum has been well established, was given in considerable excess in order to overwork the kidneys deliberately. If thi generally considered nontoxic material produces lesions under these conditions, this should provide considerable substantia for our hypothesis. Large quantities of acetate were given t experimental animals along with DTPA. Acetate has been shown to provide extra usable fuel for work of the tubule (3) and thereby can raise the tubule maximum. Acetate given under these conditions should serve as a protective agent against the formation of the lesion. A group of animals was given dinitrophenol (DNP) along with DTPA. This agent reduces the capacity of the kidneys to do work by uncoupling phosphorylat from oxidation (3). Animals treated thus should be more vul- nerable to the nephrotoxic action of the drug.

All groups of animals except for the controls were treat by the standard nephrotoxic procedure described previously (4 To determine the identity of the tubular lesion, the tissues from the DTPA and the EDTA treated animals were stained with both H and E and PAS. The para-amino-hippuric acid treated animals were given the agent in doses ranging from 50 up to 300 mg/day. The dose producing a plasma level corresponding to the tubular maximum was approximately 100 mg/day. The

group receiving acetate was given sodium acetate mixed with the diet to the extent of 10 per cent. The group receiving DNP was given 50 mg/day of the drug intraperitoneally.

RESULTS AND DISCUSSION

In this study both types of lesions, the droplet and the vacuolar degeneration, were seen in the sections from the DTPA and the EDTA animals. The droplet lesion was seen at lower doses than the vacuole lesion, and hence it is quite likely that the droplet lesion is a precursor to the vacuole lesion. It was not possible to correlate the severity of the droplet lesion with dose levels, since the severity of the lesion varied greatly from animal to animal without regard to the dose. The vacuolar lesion first appeared at much lower dose levels in the EDTA animals than it did in the DTPA animals, indicating that DTPA is less nephrotoxic than EDTA. It was possible to produce the droplet lesion with doses of para-amino-hippuric acid exceeding the tubular maximum.

The experiments using acetate and DNP were inconclusive. The droplet lesion appeared to be less severe in the acetate treated animals at all doses, when compared to animals treated with DTPA alone. However, as stated above, it was very difficult to quantitate the severity of the droplet lesion. A similar situation applied to the DNP results. It appeared

that DNP worsened the lesion, but this could not be told conclusively. It will be necessary to repeat the experiment using EDTA instead of DTPA, since the vacuolar lesion produced is much easier to quantitate and correlate with dose levels with the former drug.

REFERENCES

(1) Biological and Medical Research Group (H-4) of the Health Division - Semiannual Report July through December 1959, Los Alamos Scientific Laboratory Report LAMS-2445 (February 1960).

(2) A. C. Allen, The Kidney, p. 210, Grune and Stratton, New York (1951).

(3) G. H. Mudge and J. V. Taggart, Am. J. Physiol. 161, 191 (1950).

(4) H. Foreman, C. Finnegan, and C. C. Lushbaugh, J. A. M. A. 160, 1042 (1956).

BIOCHEMISTRY SECTION PUBLICATION

(1) C. R. Richmond, T. T. Trujillo, and D. W. Martin, Volume and Turnover of Body Water in Dipodomys deserti with Tritiated Water, Proc. Soc. Exptl. Biol. Med. 104, 9 (1960).

CHAPTER 3

LOW-LEVEL COUNTING SECTION

Milk Monitoring Program (B. E. Clinton, J. M. Allen, and E. C. Anderson)

INTRODUCTION

The program of measuring natural and fallout radioactivities in milk samples from 55 stations in the United States and Canada has continued. Because of the development of the U. S. Public Health Service's and the Canadian Department of Health and Welfare's networks for routine monitoring, the LASL network will be reduced at the end of this report period to the 16 stations listed in Table 1. These stations will be continued for another fiscal year in order to obtain the pattern of variation for an additional year without tests. While no tests were conducted during 1959, the pattern for that year was nevertheless abnormal due to the intensive high latitude tests in the fall of 1958. On the basis of previous experience, it was concluded that the reduced net would be

TABLE 1. MILK SAMPLING STATIONS TO BE CONTINUED DURING FY 1961

	State	Town
1.	California	Tipton
2.	Idaho	Idaho Falls
3.	Illinois	Minonk
4.	Kentucky	Louisville
5.	Louisiana	Franklinton
6.	Michigan	Adrian
7.	Minnesota	Stillwater
8.	Missouri	Springfield
9.	North Dakota	Bismarck
10.	New York	Binghamton
11.	South Dakota	Mitchell
12.	Texas	LaGrange
13.	Utah	Ogden
14.	Vermont	St. Albans
15.	Washington	Burlington
16.	Washington	Sunnyside

adequate for the study of meteorological and ecological factors. The stations were carefully selected on the basis of this requirement and for reliability of shipments and dating. In the absence of unexpected developments, the entire program will be discontinued at the end of fiscal 1961.

METHODS AND RESULTS

As before, direct measurements were made of the Cs^{137} and K^{40} radioactivities using the 4π liquid scintillation counter (Humco I). No processing of the 50 to 100 pound samples was required. The most striking features of the 1960 results are the lack of structure and the very low levels to which the Cs^{137} has fallen in many locations.

The characteristic feature of the 1959 data was the broad peak in milk radioactivity which occurred in all stations. The rise began as early as February or March in some stations (Missouri, Texas, California) and as late as May or June in others (North Dakota, Minnesota, Massachusetts). Extremely high levels were reached for brief periods of time (e.g., 300 $\mu\mu c$ Cs^{137}/g K in Washington, 200 $\mu\mu c$ in Missouri and Louisiana). In contrast, no station has shown a significant rise during the first 6 months of 1960; the curves are flat and structureless and generally show a steady decline over this period. This indicates that the 1959 pattern was

unusual, probably a result of the intense high latitude tes ing in the fall of 1958. The cesium levels in most station during 1960 have been at or below their values before the 1959 peak, only Missouri and Ogden, Utah being slightly elevated.

For most of the country, the 1960 to 1959 ratio is 0.4 to 0.8. Washington and Vermont, the highest points in the United States, remain at their January-February 1959 levels of about 80 μμc/g K, far below peak values, and a slow but steady decline has continued throughout the spring and summer. The lowest cesium values for milk are shown by the California points, some of which have reached levels in Jun at which the cesium is no longer detectable (less than 10 μμc/g K). These observations strongly suggested that th uptake of cesium is proportional to differential, rather th to integral, fallout. Figures 1 through 4 show typical com parisons of 1959 (solid curve) and 1960 (points) data.

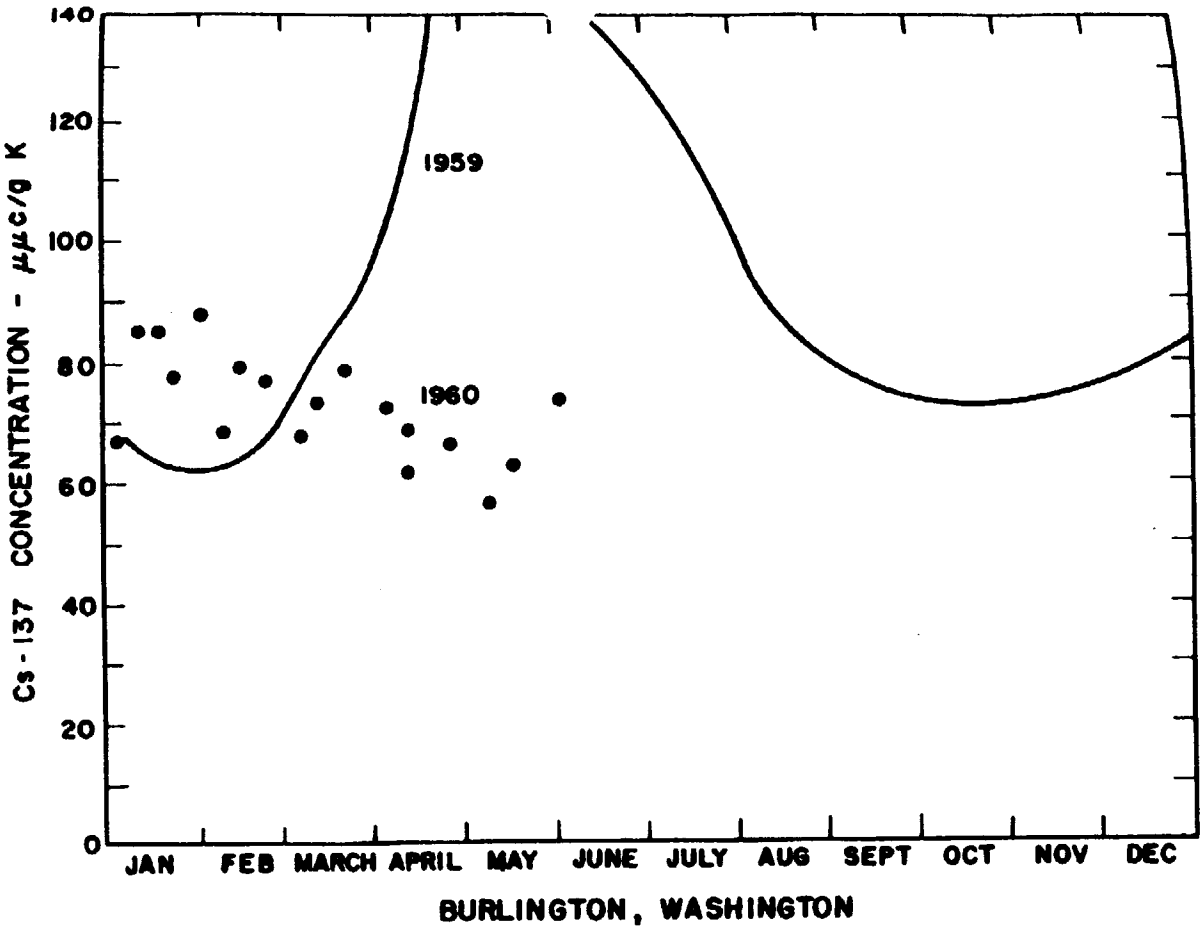

Fig. 1. Cesium^{137} in milk, 1959-1960; Burlington, Washington.

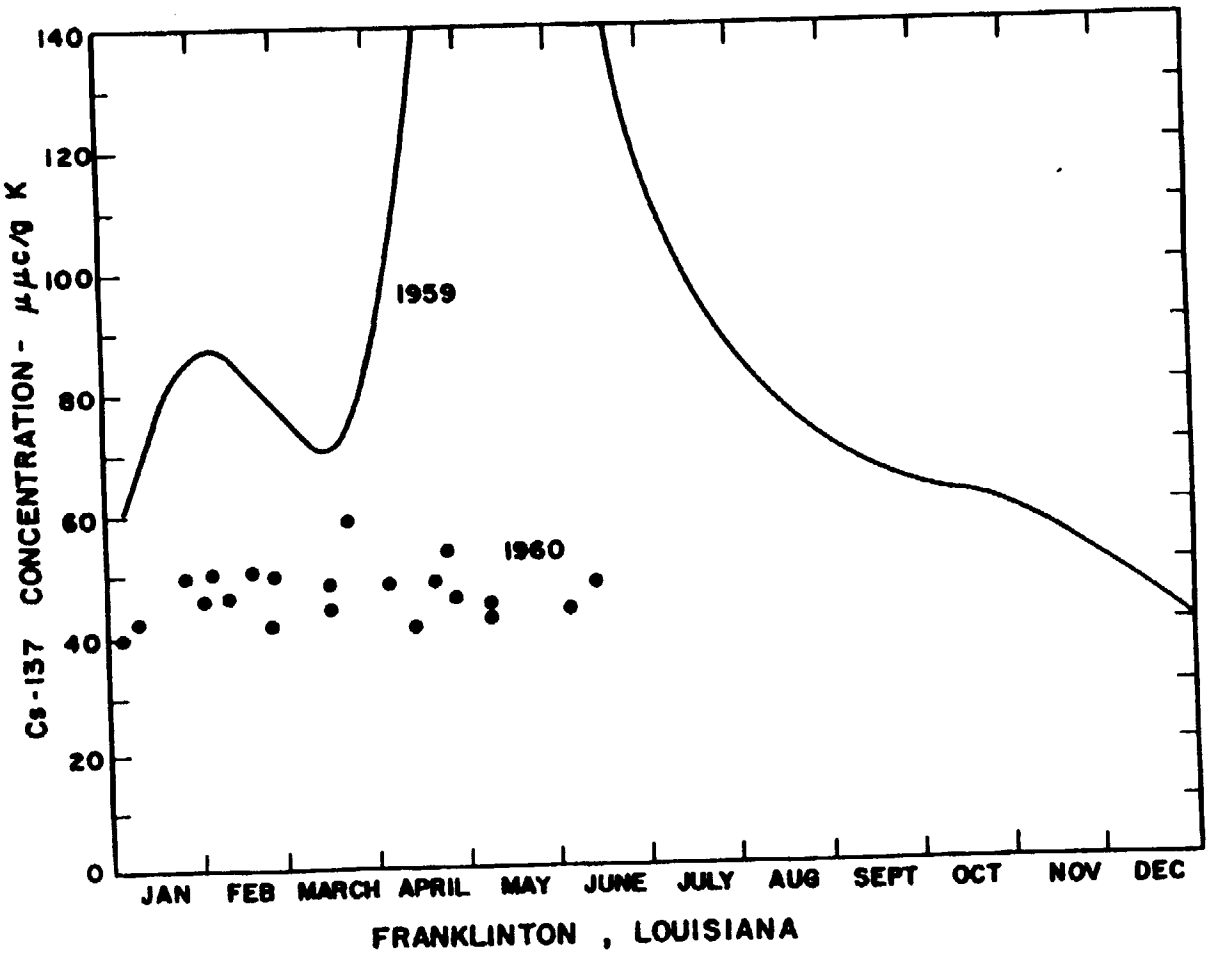

Fig. 2. Cesium^{137} in milk, 1959-1960; Franklinton, Louisiana.

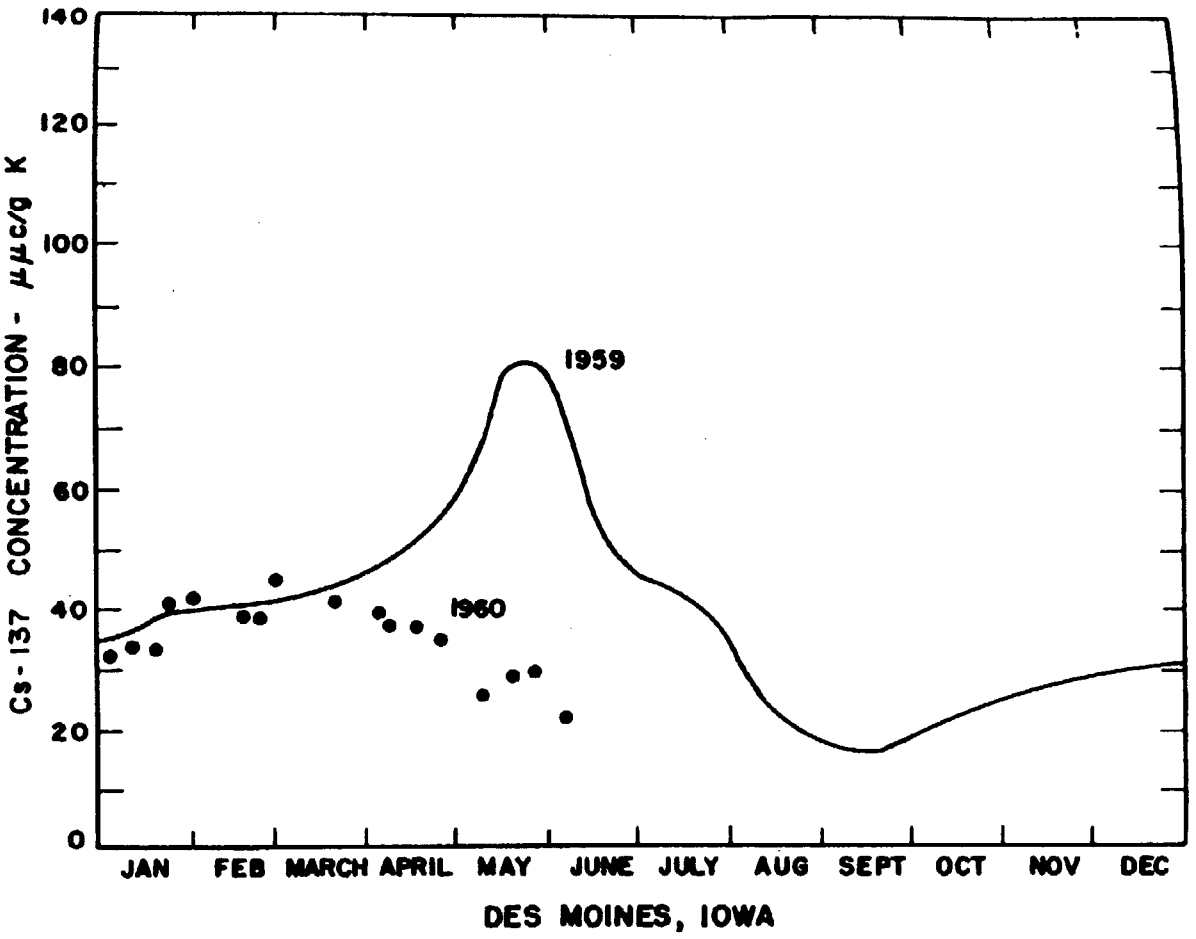

Fig. 3. Cesium^{137} in milk, 1959-1960; Des Moines, Iowa.

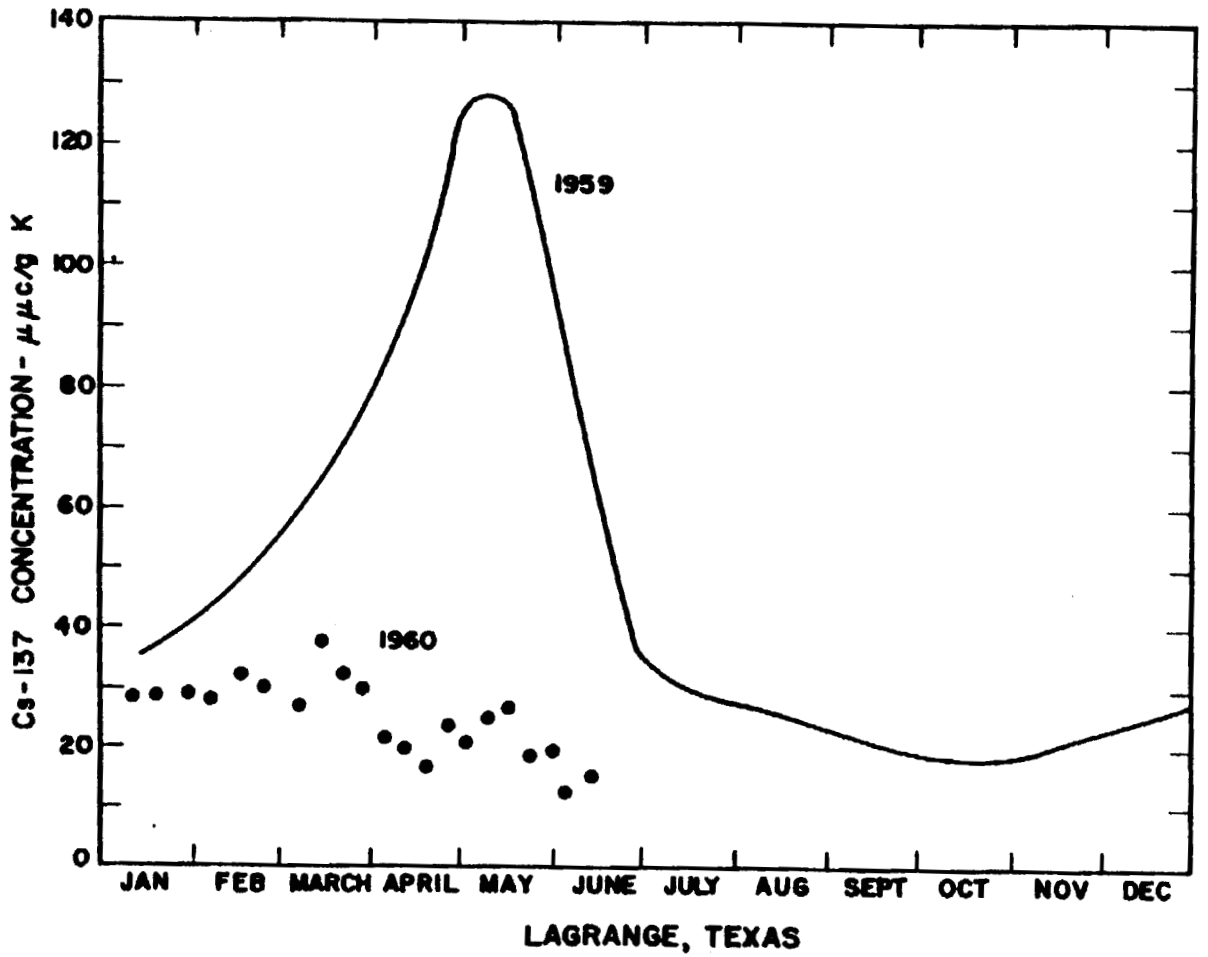

00131478.089

Fig. 4. Cesium^{137} in milk, 1959-1960; LaGrange, Texas.

Search for Zinc^{65} in General Population (M. A. Van Dilla and M. W. Rowe)

INTRODUCTION

The general food supply contains slight amounts of Zn^{65} (1,2) in addition to the well known fission products Cs^{137} and Sr^{90}. Since the uptake and retention of this radioisotope are large (3), it should be present in people. Hence, we have re-examined the gamma ray spectra of 32 candidates for the Mercury astronaut program measured in the first half of 1959 for possible traces of Zn^{65}.

METHODS AND RESULTS

These 32 men are fairly homogeneous with respect to age, weight, and general physical condition. They come from different parts of the country. All were measured in both Humco I and the Human Spectrometer, the measuring time in the latter being 30 minutes. All spectra show the usual Cs^{137} and K^{40}; it is clear from cursory inspection that any other radioactivity present must be in amounts small compared with these. However, it is easy to be misled into mistaking the Compton edge (at 1.22 Mev) of the prominent K^{40} peak for a trace of Zn^{65} (gamma ray energy = 1.11 Mev). In order to take this into account, we made phantoms of sugar and KCl, weighing 140 and 180 pounds. This permitted the Zn^{65} region (channels 46-58,

corresponding to 1.02 to 1.26 Mev) of the human spectra to be corrected for the K^{40} contribution. When this was done, the count rate in the Zn^{65} region of the human spectra was reduced from 30 to 60 c/m to nearly zero for most subjects. The statistical distribution of these residual count rates is shown in Fig. 1. The standard deviation of a single measurement due to counting statistics is $\pm$ 3 c/m.

DISCUSSION

It is clear that the spread of the data is greater than would be expected from counting statistics only. This is probably due to two factors: (a) the phantoms used are not perfect imitations of people with respect to potassium distribution and gamma ray absorption and scattering, and (b) the steel room which shields the human spectrometer has a radon background which varies erratically from negligible to appreciable amounts.

Analysis of the data from the phantoms indicates that the effect of (a) is about $\pm$ 3 c/m. This plus counting statistics would account for much of the histogram about zero; the asymmetrical positive tail is most likely due to radon in the steel room.

These considerations allow an upper limit of about 2 mμ to be placed on possible Zn^{65} present in these 32 subjects

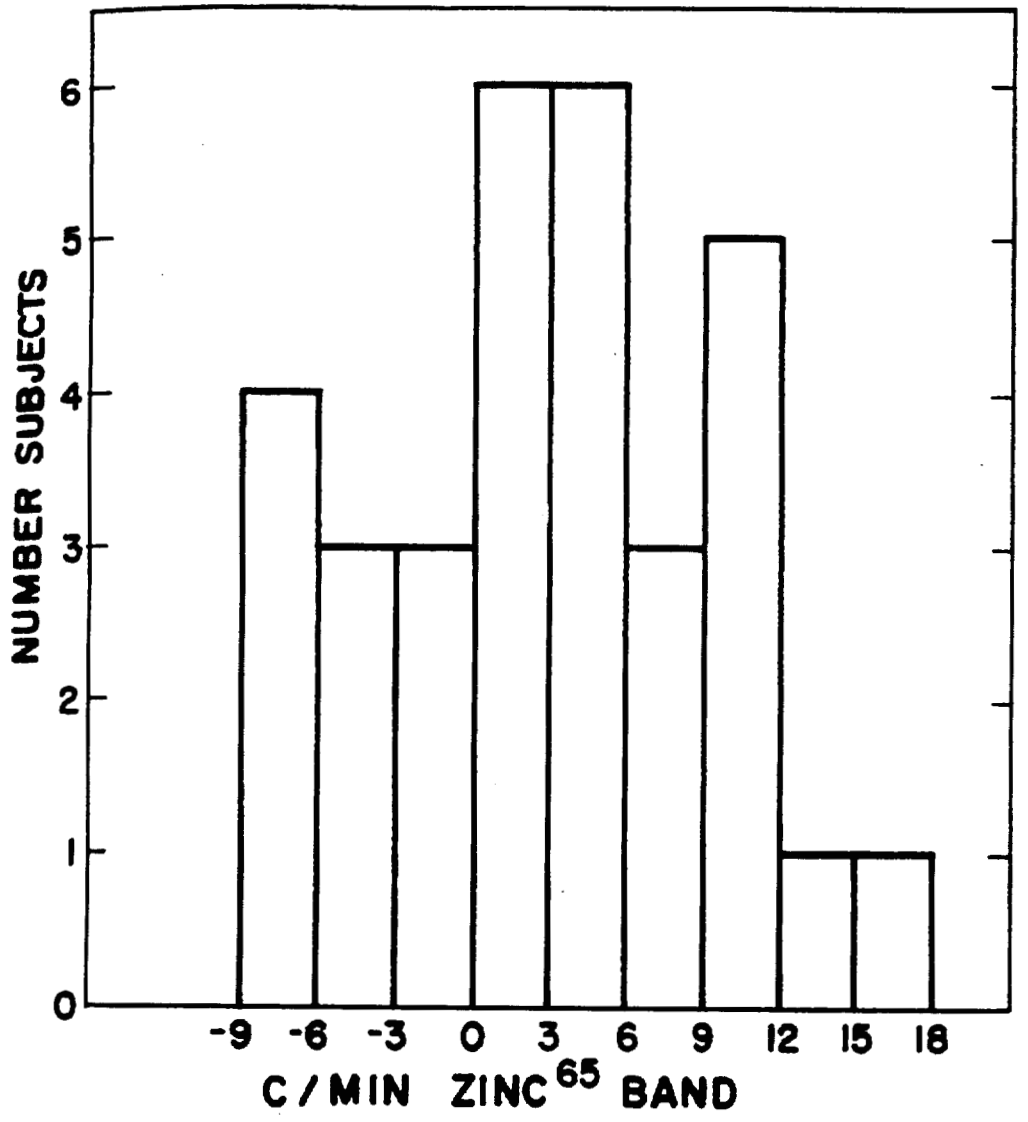

Fig. 1. Count rate in Zn^{65} band (channels 46-58), corrected for K^{40} (32 subjects).

(which may be compared with the average Cs^{137} content of these men, 10.7 mμc). Hence, we may conclude that even if Zn^{65} is present, the amount is trivial.

REFERENCES

(1) G. K. Murthy, A. S. Goldin, and J. E. Campbell, Science 130, 1255 (1959).

(2) M. A. Van Dilla, Science 131, 659 (1960).

(3) M. A. Van Dilla and M. J. Engelke, Science 131, 830 (1960).

Total Body Potassium in Man (B. E. Clinton, W. H. Langham, and E. C. Anderson)

INTRODUCTION

Whole body counting of the natural K^{40} activity of the whole body has provided an easy and rapid method of determining total body potassium. Body potassium is largely intracellular and is, therefore, related to the cellular mass. Its measurement affords an opportunity to correlate body potassium with gross body composition and with such physiological parameters as basal metabolic rate.

METHODS AND RESULTS

Total body potassium has been measured in some 4000 subjects by counting the natural K^{40} activity in the 4π liquid scintillation counter. The subjects were randomly selected in that they were all casual visitors to the Health Research Laboratory.

Analysis of previously published data has continued, and a paper has been submitted to the Journal of Gerontology on the variation of K^{40} with age. An extremely interesting correlation of total body potassium with basal metabolic rate has been noted (Fig. 1), both for 17 subjects on whom basal metabolism rates (BMR's) were determined prior to K^{40} counting and for 1590 subjects for whom BMR's were calculated from

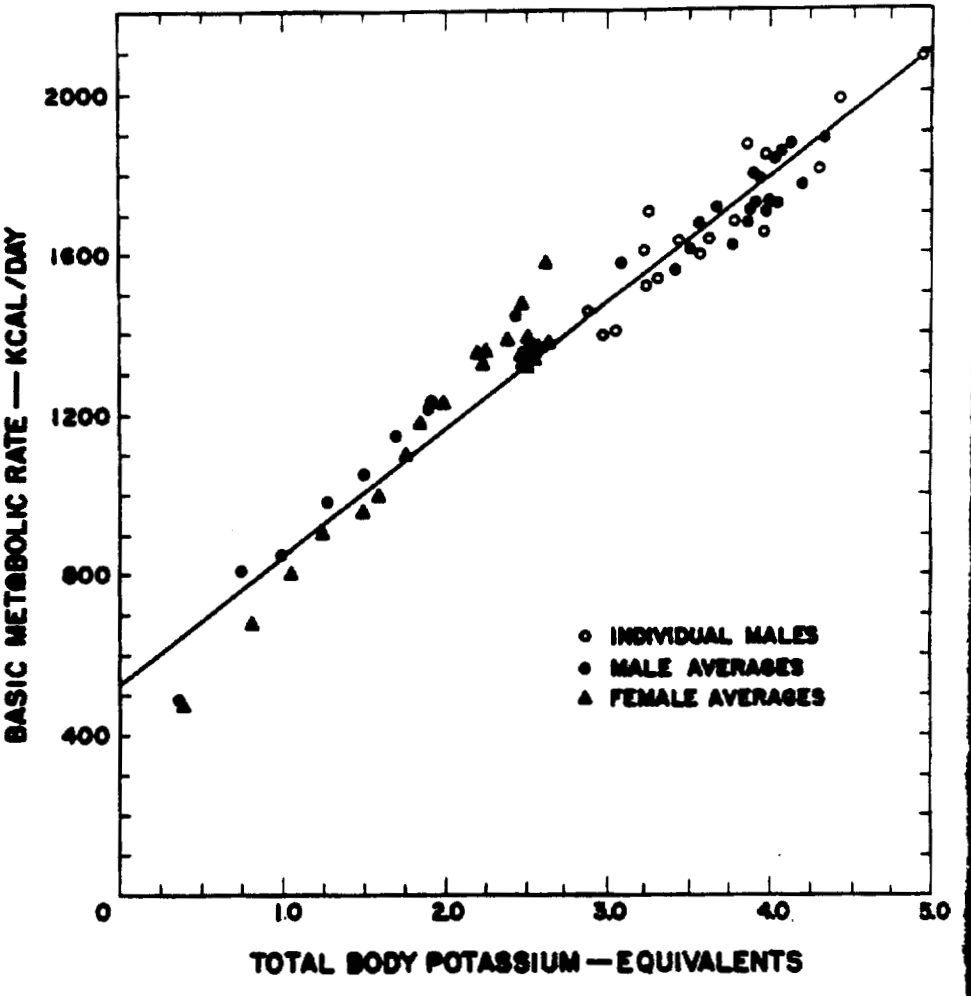

Fig. 1. Correlation between basal metabolic rate and total body potassium.

00131478.095

sex, age, and weight using the equations of Brody (1). A correlation coefficient of 0.976 is observed and an empirical equation

$$\text{BMR (kcal/day)} = 521 + 314\ K\ \text{(equivalents)}$$

has been derived from the data. The actual distribution of the points about this line suggests significant fine structure worthy of further investigation.

REFERENCE

(1) S. Brody, Bioenergetics and Growth, pp. 424-426; Eqs. 1-5 in Figs. 14.15, 14.16a, and 14.16b. Reinhold Publishing Corp., New York (1945).

Humco II: A New 4π Liquid Scintillation Counter (E. C. Anderson, R. L. Schuch, and V. N. Kerr)

INTRODUCTION

An improved liquid scintillation counter (Genco) was operated at the Second Conference on Peaceful Uses of Atomi Energy in Geneva during 1958 and proved to be a tremendous improvement over the original human counter (Humco I) in terms of energy resolution and useful energy range. This improvement was primarily a result of the improved efficien of collection of the scintillation light resulting from the use of the large (nominal 14-1/2 in.) photocathode diameter of the new K-1328 multiplier phototubes. Genco has been in routine operation at the U. S. Army Medical Center in Landstuhl, Germany, since the Conference, and accurate measurements of K^{40} and Cs^{137} in some 4000 German civilians have been completed in addition to other studies on thorotrast patients, foodstuffs, and some tracer investigations.

In view of the success of this detector, the replacemen of Humco I with an improved version was decided upon in 195 The new counter was to embody the following basic improvemen

(a) Increased efficiency of collection of the scintil lation light through the use of 24 large multiplier photo- tubes.

(b) Increased counting efficiency and energy discrimination through the increase of liquid scintillator thickness from 6 to 12 in.

(c) Increased data processing efficiency through the use of automatic card punching directly from the 6 energy channels with no manual transcription of data.

(d) Increased safety and simplicity through the use of a nonvolatile scintillation solvent.

METHODS AND RESULTS

The new counter is shown during assembly, in Fig. 1. The tank has a capacity of 450 gallons of scintillator and is hexagonal in cross section. Four 14-1/2 in. diameter multiplier phototubes are mounted on each flat face, giving a cathode area amounting to 22 per cent of the total wall area of the counter. The subject well has the same dimensions as in Humco I (i.e., 18 in. in diameter by 72 in. long). The counter is shielded by a steel (naval armor plate) room with 7 in. thick walls. Access to the room for counter servicing is through a large door; subjects and samples enter the counter by a trough and sling arrangement, as in Humco I. The transistorized electronics and card punch* are shown in Fig. 2.

* We are grateful to J. Gallagher, J. Gilland, and R. D. Hiebert of the Electronics Group (P-1) for the design and construction of this apparatus.

00131478.099

Fig. 2. Transistorized electronics for Humec II.

The counter was successfully operated in the fall of 1959, and some results were reported at the Vanderbilt Symposium (1). A slight warping of the tank resulted in cracking of the glass face-plates of several of the multiplier phototubes, and the counter was disassembled for repair of this difficulty. During the repair operation, th leakage of a Co^{60} irradiation source elsewhere in the build- ing resulted in low level contamination of the shield and counter. Decontamination operations with grease solvents, rust remover, complexing agents, hydrochloric acid, and finally abrasion of the surface with disc sanders and shot- blasting required several months. During this period, a ne method of tube mounting was designed and tested, to compen- sate for the warped tank.

The counter is now (July 1960) reassembled and tests o new scintillation solvents are continuing. Routine opera- tion is expected in the fall.

Toluene is still the best solvent in terms of maximum output pulse height. The performance of Humco II with a to terphenyl-POPOP filling is shown in Fig. 3. Resolution is 35 to 40 per cent full-width at half-height for K^{40}, which adequate to determine simultaneously Zn^{65} and K^{40}, for ex- ample. $Zinc^{65}$ has been identified with Humco II in one sub ject on the basis of the measured pulse height spectrum.

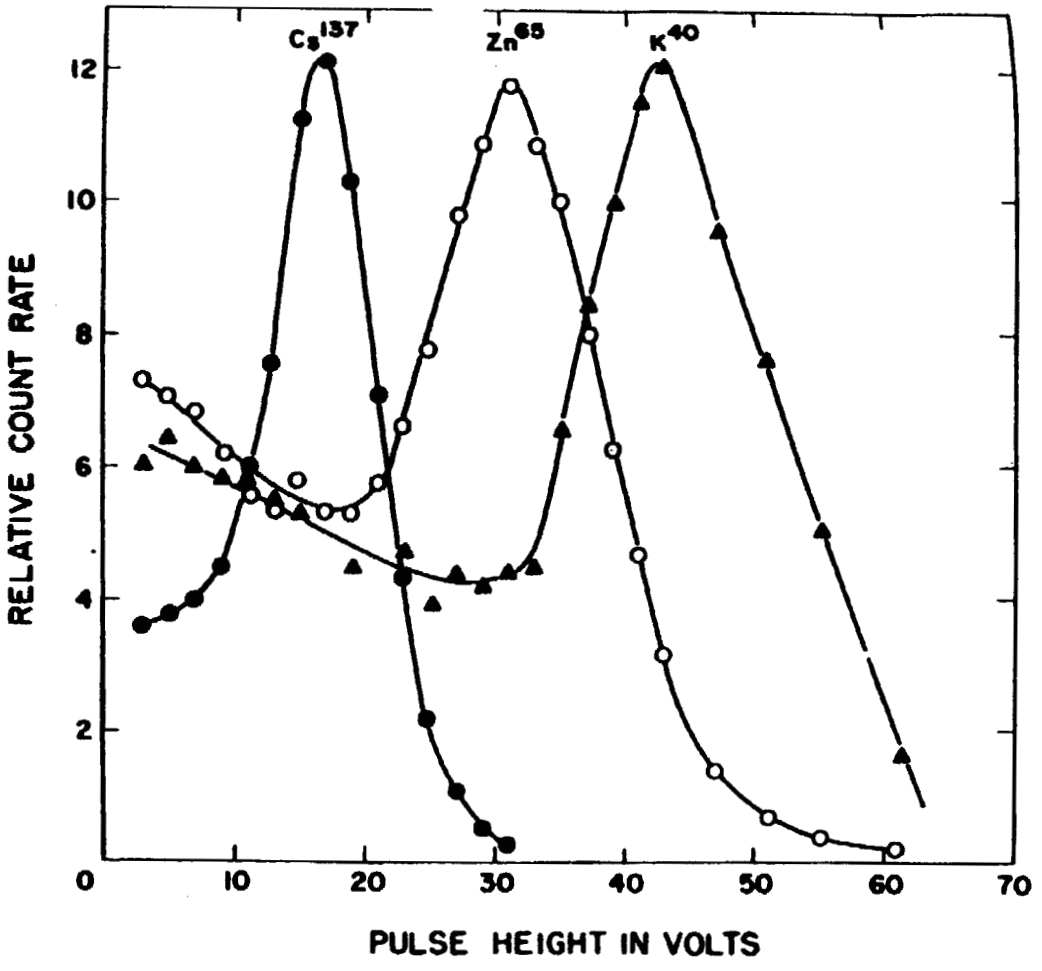

Fig. 3. Energy spectra from Humco II.

Of the other solvents so far investigated, a commercial paint solvent TS-28* appears to be the most promising. Its volatility is similar to that of kerosene, so that it does not constitute a fire hazard. The pulse height ranges from 80 to 90 per cent of that of toluene solutions, and optical transmission for a 10 cm light path is 97 to 100 per cent relative to toluene. Simple purification on an Al_2O_3 adsorption column is adequate. This solvent will probably be used in Humco II instead of triethylbenzene, which was used in Genco. The latter is much more expensive and requires distillation from sodium for purification.

REFERENCE

(1) E. C. Anderson, R. L. Schuch, V. N. Kerr, and M. A. Van Dilla, Humco II: A New 4π Liquid Scintillation Counter presented at the Vanderbilt University Symposium on Radioactivity in Man (April 18-19, 1960), Nashville, Tennessee. To be published in the Proceedings.

*TS-28, available from the Shell Oil Company, Martinez, California.

The Los Alamos Small-Animal Counter III (LASAC III)

(R. L. Schuch)

INTRODUCTION

The proved utility and increasing demand for whole-body small-animal counters prompted the development and construction of an improved liquid scintillation detector. A well-type detector (LASAC III, Fig. 1) was designed to include maximum photomultiplier cathode area, to improve tube mounting techniques, and to keep the over-all detector as small as possible without loss of efficiency or sensitivity. This system permits low-level measurements of a wide range of gamma-emitting isotopes with counting efficiencies to 60 per cent. The lower limit of energy measurement is 52 kev (Compton energy), which permits bremsstrahlung counting. Further improvements utilizing standard transistorized electronics and selected low background shielding have been incorporated.

RESULTS AND DISCUSSION

The detector tank was constructed similar to prototype LASAC II (1) except that the photomultipliers are fitted with windowless tube holders (Fig. 2) and the tube faces are in direct contact with the scintillator. This unit consists of a tank with an ellipsoidal head 12-1/4 in. in diameter and

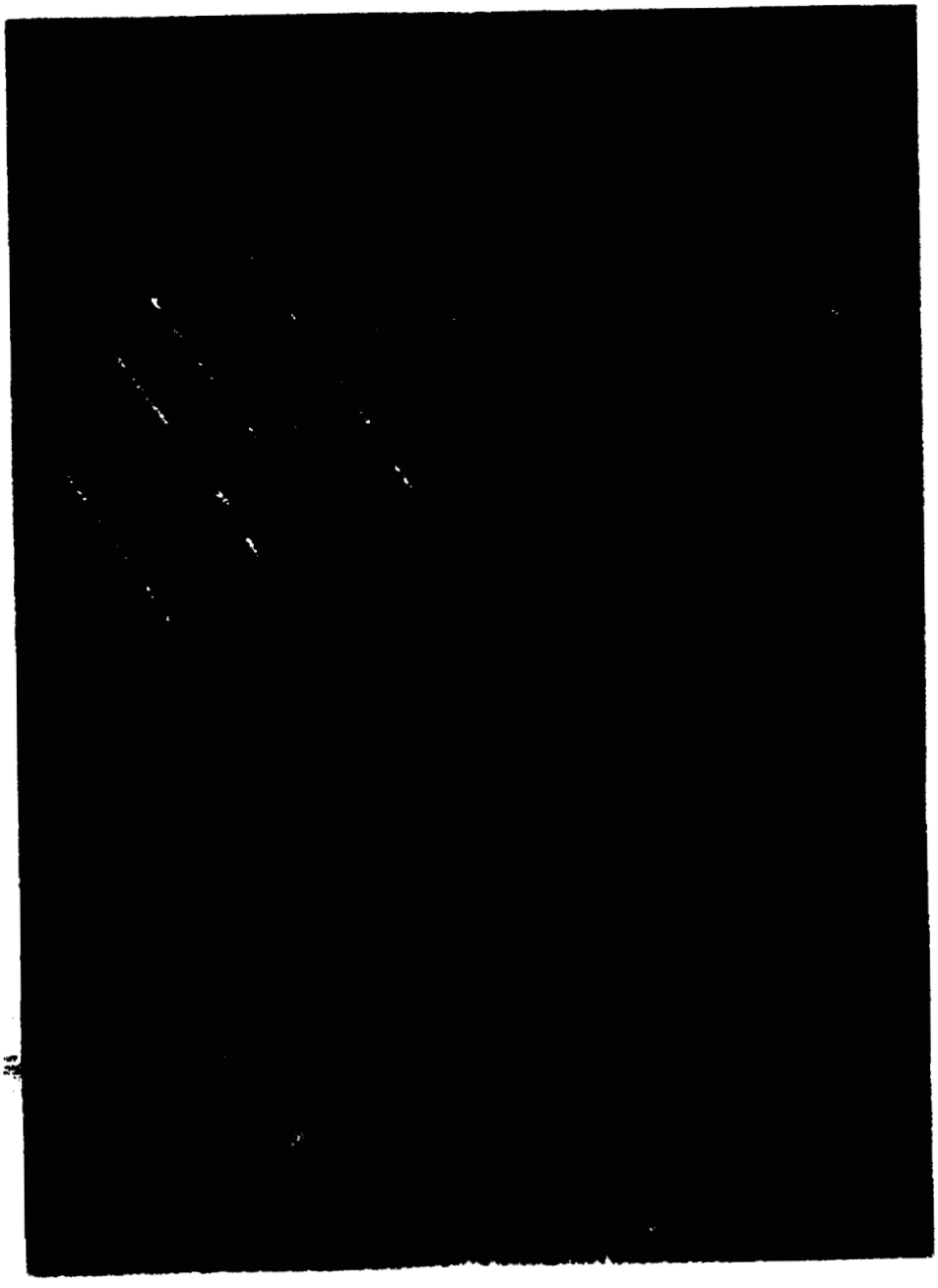

00131478.105

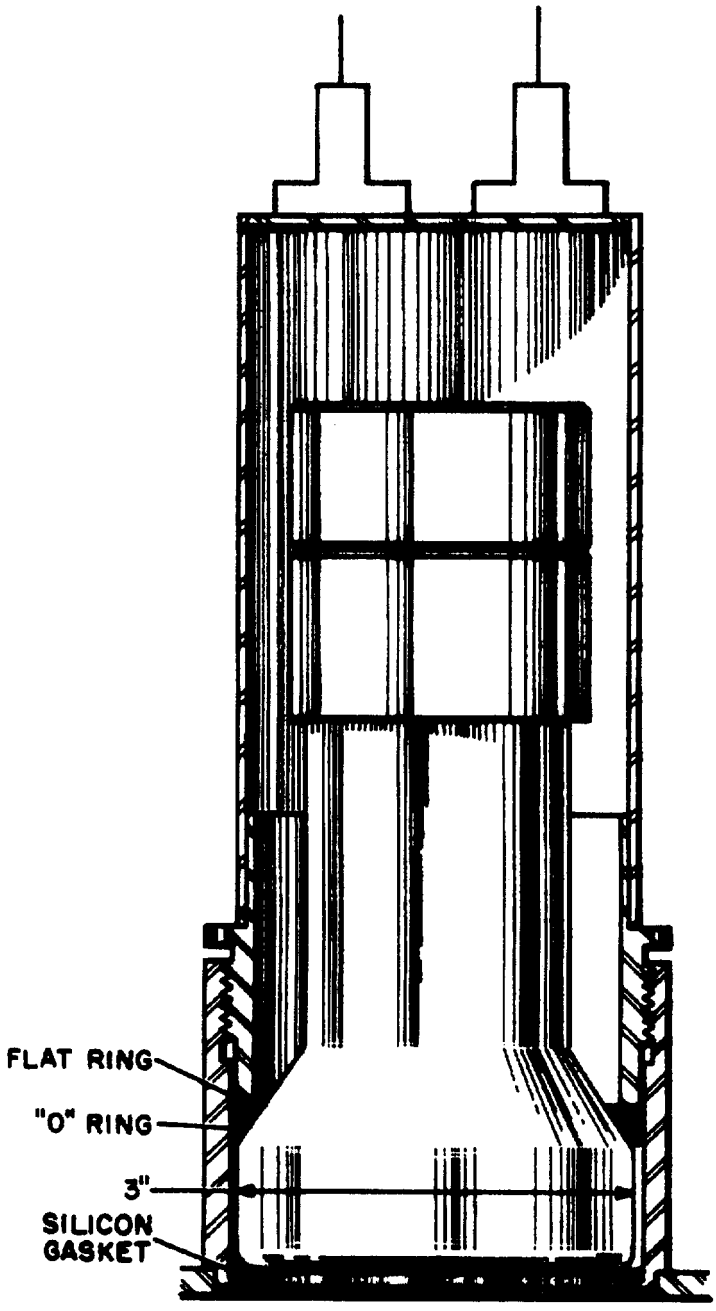

Fig. 2. Photomultiplier tube holder.

12 in. long with 7, 3-in. diameter DuMont photomultipliers fitted into a flat plate on one end. A central counting well 4-1/4 in. in diameter is surrounded by an annular ring of scintillator solution 4 in. thick, containing 4 g/l terphenyl plus 0.05 g/l POPOP in toluene. The inside surface of the detector is painted with a TiO_2 pigmented epoxy resin, which serves as a reflective coating.

Background Shielding

The bulk of the background shielding was fabricated from selected 7-1/4 in. armor plate forming an inner cubical measuring 29 in. long, 18 in. high, and 18 in. wide. The door of the shield is constructed of a stainless steel shell filled with a low background lead and fitted with a sliding lead plug to permit access to the counter well for routine operation (Fig. 3). As the unit was not to be portable and floor loading was no problem, the shield was made large enough to accommodate other detectors, should the need arise. Total weight of the shield is approximately 3 tons.

Electronics

Photomultiplier tubes are individually balanced for pulse height output and their signals are connected in parall The output of the photomultipliers is fed into standard

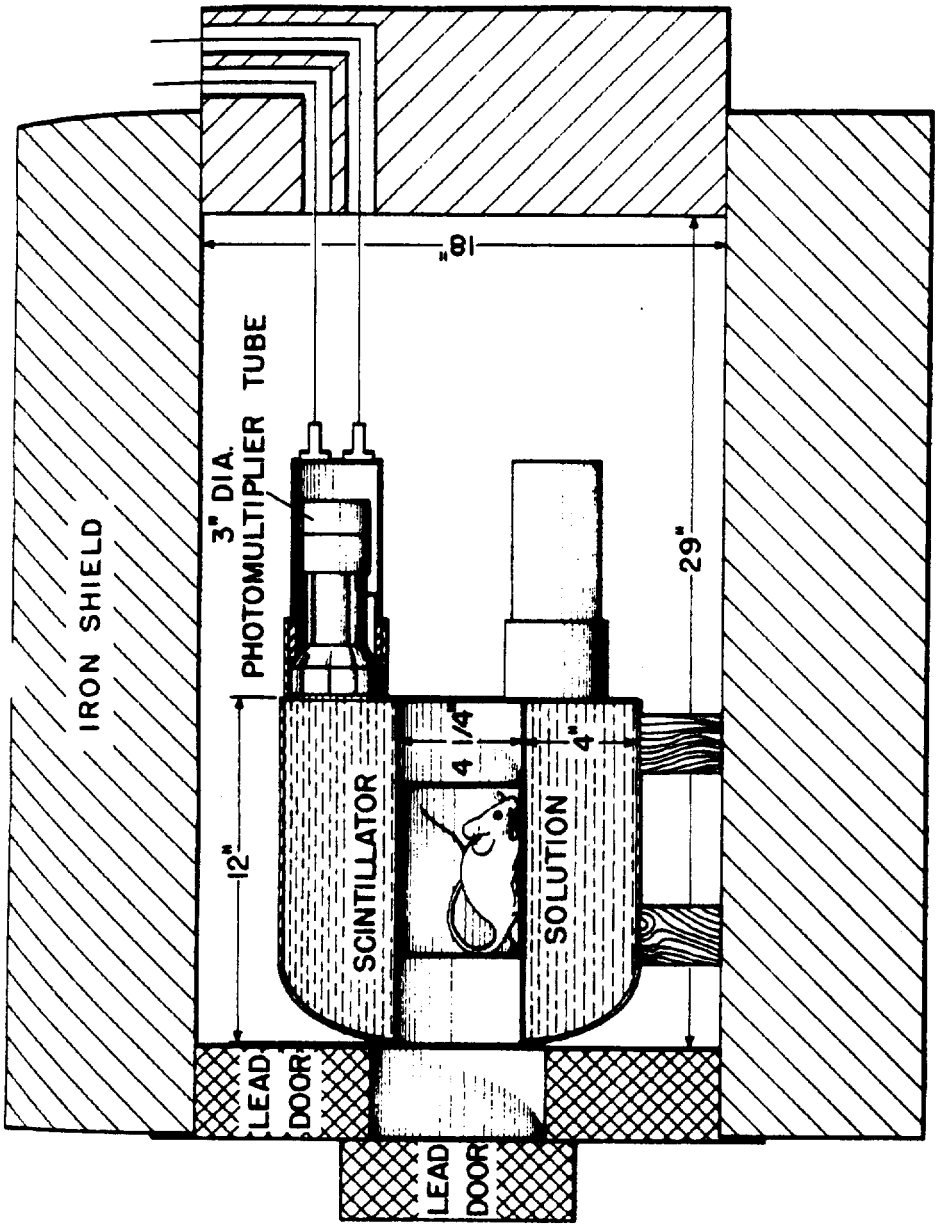

Fig. 3. Cross section of LASAC III in shield.

transistorized electronics circuitry consisting of preamplifier, five-step amplifier, and a single-channel analyzer of the threshold plus slit type. The information is read directly from a scaler controlled through a preset timer (Fig. 4).

Operational Results

Data obtained with a Cs^{137} source were analogous to those of prototype LASAC II. The signal-to-noise ratio was 10.1, and tube noise interference appeared at 52 kev (Compton edge) or 150 kev E_γ. Optimum operating conditions for a given isotope are selected by changing the amplifier gain. The slit width range is calibrated in gamma energy. A wide slit (700 units) was used because background remained low regardless of the operating level, as shown in Table 1.

REFERENCE

(1) Biological and Medical Research Group (H-4) of the Health Division - Semiannual Report July through December 1959, Los Alamos Scientific Laboratory Report LAMS-2445 (February 1960).

Fig. 4. Electronics and shield for LASAC III.

TABLE 1. SLIT WIDTH RANGE AS A FUNCTION OF AMPLIFIER GAIN

Gain	Slit Width Range (kev)	Full Range of Analyzer (Mev)	Background (c/s)
1/16	400-3200	4.0	42
1/8	200-1600	2.0	50
1/4	100-800	1.0	51
1/2	50-400	0.5	55
1	25-200	0.25	56

Absorption of Radioisotopes through the Skin: Feasibility Study (M. A. Van Dilla and M. W. Rowe)

INTRODUCTION

One of the routes of entry of radioisotopes into man is penetration through the skin. Very little is known about this subject. Since it seemed possible to investigate the matter with low level whole body counters, we carried out a feasibility study with the human spectrometer.

METHODS AND RESULTS

The main difficulty in carrying out a skin absorption experiment is that fractional absorption is likely to be small. Hence, the radioactivity on the test area (hand or arm, probably) may "swamp" the radioactivity absorbed through the skin and distributed through the body. This means that the test area on the skin should be heavily shielded from the crystal, and any other means of improving the body test area ratio should be used.

In our experiments, we built a small lead cave adjacent to the arm of the lawn chair in which subjects recline during a measurement. The lead cave was so placed that a subject might thrust his hand and forearm into it while in the lawn chair. The opening pointed horizontally and toward the rear

of the steel room (away from the crystal). The lead thickness was 2 in., except for the two sides closest to the crystal which were 4 in. thick.

In the first experiment we measured background, then ran with about 100 μc Cs^{137} (0.66 Mev gamma rays) in the cave, and lastly ran with about 0.1 μc Cs^{137} in the seat of the lawn chair. Cesium^{137} was chosen because of its convenience and because the absorption coefficient of lead is large at 0.66 Mev and rises rapidly at lower energies; thus, softer gamma ray emitters (as Sr^{85}, I^{131}, Cr^{51}, etc.) would be easier to shield. The spectra obtained in the Cs^{137} experiment are shown in Fig. 1. Although there is a large backscatter peak due to those gamma rays which escape through the cave opening, the photopeak region (channels 55-70) is only slightly above background. The count rate due to 0.1 μc Cs^{137} in the lawn chair is much larger than the interference from the 100 μc in the arm cave. These data are summarized in Table 1.

In the second experiment, we did a repeat using Co^{60}. This case is less favorable, since the absorption coefficient of lead is close to its minimum value for Co^{60} gamma rays (1.25 Mev average), so that shielding is less effective. However, even so, the results were very encouraging, as the data in Table 1 show.

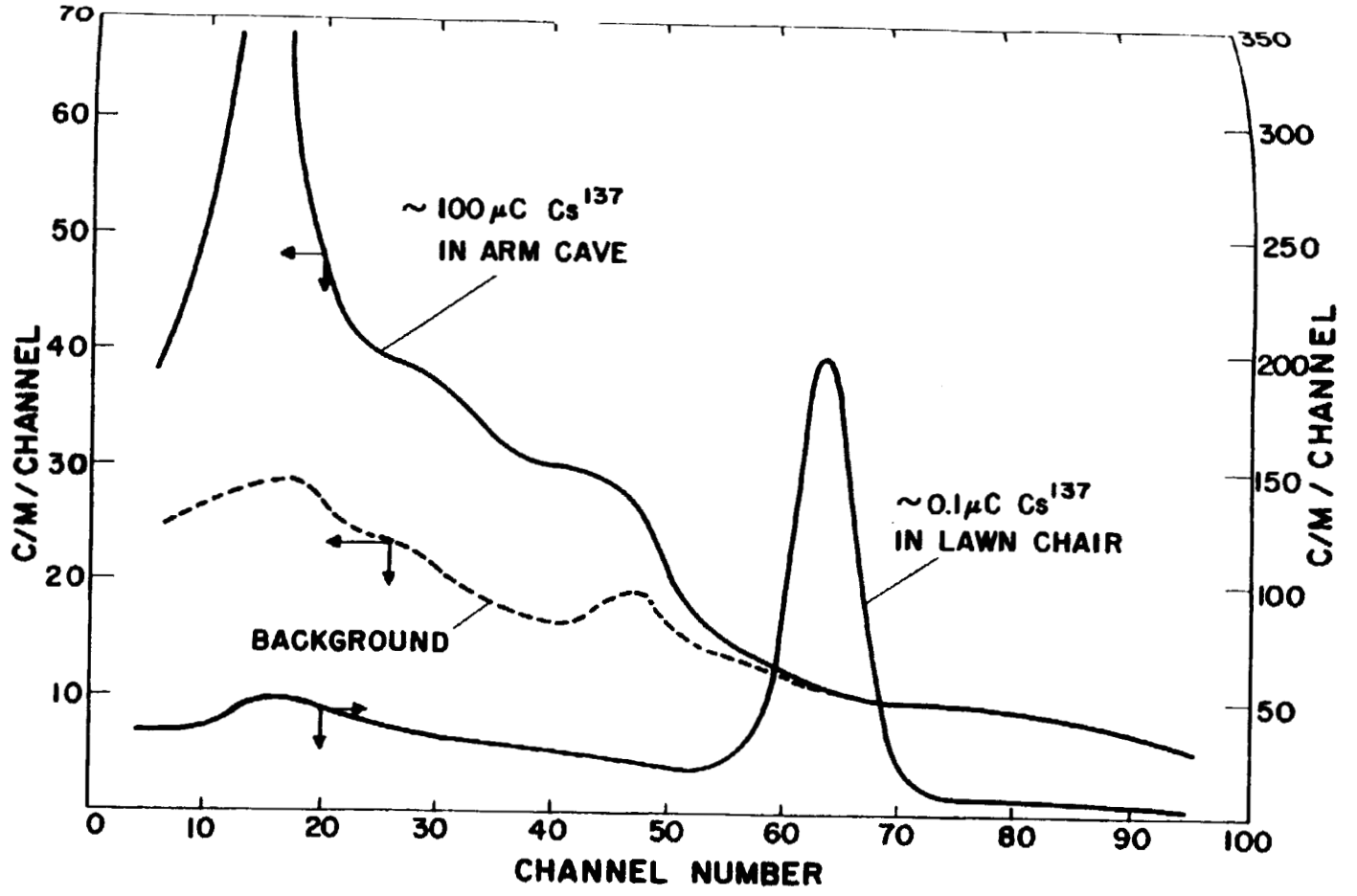

Fig. 1. Absorption of radioisotopes through the skin: feasibility study with Cs^{137}

TABLE 1. SKIN ABSORPTION OF RADIOACTIVITY FEASIBILITY STUDY

Source	Gamma Ray Energy (Mev)	Position	Net Count Rate in Photopeak, in c/s
~100 μc Cs^{137}	0.66	Arm cave	11
~0.1 μc Cs^{137}		Lawn chair	1337
Background			179
~10 μc Co^{60}	1.17; 1.33	Arm cave	91
~0.1 μc Co^{60}		Lawn chair	1265
Background			245

DISCUSSION

In view of the results shown in Table 1, it seemed desirable to speculate on possible experimental design for a skin absorption study on people. The result is shown in Table 2; using 10 μc on the hand or forearm and a 30-minute counting time, an absorption through the skin of as little as 0.02 per cent can be measured with a 10 to 16 per cent counting error.

We may conclude that the detection of very small amounts of radioactivity absorbed through the skin is quite feasible using the method described above. It is important, however,

TABLE 2. POSSIBLE EXPERIMENTAL DESIGN FOR SKIN ABSORPTION

Amount on Hand or Arm (μc)	Position		Counting Time (minutes)	Counting Error, if Absorbed	
	Subject	Arm		0.1%	0.02%
10	Lawn chair	Lead arm cave	30	3-4%	10-16%

that care be taken to avoid slight contamination of the equipment, because the skin test area will contain a large amount of radioactivity relative to what is being detected. With good technique, this can be readily accomplished. We plan to enlist the aid of medical or biological people elsewhere in the Group to continue this project.

Radiation Dose Rates above the Atmosphere (M. A. Van Dilla, M. W. Rowe, R. D. Hiebert, and J. A. Sayeg)

INTRODUCTION

The discovery, in 1958, by Van Allen and his collaborators of large zones of high energy charged particles trapped in the earth's magnetic field has stimulated extensive geophysical investigation and provoked a good deal of thought as to potential hazards to man in space. In the spring of 1959, the Air Force Special Weapons Center at Kirtland Air Force Base requested the cooperation of H-4 in an effort to measure dose rates in the Van Allen belts. As a result, we designed and built 5 tissue-equivalent ion chambers which were described in the previous semiannual report (1). These are slated for Atlas and 609-A flights for the summer and fall of 1960. Twelve additional units were made for AFSWC under contract to the Eberline Instrument Company for other flights.

METHODS AND RESULTS

The LASL space ion chambers now operational are made of Lucite and have been calibrated with Co^{60} gamma rays. Lucite was chosen originally because it is a reasonable approximation to soft tissue, it is readily available, and fairly easy

to fabricate. Since time schedules were short, these considerations were overriding. Calibrations with Co^{60} gamma rays are easy to make quickly and accurately at this Laboratory, so again this was the method of choice. Now that these instruments are in the hands of AFSWC for dose rate measurements in space, improvements and refinements are possible. These involve tissue equivalence and neutron-proton calibration.

DISCUSSION

It was pointed out to us by John Rose of the Argonne National Laboratory that the tissue-equivalent plastics developed by Shonka et al. have improved to the point where they compare with or surpass Lucite in ease of fabrication and availability. As a result of discussions with Dr. Shonka and our colleagues at AFSWC, it was agreed that Shonka would make a prototype front end of tissue-equivalent plastic and LASL would redesign and build the rest of the unit (electrometer circuit, transistorized amplifier, and power supply). The tissue-equivalent plastic and gas filling are equivalent to muscle for X rays, gamma rays, and neutrons, and so represent an improvement over Lucite. In addition, an effort would be made to minimize the amount of metal near the sensitive volume because of the possibility of radioactivity

produced by spallation reactions. At the present writing, the tissue-equivalent plastic front end has just arrived from Dr. Shonka and design of the rest of the instrument is under way.

In addition to this redesign using tissue-equivalent plastic, the calibration and response of the Lucite ion chambers are being extended to include neutrons and high energy protons. When the hard protons of the inner belt strike the space vehicle (and the ion chamber itself), both neutrons and radioactive spallation products can be produced. Arrangements have been made by AFSWC with Dr. Tobias of the University of California at Berkeley to expose one of the Lucite chambers (Eberline Serial No. 3) to high energy protons in one of their big accelerators. In the meantime, the response of this chamber to both Co^{60} gamma rays and neutrons has been measured at LASL. The Co^{60} calibration covered the range 0.01 to 100 r/hr and is shown in Fig. 1. The neutron measurements, made with 2, 8, and 20 Mev monoenergetic neutron beams at the vertical Van de Graaff generator, are shown in Table 1. These data show that the neutron response of the Lucite chamber at the two higher energies is quite good, while at the lowest energy it falls off considerably. This latter effect may be due to the fact that the dimensions of the sensitive volume of the ion chamber (about 3 in. acr

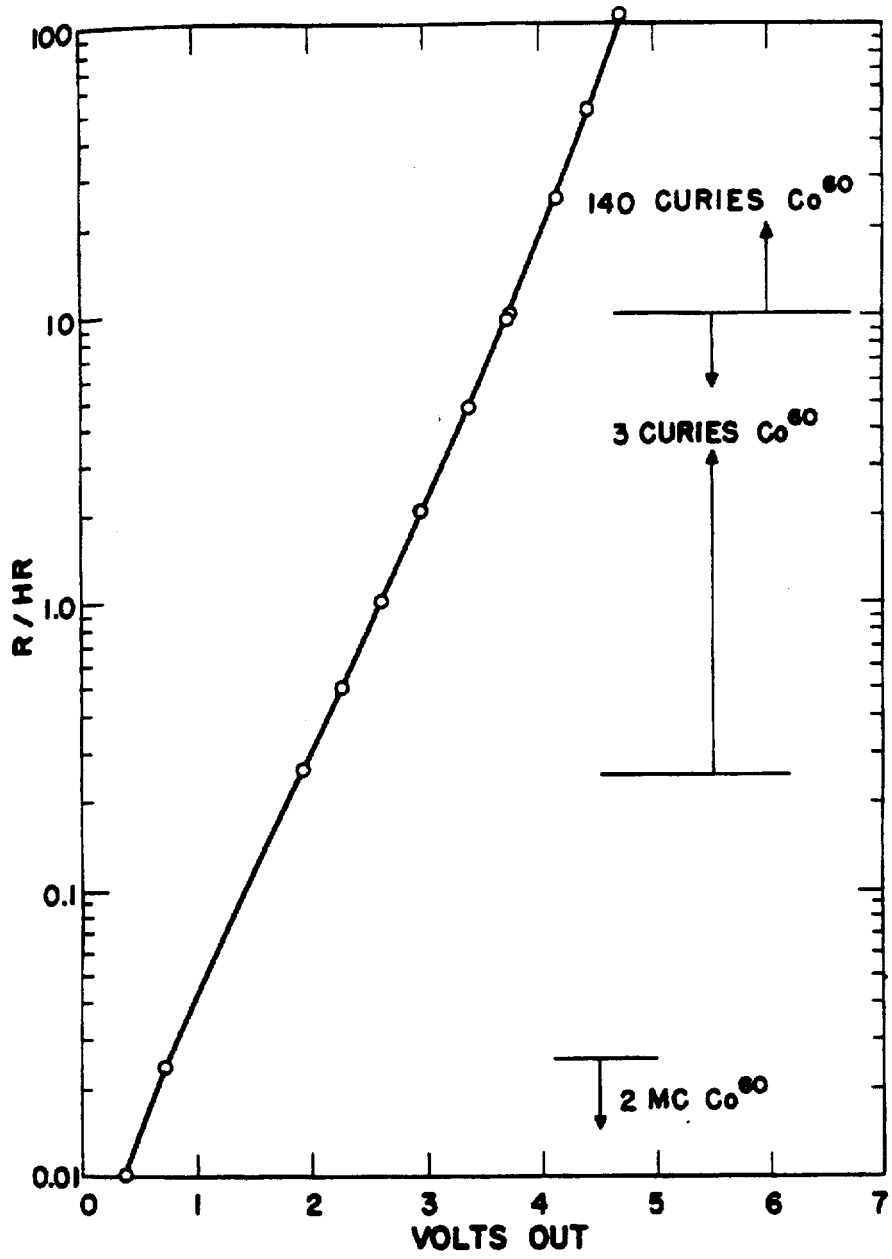

Fig. 1. LASL space ion chamber (Eberline Serial No. 3), W-128 Co^{60} facility, 8200 ohms load.

TABLE 1. RESPONSE OF LUCITE SPACE ION CHAMBER TO MONO-ENERGETIC NEUTRONS

Neutron Energy (Mev)	Neutron Dose Rate* (rads/hr)	Lucite Ion Chamber Response (Eberline Serial No. 3) (rads/hr)
2	2.10	0.7
8	1.30	1.2
20	0.83	1.2

*Calculated from the neutron flux and first collision theory.

are similar to the recoil proton range in air (about 2.75 in. for 2 Mev protons), while the range in air of 8 Mev protons is 30.6 in. (2). This error will be eliminated in the chamber now under development because both walls and gas filling will be tissue-equivalent.

REFERENCES

(1) Biological and Medical Research Group (H-4) of the Health Division - Semiannual Report July through December 1959, Los Alamos Scientific Laboratory Report LAMS-2445 (February 1960).

(2) R. D. Evans, The Atomic Nucleus, p. 651 (1955). McGraw-Hill Book Company, Inc., New York.

Moonspec: Measurement of Radioactivity of the Lunar Surface

(M. A. Van Dilla and E. C. Anderson)

INTRODUCTION

The feasibility study outlined in the previous semiannual report (1) has now developed into a firm project, the objective of which is to provide information on the composition and history of the moon and its surface radiation. This will be done by detection of the gamma radiation from the natural radioactivity (K^{40} mainly) of the lunar surface.

METHODS AND RESULTS

The project has moved forward considerably and has changed, in some respects, since the previous semiannual report. The arrangement with the National Aeronautics and Space Administration through its contractor, the Jet Propulsion Laboratory of the California Institute of Technology at Pasadena has become firm; we are responsible for the detector package, Radiation Instruments and Development Laboratories of Chicago has a contract for the 32-channel analyzer and most of the pulse circuitry, and the Jet Propulsion Laboratory handles matters concerning the vehicle, telemetering, thermal control, mechanical design, etc. Professor J. R. Arnold of the University of California at La Jolla (who, with

Professor H. C. Urey, conceived the original ideas for the experiment) is making theoretical predictions of the lunar radiation levels and will assist in data interpretation.

The gamma ray spectrometer has been scheduled on flights 3, 4, and 5 of the so-called "Ranger" series of rockets to be launched in 1962. The vehicles on which the spectrometer will fly are designed for lunar impact; it is during the last 10 minutes before impact that the spectrometer will be close enough to the moon to respond to its gamma radiation. During this short time, the contents of the analyzer's memory will be periodically telemetered back to earth; at impact, the vehicle will be wrecked.*

The design of the detector package has also become firmer in the past few months. It will consist of a phoswich, a CBS CL-1003 photomultiplier, and a fast pulse rejection circuit. The phoswich will be a cylindrical CsI (Tl) crystal, 2-3/4 x 2-3/4 in., completely surrounded by plastic scintillator of 1/8 in. wall thickness. The CsI is the gamma ray detector, while the plastic acts as a guard counter (or anticoincidence shield) to reject pulses due to fast charged particles (cosmic rays). The detector package will be situa

*That is, all but the seismograph; this separates at about 12 miles from the moon and is eased down by a retro-rocket.

on the end of a 3 to 4 foot boom to minimize the effect of photons generated by a cosmic ray bombardment of the vehicle; this decision was based on the results of the Russian rocket Lunik II.

DISCUSSION

If the lunar surface radioactivity resembles the chondritic meteorites and has a minimum value, K^{40} will be the most hopeful natural radioactive species to look for. Our estimates of the K^{40} signal and the background in the 1.36 to 1.56 Mev region are as shown in Table 1.

TABLE 1. ESTIMATES OF THE RADIATION FROM THE LUNAR SURFACE

K^{40} signal (average, final 10 minutes)	3 c/m
Background (cosmic rays, edge-clipping)	45
Background (secondary photons from vehicle, inside)	180
Background (secondary photons from vehicle, 3 foot boom)	14
Background (lunar surface, 500 km altitude)	2.7

The first of the contributions to background will be eliminated by use of the phoswich, and since we will have the advantage of a boom the total estimated background will be 14 + 2.7 = 16.7 c/m. If the background is well determined during the long coast toward the moon, the standard deviation of the K^{40} signal will be

$$\sigma = \sqrt{\frac{3 + 16.7}{10}} = 1.4$$

for a 10-minute counting period. Thus, if the natural potassium level of the lunar surface is chondritic, the chance of detecting its presence seems marginal. However, if the lunar surface resembles the earth's surface as a consequence of segregation following extensive melting, then the potassium concentration will be higher by a factor of about 30 and be very obvious (as will be the uranium and thorium series also). Some current theories of lunar composition and history predict either chondritic or terrestrial composition, so the experiment should provide important evidence.

REFERENCE

(1) Biological and Medical Research Group (H-4) of the Health Division - Semiannual Report July through December 1959. Los Alamos Scientific Laboratory Report LAMS-2445 (February 1960).

CHAPTER 4

ORGANIC CHEMISTRY SECTION

World-Wide Biospheric Carbon^{14} (F. N. Hayes, V. N. Kerr, E. Hansbury, and D. L. Williams)

INTRODUCTION

Much information of direct physiological and geochemical benefit and also providing starting data for genetic extrapolations into the future can come from careful assays of the distribution of the massive quantity of C^{14} injected into the atmosphere from 1954 through 1958 by nuclear weapons testing. Botanical essential oils and zoological lipids, widely distributed in time and geography, and amenable to liquid scintillation counting, are being assayed and results are being analyzed for their tracer implications in the biospheric appearance, mixing, and disappearance of carbon.

METHODS AND RESULTS

One publication on some of the methods of this program and another on results with lemongrass oil have appeared in print since the last report. During this period, efforts have been almost exclusively directed toward chemical processing, and there are no corrected counting results to report. The following inventory of samples now ready to count has been prepared: 36 from turpentine, 19 from citrus oils, 8 from eucalyptus oil, and 8 from lemongrass oil. Carbon dioxide has been quantitatively derived from these samples and has been sent to Dr. Wallace Broecker at the Lamont Geological Observatory for C^{13} analysis to allow us to correct the counting results of these samples for C^{14} fractionation.

In order to determine the feasibility of measuring C^{14} uptake in humans, preliminary studies of methods of isolation and purification of cholesterol have been made. A commercial sample of cholesterol has been purified and counted. Choles-

Chemical Systems for Liquid Scintillation Dosimetry (D. L. Williams and F. N. Hayes)

INTRODUCTION

A system of "paired" liquid scintillators has been developed (1) for making simultaneous gamma ray and fast neutron dose rate measurements in mixed radiation fields, such as those arising from the prototype Kiwi series of rocket propulsion nuclear power units. This system is dependent upon electrons, and response to fast neutrons is dependent upon hydrogen atoms. Hexafluorobenzene, which is hydrogen-free, is used as solvent in the scintillator which is sensitive only to gamma rays. A solution of a suitable solute in p-xylene has been employed as the hydrogen-rich liquid scintillator which responds to both gamma rays and fast neutrons. Thus, with the essential calibrations, the fast neutron rate is obtained as a calculated difference value.

As used in photodetectors for measuring radiation rates, the neutron response of the p-xylene system is only 0.22 time the gamma response. With the precision of these measurements considered to be ±5 per cent, it follows that the ratio 0.22/0.05 = 4.4 is the maximum ratio of gamma-to-fast neutron energy deposition rates at which a significant neutron measurement may be made. Since, in actual practice, situations have

been encountered in which the gamma-to-neutron ratio was as high as 10 to 1, it was considered highly desirable to increase the response of the hydrocarbon system to fast neutrons, if possible.

METHODS AND RESULTS

A solution of 9,10-diphenylanthracene solute in mineral oil (2 g/l) gives a scintillation response to electrons measured as a relative current (2) which is about 23 per cent that shown by a similar solution in p-xylene. Mineral oil has 51.5 per cent more hydrogen than p-xylene, on a weight basis. Therefore, despite the lower scintillation efficiency of its solution, mineral oil should show about 50 per cent more response to fast neutrons than p-xylene, relative to their respective gamma sensitivities. Calibration of the paired liquid scintillators, using a Co^{60} gamma source and the Los Alamos Godiva II reactor for a neutron source, showed that the relative fast neutron-to-gamma response of the mineral oil scintillator is 0.22, no different than that of the p-xylene system. This suggests that the 50 per cent greater hydrogen density of mineral oil relative to p-xylene is counterbalanced by a 0.67 fold less efficient sensitivity to recoil protons produced from the neutron spectrum of the Godiva source.

Another approach to the problem of increasing the fast neutron response of the hydrocarbon liquid scintillator was made by the inclusion of a soluble gadolinium salt. The fast neutron capture cross section of gadolinium is approximately 10 barns. In a solution of 9,10-diphenylanthracene in p-xylene (3 g/l) was dissolved 1 per cent by weight of gadolinium as the 2-ethylhexanoate salt. The fast neutron response of the gadolinium-loaded solution was compared with that of the untreated p-xylene solution at various neutron energy levels. Each solution was exposed to monoenergetic neutrons from the Los Alamos Van de Graaff accelerator. The response data for the gadolinium solution were corrected for quenching due to the gadolinium salt by means of relative current measurements (2). The results, which are shown graphically in Fig. 1, show an increase in response of about 22 to 28 per cent in the 1 to 2 Mev region, with lesser increases at the higher energy levels.

DISCUSSION

In comparison to the standard 9,10-diphenylanthracene/p-xylene liquid scintillator, neither mineral oil/9,10-diphenylanthracene nor the gadolinium-loaded p-xylene solution show an increase in fast neutron sensitivity which is considered of sufficient consequence to warrant further study.

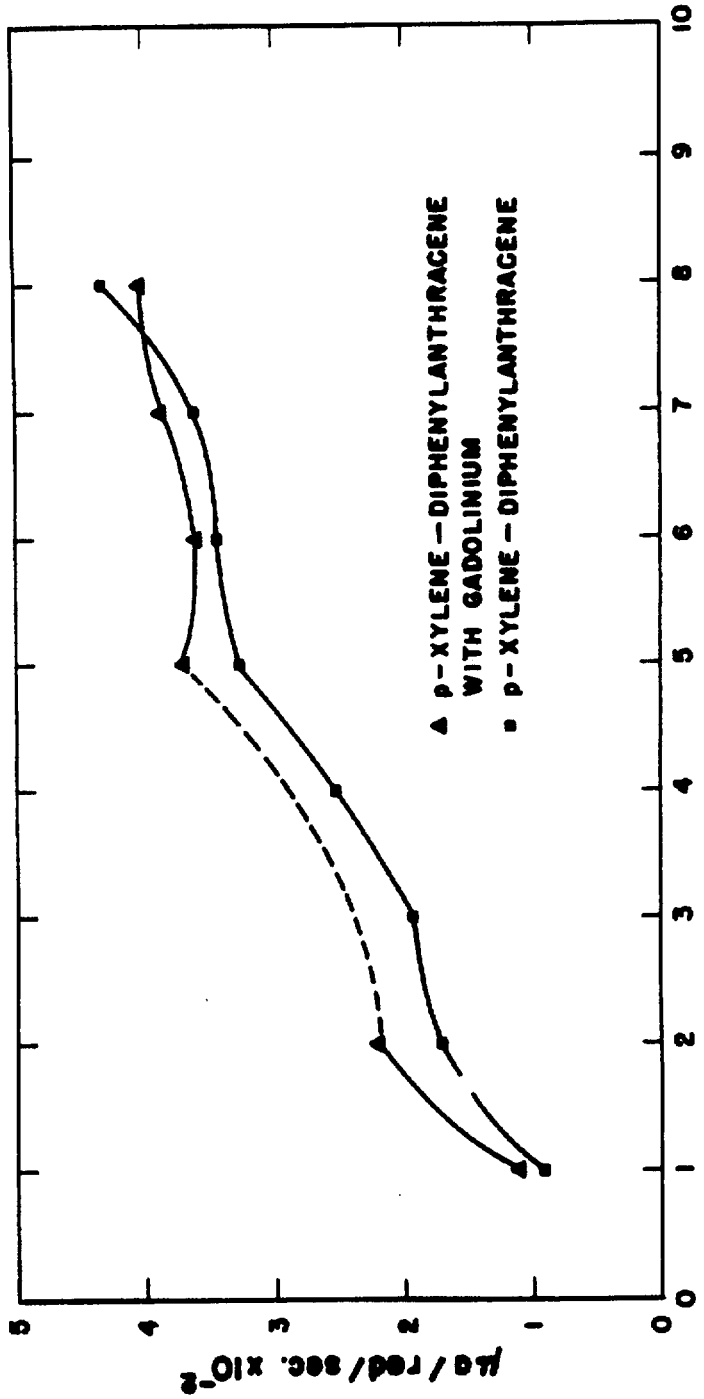

Fig. 1. Effect of 1 per cent gadolinium on the fast neutron response of p-xylene/diphenylanthracene liquid scintillator.

00131478.131

REFERENCES

(1) D. L. Williams, F. N. Hayes, R. L. Schuch, R. L. Crawford, and R. D. Hiebert, Los Alamos Scientific Laboratory Report LA-2375 (1959).

(2) B. S. Rogers, P. C. Sanders, R. L. Schuch, D. L. Williams, and F. N. Hayes, Los Alamos Scientific Laboratory Report LA-1639 (1953).

Photodetectors for Scintillation Dosimetry in the Field

(D. L. Williams and F. N. Hayes)

INTRODUCTION

Dose rate devices are needed which are capable of measuring low gamma ray dose rates in the field. These devices should be dose rate and energy independent. Other desirable features are small size, mobility, a minimum requirement for associated electronic equipment, and no requirement for AC electrical power.

METHODS AND RESULTS

A suitable photodetector and scintillation unit was constructed by optically coupling a 25 cc right cylinder of NE 102* plastic scintillator to the cathode of a 1 in. diamet DuMont No. 6467 photomultiplier tube. Before cementing with Armstrong A-6 epoxy resin, the piece of plastic (1 in. in diameter by 2 in.) was sprayed with white Tygon paint with th exception of the polished surface at one end. To minimize internal reflection at the plastic and glass interfaces, the polished surface of the plastic was coated with a colorless grade of Dow-Corning silicone grease before joining it to the

*Nuclear Enterprises, Inc., Winnipeg, Canada.

cathode of the photomultiplier tube. To protect the plastic and phototube, an aluminum cylinder (1-1/8 in. inside diameter by 3 in. in length) was machined to fit over the plastic and then for about 1/2 in. over the glass envelope of the tube. The junction between the aluminum cylinder and the phototube and the glass envelope of the phototube were covered with black electrical tape to eliminate light leaks.

The necessary interdynode DC voltages were supplied to the photomultiplier tube from a battery pack made up of 46, 22.5-volt batteries. The batteries were arranged in series to give a difference in potential of 135 volts between the cathode and the first dynode, 90 volts between each of the next 9 stages, and 90 volts from the tenth dynode to ground. Since current is drawn only during the time that the phototube sees light from the scintillator, the useful life of the battery pack approaches shelf-life of the batteries.

The current generated by the photomultiplier tube is transmitted over low impedance coaxial cable to a galvanometer with a net input resistance of 1000 ohms. The gamma dose rate range of this device, as described, was about 2 mr/hr to 36 r/hr. By making suitable adjustments of the voltage across the dynodes of the photomultiplier tube, gamma dose rates up to several hundred r/min can be monitored with a dynamic range of at least 1000 fold.

Linearity of response of this type of gamma dose rate device has been well established (1) over a wide range of dose rates. However, one limitation* must be observed in adjusting the sensitivity of the detector for the probable dose rate range which is to be monitored. When relatively large anode currents ($\geq$1 μa) are delivered for more than a few minutes, a change in the response of the photomultiplier tube is observed. Different brands of tubes behave differently under these circumstances. For example, DuMont No. 6467 tubes show an increase in sensitivity, whereas RCA No. 6199 tubes always decrease in sensitivity. From a study of this feature, the following generalizations may be made for DuMont No. 6467 tubes. At about 2 μa anode current, the tubes are stable for about 15 minutes; at about 1 μa, the response is constant for at least 30 minutes; and at $<$ 0.5 μa, stability is good over several hours. Tubes which have had a change in response recover over a period of time which is roughly proportional to the magnitude of the change.

DISCUSSION

By making the appropriate adjustment of the voltage applied across the dynodes of the photomultiplier tube, the

*This feature of photomultiplier tube response was first brought to our attention by R. D. Hiebert of Group P-1.

dose rate device described above can be used to monitor gamma dose rates in the field over an extremely wide range, e.g., 1 mr/hr to several hundred r/min.

No further work on this project is anticipated in the near future.

REFERENCE

(1) D. L. Williams, F. N. Hayes, R. L. Schuch, R. L. Crawford, and R. D. Hiebert, Los Alamos Scientific Laboratory Report LA-2375 (1959).

Chromatography of Deoxyribonucleic Acids (A. Murray)

INTRODUCTION

The mild chromatographic method of Bendich (1) for the characterization of biologically active nucleic acids, by partial separation of the polynucleotide components of the total DNA (or RNA) from single sources, has established the heterogeneous nature of DNA. This essentially reproducible fractionation on the anion exchanger ECTEOLA (2) appears to depend largely on the molecular size or aggregation state of the various polynucleotide species as well as their base composition. Although this nitrogen-containing cellulose derivative has found widespread application in the chromatography of DNA, RNA, and viruses and in the purification of bacteriophages, there has been no report of attempts to improve the resolution of the chromatographic profiles.

As greater discrimination in separating macromolecules would be welcomed by every worker in the field, it appeared desirable to (a) evaluate all reported chromatographic methods through a single DNA specimen, (b) prepare an improved cellulose derivative, (c) correlate the profiles yield by various chromatographic media to those with the now commercially available ECTEOLA,* (d) determine the common physic

*Eastman Kodak Company.

parameters of the separated fractions, and (e) attempt to differentiate the natural heterogeneity of a given DNA from that arising through denaturation during the many and varied procedures reported for its isolation.

METHODS AND RESULTS

The usual procedures of cellulose chemistry have been employed in the preparation of some 30 different nitrogen-containing cellulose anion exchangers. The titration curve and nitrogen analysis of each have been determined. In order to screen the effects of type of nitrogen grouping, amines were selected from 19 aliphatic, 7 aromatic, and 7 heterocyclic classifications. In order to screen for spatial effects, bonding of the amine group to the cellulose chain was effected through both ether and ester links of varying length.

The intent is to pursue the screening with DNA and investigate variations of any type that those results may warrant.

REFERENCES

(1) A. Bendich, J. R. Fresco, H. S. Rosenkranz, and S. M. Beiser, J. Am. Chem. Soc. 77, 3673 (1955); A. Bendich, H. B. Pahl, G. C. Korngold, H. S. Rosenkranz, and J. R. Fresco, J. Am. Chem. Soc. 80, 3949 (1958).

(2) E. A. Peterson and H. A. Sober, J. Am. Chem. Soc. 78, 751 (1956).

Preliminary Studies on the Chemistry of Nucleic Acids (F. N. Hayes, A. Murray, and D. G. Ott)

INTRODUCTION

In line with the recent desire to increase fundamental research efforts, a study of the field of nucleic acid chemistry was begun to determine how best our interests and talents could be channeled into this rapidly expanding and eminently important field.

DISCUSSION

Our efforts thus far have primarily been directed toward self-education by studying all the available literature and holding discussion sessions. Some laboratory work is in progress for familiarization with some of the synthetic and analytical techniques in the field and for preparation of chemicals and fabrication of apparatus which will be useful in the near future, when this program gets under way.

Labeling of Biologically Important Compounds with Radioisotopes

(A. Murray)

The programs of the Biochemistry Section, the Industrial Waste Treatment Group, and the Department of Plant Pathology of Purdue University have been supported by the synthesis of the following labeled compounds, the figures in parentheses being specific activity of the radiochemically pure compound (in μc/g) on a carrier-free basis:

(a) H^3-Deoxyribonucleic acid

(b) Dihydrolanosterol-25,26-H_2^3 (42.6)

(c) 2,4,6-Trinitrotoluene-1-C^{14} (11.25)

(d) H^3-1-Octanol (81.4)

In the last case (d), where difficult handling of small liquid samples of high specific activity was necessary, purification was effected by formation of inclusion compounds, column adsorption chromatography, fractional recrystallization of temporary solid derivatives, fractional microdistillation with low and high boiling inert carriers, and gas-liquid partition chromatography.

ORGANIC CHEMISTRY SECTION PUBLICATIONS

(1) M. D. Barnett, G. H. Daub, F. N. Hayes, and D. G. Ott, Liquid Scintillators. XI. 2-(2-Fluorenyl)-5-aryl-substituted Oxazoles and 2-(2-Fluorenyl)-5-phenyl-1,3,4-oxadiazole, J. Am. Chem. Soc. 82, 2282 (1960).

(2) F. R. Domer and F. N. Hayes, Background vs. Efficiency in Liquid Scintillators, Nucleonics 18(1), 100 (1960).

(3) F. N. Hayes, E. Hansbury, V. N. Kerr, and D. L. Williams, Contemporary Carbon^{14} in Lemongrass Oil, Z. Physik 158, 374 (1960).

(4) F. N. Hayes, E. Hansbury, and V. N. Kerr, Contemporary Carbon-14: The p-cymene Method, Anal. Chem. 32, 617 (1960).

(5) V. N. Kerr, D. G. Ott, and F. N. Hayes, Quaternary Salt Formation of Substituted Oxazoles and Thiazoles, J. Am. Chem. Soc. 82, 186 (1960).

(6) D. G. Ott, V. N. Kerr, F. N. Hayes, and E. Hansbury, Liquid Scintillators. XII. Absorption and Fluorescence Spectra of 2,5-diaryl-1,3,4-oxadiazoles, J. Org. Chem. 25 872 (1960).

(7) D. F. Petersen and A. Murray, III, Simple Fluorescent Intensification Screen for Ultraviolet Scanner Cameras, Anal. Chem. 32, 443 (1960).

(8) D. L. Williams, F. N. Hayes, R. L. Schuch, R. L. Crawford, and R. D. Hiebert, Liquid Scintillator Radiation Rate Meters for the Measurement of Gamma and Fast Neutron Rates in Mixed Radiation Fields, Los Alamos Scientific Laboratory Report LA-2375 (March 1960).

PUBLICATION SUBMITTED

(1) S. P. Birkeland, G. H. Daub, F. N. Hayes, and D. G. Ott, Liquid Scintillators. X. Some Aryl Substituted Phenanthrenes and Dihydrophenanthrenes, and Related p-Terphenyls and p-Quaterphenyls. Determination of Kallmann Parameters, submitted to Zeit. Physik.

CHAPTER 5

RADIOBIOLOGY SECTION

The Inheritance of Radiation-Induced Mutations Deleterious to the Reproductive Efficiency in the Mouse. Part I. The Reproductive Performance of the Sixth Filial Generation from Five Generations of X-Irradiated Male Mice (J. F. Spalding and V. G. Strang)

INTRODUCTION

The genetic hazards of ionizing radiation are the subject of much concern and controversy, and the urgent need for more information on the inheritance of radiation-induced genetic damage in mammals has been stressed (1). Evidence that many mutations may have slight dominant deleterious effects or that the genetic load of recessive mutations may accumulate through the germ line has been suggested by the Russells (2). This study was designed to observe the reproductive performance and life span of the sixth filial generation from 5 generations of X-irradiated male mice. For an earlier report on this experiment, the reader is referred to Chapter 5 of the previous semiannual report (3).

METHODS

The mice used in this experiment were obtained from the mating of 1 pair of RFM mice, which were treated as described in Fig. 1. The X-ray treated male mice in the experimental line were exposed to a single acute dose of X rays at 28 days of age. A control line was maintained parallel to the experimental line to check for possible loss of vigor through inbreeding.

RESULTS AND CONCLUSIONS

The reproductive performance of the sixth filial generation of 25 pairs each of experimental and control line mice has been completed and analyzed. Nine breeding characteristics were evaluated as follows: age at first litter, age at last litter, reproductive life, number of conceptions, number of mice born, number of mice weaned, average litter size born, average litter size weaned, and weaning weights.

The mean of the experimental group was less than the mean of the control group for all characteristics observed. Although only 1 of the characteristics tested (average weaning weight) was statistically significant, the results of F and sign tests justified the conclusion that 200 rads of X irradiation, delivered to the male mouse for 5 consecutive generations, resulted in heritable genetic damage to the unexposed F_6 generation.

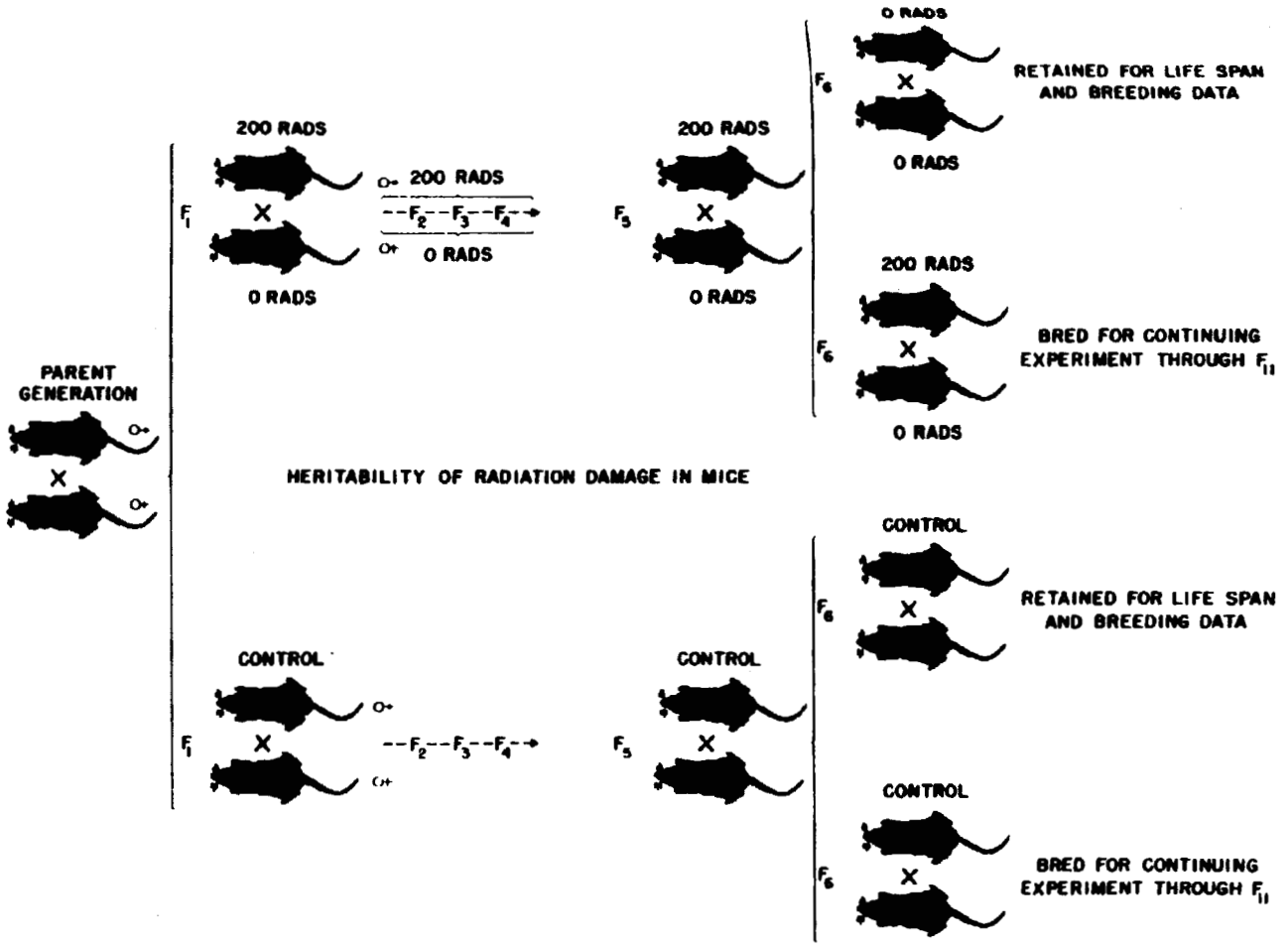

Fig. 1. Experimental design.

REFERENCES

(1) Report of the United Nations Scientific Committee on the Effects of Atomic Radiation, General Assembly Official Records: Thirteenth Session, Supplement No. 17 (A/3838), New York (1958).

(2) W. L. Russell, L. B. Russell, and E. F. Oakberg, Radiation Genetics of Mammals, In: Radiation Biology and Medicine, W. D. Claus (ed.), Addison-Wesley, Reading, Mass. (1958).

(3) Biological and Medical Research Group (H-4) of the Health Division - Semiannual Report July through December 1959, Los Alamos Scientific Laboratory Report LAMS-2445 (February 1960).

The Inheritance of Radiation-Induced Mutations Deleterious to the Reproductive Efficiency in the Mouse. Part II. The Reproductive Performance of the Eleventh Filial Generation from Ten Generations of X-Irradiated Male Mice (J. F. Spalding and V. G. Strang)

INTRODUCTION

This is a continuing experiment to observe the reproductive performance, resistance to nonspecific stress (low temperature and chronic gamma ray exposures), and life span of the eleventh filial generation from 10 generations of X-irradiated male mice. The data obtained from Part I of this study (observations on the sixth filial generation) indicated the necessity for continuance of this project.

METHODS

The population of mice used in this study originated from the sixth filial generation of control and experimental mice in Part I. The X-ray treated male mice were exposed acutely at 4 weeks of age, and offspring from the tenth filial generation of the control and experimental groups (nonirradiated eleventh generation mice) are being observed for reproductive performance, resistance to nonspecific stress, and life span. Five groups are under study, as shown in Fig. 1, and are mated in the following manner:

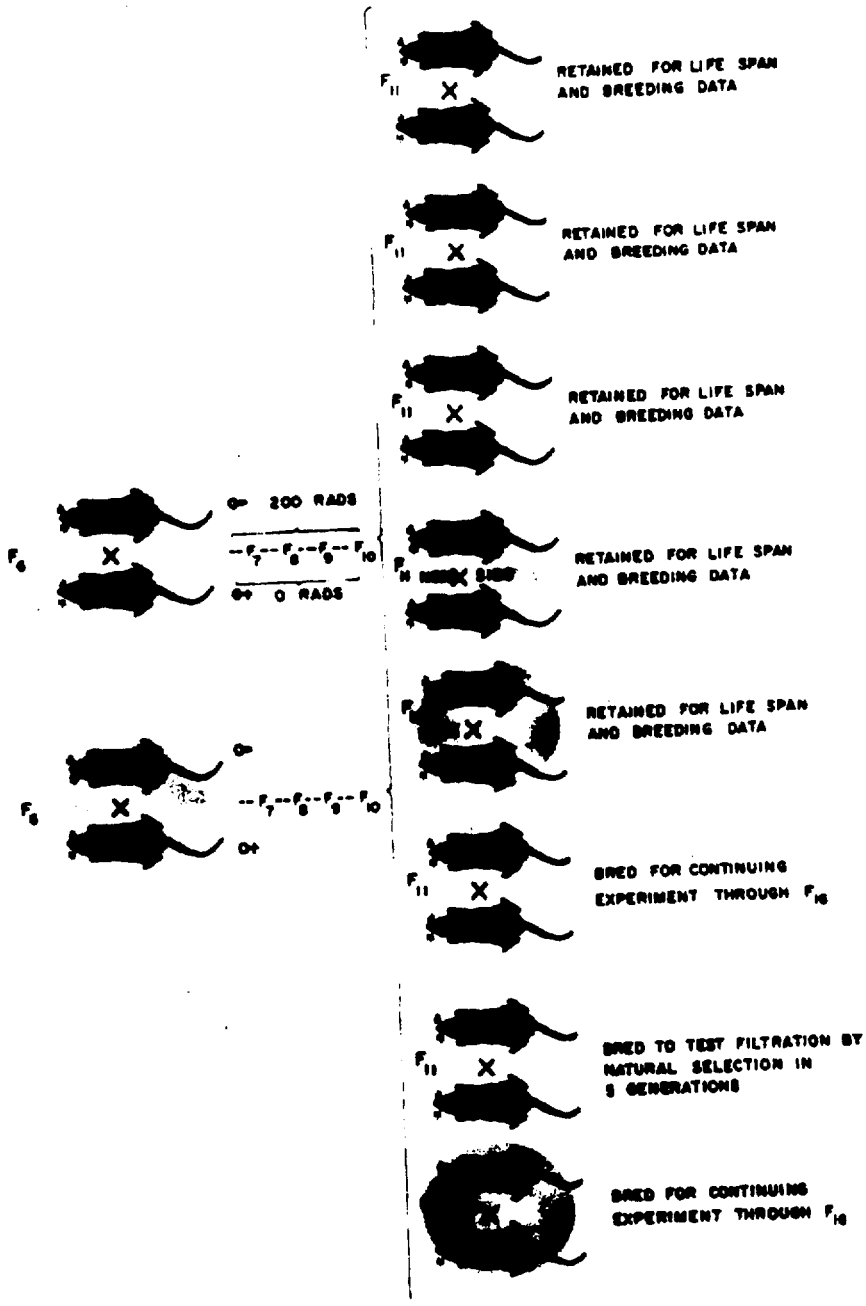

Fig. 1. Experimental design.

00131478.148

Group I	Control line male x irradiated line female
Group II	Irradiated line male x control line female
Group III	Irradiated line male x irradiated line female
Group IV	Sister-brother mated control
Group V	Nonsister-brother mated control
Group VI	Irradiated line male x irradiated line female, bred to continue experiment through F_{16} with X-ray exposures to each generation of males
Group VII	Irradiated line male x irradiated line female with no further X-ray exposures, bred to test filtration by natural selection through 5 generations
Group VIII	Control male x control female bred to continue experiment through F_{16}

RESULTS

The reproductive performance of the first 5 groups listed under Methods is under study. Expected completion date is March 1961. For reports of earlier data, see Part I of this report (1) and Chapter 5 of the previous semiannual report (2).

REFERENCES

(1) J. F. Spalding and V. G. Strang, The Inheritance of Radiation-Induced Mutations Deleterious to the Reproductive Efficiency in the Mouse. Part I. The Reproductive Performance of the Sixth Filial Generation from Five Generations of X-Irradiated Male Mice, this report.

(2) Biological and Medical Research Group (H-4) of the Health Division - Semiannual Report July through December 1959, Los Alamos Scientific Laboratory Report LAMS-2445 (February 1960).

Dependence of Recovery Half-Time on Magnitude of Conditioning Dose of Cobalt^{60} Gamma Rays (J. F. Spalding and T. T. Trujillo)

INTRODUCTION

It has been stated that the recovery half-time following acute irradiation damage is strongly dependent on the size of the dose (1). A series of studies are being conducted to determine recovery or repair rates in irradiated mice and if possible, to establish the actual relationship between recovery rate and radiation dose.

METHODS AND RESULTS

Three approaches are being undertaken to determine radiation repair rates. In the first approach, groups of mice are given a single acute challenging dose of Co^{60} gamma rays. After allowing various times for recovery, the LD_{50} for each group is determined. The residual damage is determined at each repair time interval to obtain the repair half-time (RT_{50}). Tables 1 and 2 show this method and the results obtained to date.

In the second approach, several groups of mice are conditioned with different challenging doses and all groups are allowed the same repair interval prior to determining the LD_{50}. The residual damage is then determined for each

TABLE 1. RADIATION REPAIR RATE FOLLOWING FIXED CONDITIONING DOSE (600 rads) AND VARIABLE REPAIR TIME (1 to 23 days)

Group (No.)	Mice (No.)	Conditioning Dose (rads)	Repair Time (hr)	LD_{50}^{30}	Residual Damage (rads)	Repair Half-time (RT_{50})
1	180	600	546	722	37	150 ± 9 hr
2	180	600	312	677	82	150 ± 9 hr
3	180	600	237	525	233	150 ± 9 hr
4	180	600	172	409	350	150 ± 9 hr
5	180	600	69	364	395	150 ± 9 hr
6	180	600	21	199	560	150 ± 9 hr
7	180	Zero	Control			

TABLE 2. RADIATION REPAIR RATE FOLLOWING FIXED CONDITIONING DOSE (205 rads) AND VARIABLE REPAIR TIME (1 to 23 days)

Group (No.)	Mice (No.)	Conditioning Dose (rads)	Repair Time (hr)	LD_{50}^{30}	Residual Damage (rads)	Repair Half-time (RT_{50})
1	180	205	546	No data at time of writing		
2	180	205	312			
3	180	205	237			
4	180	205	172			
5	180	205	69			
6	180	205	21			
7	180	Zero	Control			

challenging dose. Table 3 shows this method and the results obtained to date.

The third approach is the fractionated dose method, as tabulated in Table 4. One hundred and eighty mice were exposed to 500 rads of Co^{60} gamma rays biweekly for 7 exposures. The dose required to kill 50 per cent of the mice will be determined, and with this information the repair half-time will be estimated.

These studies are incomplete as of this date, and analyses and interpretation of the present and subsequent data will be presented in a future semiannual report.

REFERENCE

1) G. A. Sacher, Reparable and Irreparable Injury: A Survey of the Position in Experiment and Theory, In: Radiation Biology and Medicine, W. D. Claus (ed.), Addison-Wesley, Reading, Mass. (1958).

TABLE 3. RADIATION REPAIR RATE FOLLOWING VARIABLE CONDITIONING DOSE (205 to 692 rads) AND FIXED REPAIR TIME (6 days)

Group (No.)	Mice (No.)	Conditioning Dose (rads)	Repair Time (hr)	LD_{50}^{30}	Residual Damage (rads)	Per cent Residual
1	180	205	143	677	105	51
2	182	302	146	690	92	30
3	181	408	145	510	272	67
4	183	512	144	519	263	51
5	180	603	143	474	306	51
6	180	692	147	385	397	57
7	180	Zero	---	782	---	--

TABLE 4. FRACTIONATED DOSE APPROACH TO REPAIR HALF-TIME[a]

Exposure Date	Group I			Group II[c]		
	Mice (No.)[b]	Single Dose (rads)	Accumulated Dose (rads)	Mice (No.)[b]	Single Dose (rads)	Accumulated Dose (rads)
4-21-60	180	500	500	172	500	500
5-5-60	180	500	1000	172	500	1000
5-19-60	179	500	1500	165	500	1500
6-2-60	167	500	2000	146	500	2000
6-16-60	139	500	2500	112	500	2500
6-30-60	97	500	3000	58	500	3000

To be continued

(a) The acute LD_{50} for this experiment was 759 rads.

(b) Number of mice on exposure date.

(c) Group II is a replication of Group I.

Comparison of Natural and Radiation Aging Mechanisms: Response of Irradiated and Nonirradiated Mice to Cold Stress

(T. T. Trujillo and J. F. Spalding)

INTRODUCTION

Young animals demonstrate the ability to withstand a nonspecific stress, such as subnormal temperature, better than old animals as indicated by the per cent of survivors. Numerous investigations also indicate that single or multiple doses of whole body irradiation, at least above a certain threshold, result in the life shortening of mammals. Both the normal and radiation aging processes are poorly understood; however, the above observations provide a means to compare the natural process with radiation aging.

This investigation, reported in the previous semiannual document with some of the early results (1), was designed to observe differences in the two aging mechanisms in a single strain of irradiated and nonirradiated mice when exposed to a nonspecific stress such as cold.

METHODS AND RESULTS

Female mice of the RF strain were used in this study. The radiation exposure came from a low intensity Co^{60} source. The 4 irradiated groups were exposed at the age of 3 to 5 months; however, the beginning of exposure of each group

varied to allow for exposure termination of all groups to occur at the same time. This was followed by a 90-day recovery period before the animals were subjected in individual cages to cold stress for 14 days at 6 to 7°C in a walk-in refrigerator. All animals surviving the cold stress period were observed for an additional 10 days following the stress period. The per cent mortality reported is from both periods. A nonirradiated group of the same chronological age was stressed along with irradiated groups.

In the study to observe the effect of natural aging on resistance to cold of the RF strain, 5 different age groups (4, 8, 12, 20, and 24 months) have been stressed. Table 1 shows the results of 4 irradiated groups observed since the last report. The per cent mortality in the irradiated groups is higher than the control group with significant differences corresponding to the whole body dose received by each group.

Table 2 shows the response of 5 nonirradiated groups of different ages when exposed to a subnormal temperature. The 16 month old group remains to be exposed to cold stress.

DISCUSSION

From these additional data, it again is evident that the response of radiation-aged mice is similar to the response of naturally-aged animals, when both groups are exposed to a

TABLE 1. EFFECT OF COLD STRESS ON THE SURVIVAL OF YOUNG IRRADIATED AND NONIRRADIATED MICE

Group (No.)	Mice (No.)	Dose (rads)	Duration of Irradiation* (days)	Age at Start of Stress** (months)	Deaths during 14-Day Stress (No.)	Deaths during 10-Day Post Stress Period (No.)	Total Deaths (per cent)
I	96	0	0	9	19	1	21
II	96	500	10	9	23	2	26
III	96	1502	30	9	35	2	39
IV	86	2581	51	9	46	4	58
V	69	3633	72	9	46	4	72

*Dose rate = 50 rads/22-hr day from Co^{60} source. Exposure terminated at the same time for all groups.

**Animals were allowed a 90-day recovery period between termination of irradiation exposure and start of cold stress test.

TABLE 2. AGE VERSUS RESISTANCE TO COLD STRESS OF RF FEMALE MICE

Mice Stressed* (No.)	Age (months)	Mortality** (per cent)
100	4	14
100	8	36
96	12	27
96	16	--
83	20	87
44	24	100

*Stress period 14 days at 6 to 7°C.

**Includes deaths during 10-day post stress period.

nonspecific stress such as cold. It can be concluded that the aging mechanisms of the natural and radiation processes are very similar, at least insofar as the ability of the animals to withstand a specific environmental stress (in this case, cold) is concerned.

REFERENCE

(1) Biological and Medical Research Group (H-4) of the Health Division - Semiannual Report July through December 1959, Los Alamos Scientific Laboratory Report LAMS-2445 (February 1960).

Effect of Preirradiation Treatment with Glutathione on the Age Specific Log Rates of Mortality (Gompertz Function)

(I. U. Boone, G. A. Trafton, and L. M. Conklin)

INTRODUCTION

The administration before irradiation of agents such as cysteine, cysteamine, glutathione, S,2-aminoethylisothiuronium bromide (AET), etc., have been shown to exert a protective effect against acute lethal doses of X irradiation. Very little information is available as to the long-term effects that these protective agents may have. In this study, glutathione was administered to CF_1 female mice prior to a single lethal or sublethal dose of X irradiation.

Life span and tumor incidence of animals given glutathione before 400 and 700 rads of X irradiation have been reported previously and compared to animals receiving a single dose of 400 rads of whole body X irradiation and to nonirradiated animals (1,2). Glutathione had a definite protective effect in terms of life shortening and tumor incidence at both the lethal and sublethal dose levels. Additional data on the age specific log rates of mortality of irradiated animals, pretreated and nontreated with glutathione, are presented here.

METHODS

The irradiation was delivered as a single dose of 250 KVP X rays. The air dose was 52 r/min with a tissue dose of 50 rads/min. Glutathione (4 g/kg body weight) was administered subcutaneously 30 minutes before irradiation. The mice were treated and irradiated at 17 weeks of age with approximately 150 per group. The groups were as follows:

Group I	400 rads whole body X irradiation
Group II	glutathione + 400 rads X irradiation
Group III	glutathione + 700 rads X irradiation
Group IV	specific control group, which received glutathione only
Group V	a general control group, which received nothing

RESULTS AND DISCUSSION

Following irradiation, the Gompertz function (logarithm of the daily rate of mortality) was displaced upward from the control mortality rate. Figure 1 represents the data of the age specific rates of mortality for nonleukemia deaths in all groups as listed under Methods. Leukemia deaths have been removed because of the characteristic phasic time pattern of appearance. Least square estimates of the linear regression of log mortality rate on age were obtained

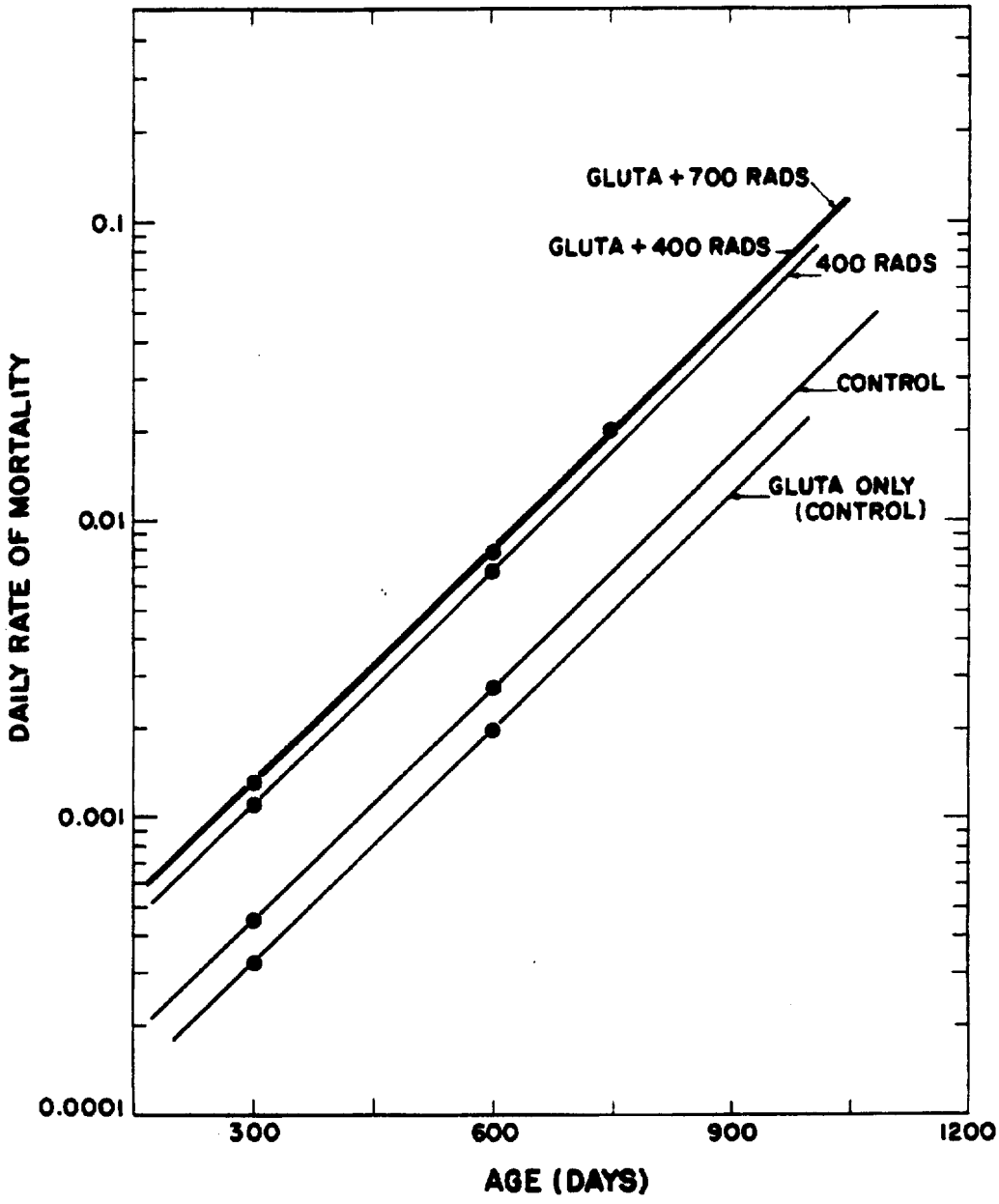

Fig. 1. Age specific rates of mortality for CF_1 protected and nonprotected mice following whole body X irradiation.

for each group. In all instances, the regression coefficients (i.e., the slopes) did not differ significantly from that of the control lines, and the lines could be drawn parallel as shown.

The Gompertz lines of all irradiated groups, whether treated or untreated with glutathione, were displaced upward from the control groups. Interestingly, the Gompertz lines for the glutathione pretreated groups which received 400 or 700 rads were identical. These lines did not differ significantly from that representing the group which received 400 rads of whole body X irradiation only. Although the glutathione treatment had little effect on the mortality rates of animals that received 400 rads, it appears to have significant influence on the death rate of animals that received 700 rads. Glutathione modified the death rate of animals receiving 700 rads such that the death rate of these animals was not different from the animals which received 400 rads of whole body X irradiation, with or without pretreatment with glutathione.

REFERENCES

(1) I. U. Boone, Incidence of Tumors in Animals Exposed to Whole-Body Radiation, In: Proceedings of the Symposium on the Delayed Effects of Whole-Body Radiation, B. B. Watson (ed.), ORO-SP-127, pp. 19-37 (1960).

(2) Biological and Medical Research Group (H-4) of the Health Division - Semiannual Report July through December 1959, Los Alamos Scientific Laboratory Report LAMS-2445 (February 1960).

Effects of Sublethal Whole Body X Irradiation at Different Age Levels in CF_1 Mice (I. U. Boone, G. A. Trafton, and L. M. Conklin)

INTRODUCTION

This study was designed to investigate the chronic effects of sublethal whole body X irradiation as a function of age of CF_1 mice at time of exposure. Of the several radiation effects observed, the acute mortality, per cent life shortening, and tumor incidence have been reported (1,2,3). The results indicated that the sensitivity to acute effects of irradiation appeared to be increased with the age of the animal, while the chronic delayed effects on life shortening decreased with age. The tumor incidence data for all mature age groups showed that the leukemia incidence varied with age in this strain of mice. The greatest susceptibility was seen at 2 months and then at 18 months of age.

In addition to the above observed radiation effects on life shortening and tumor incidence, age specific log rates of mortality (commonly known as the Gompertz function) were also determined.

METHODS

CF_1 female mice from the same original random group were exposed to whole body X irradiation of 100, 200, and 400 rads at 2, 6, 12, and 18 months of age. Groups of animals exposed at 18 months of age contained 40 to 50 animals. All other irradiated groups had 150 animals. There were 300 animals in the control group. Also from the same original random group nonirradiated mothers were chosen for breeding purposes, and their babies were exposed at 1 to 7 days of age. This part of the study included females and males. Following irradiation, the babies were placed with their mothers for 30 days, weaned, and rerandomized. The number of animals in each group varied between 80 and 100 at time of exposure.

RESULTS AND DISCUSSION

The Gompertz function (or logarithm of the daily rate of mortality) has been widely used as a means of measuring the "aging" process following irradiation. The rate of mortality increases exponentially with age. This exponential increase is characteristic of most mammalian species. Following irradiation, the Gompertz function is displaced upward from the control mortality rate. Figure 1 illustrates representative data of the age specific rates of mortality for nonleukemia deaths at 2, 6, and 12 months of age. In these

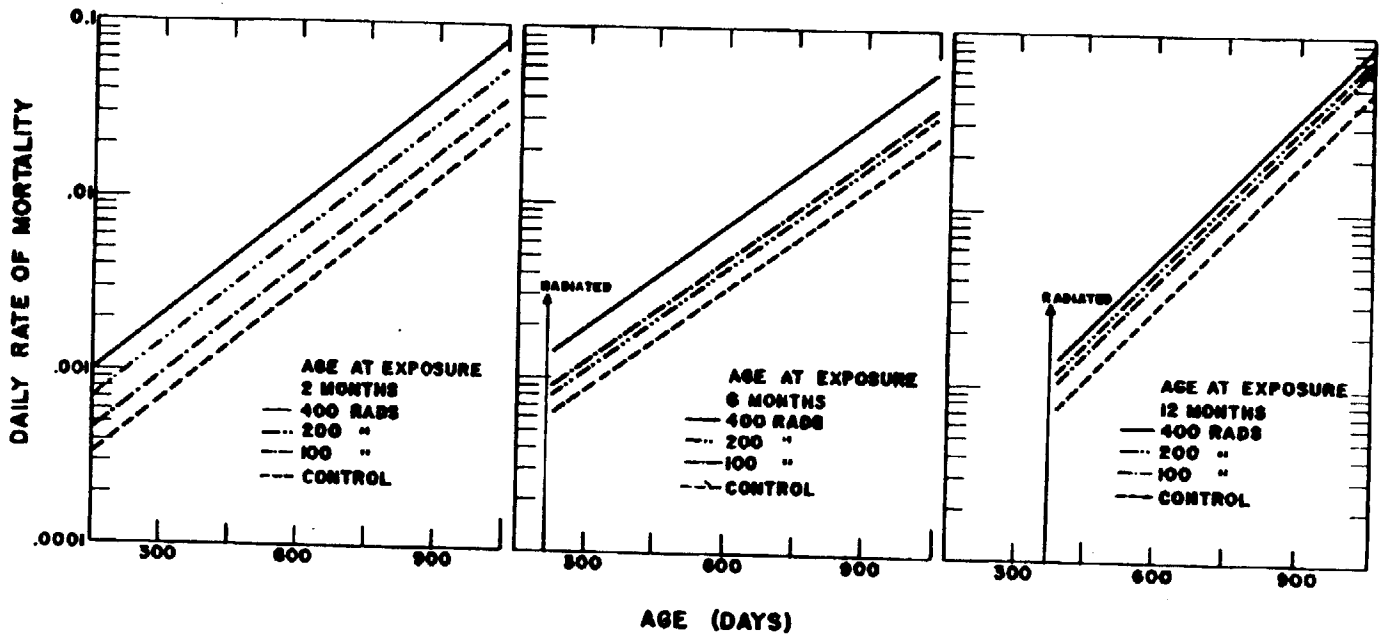

Fig. 1. Age specific rates of mortality for nonleukemia deaths of CF_1 female mice irradiated at various age levels.

particular calculations, leukemia deaths have been removed because of the characteristic phasic time pattern of appearance.

Least square estimates of the linear regression of log mortality rate on age were obtained for all control and irradiated groups. In all instances, the regression coefficients (i.e., the slopes) did not differ significantly from that of the control lines, and the lines could be drawn parallel as shown. As can be seen, the log of the daily mortality rate in the irradiated groups was displaced upward from the control group. This displacement was not as pronounced in animals which were irradiated at 6 and 12 months of age, as compared to those irradiated at 2 months of age.

Figure 2 represents the Gompertz lines of male and female mice irradiated at 1 to 7 days of age. Figure 3 gives the data for mice irradiated at 18 months of age.

These changes in displacement can be further illustrated if one plots the ratio of displacement at each dose level versus the age at which the animals were irradiated, as shown in Fig. 4. This decrease in displacement of mortality rate as a function of age at exposure is well demonstrated at the 400 rad dose level, the greatest displacement occurring in animals irradiated at 2 months of age. The displacement was even greater than that seen in mice irradiated in the first week of life.

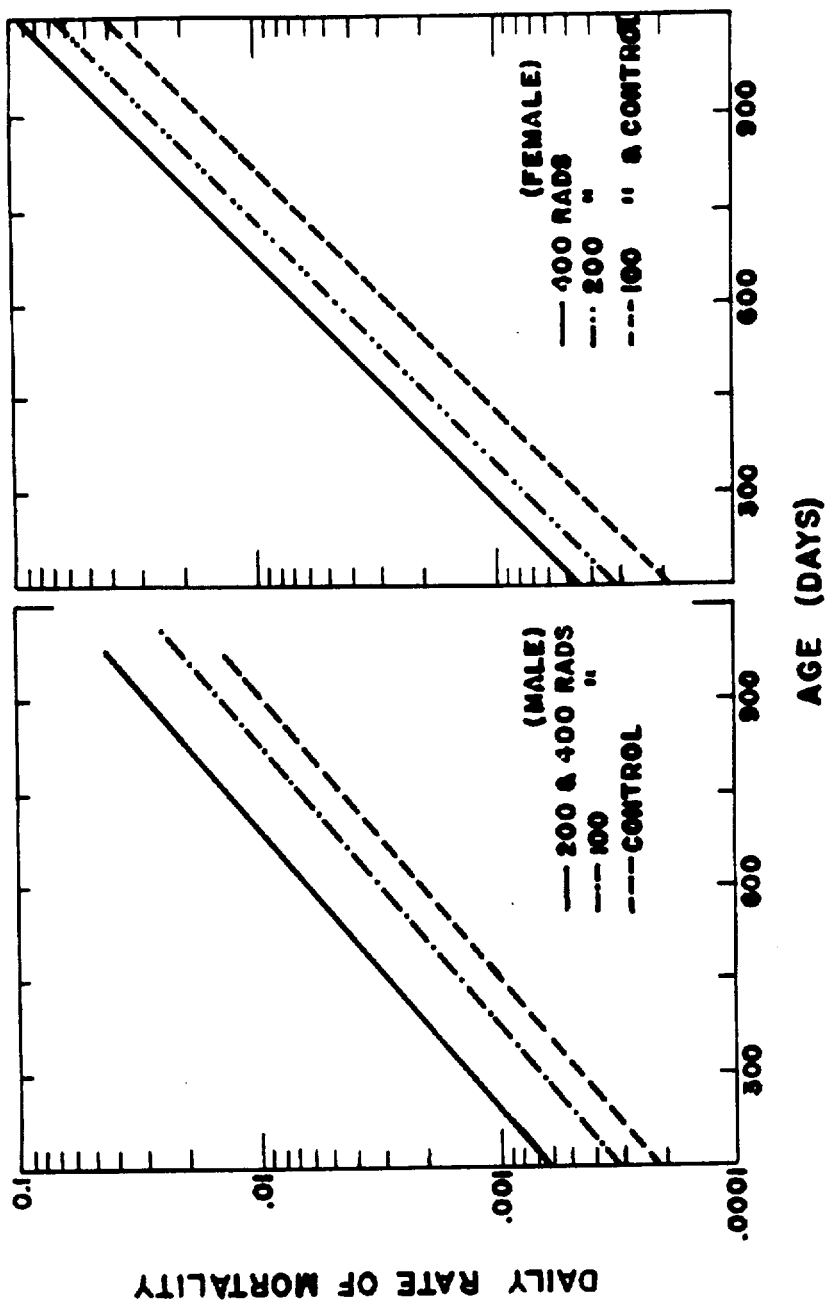

Fig. 2. Age specific rates of mortality for nonleukemia deaths of CF_1 mice irradiated at 1 to 7 days of age.

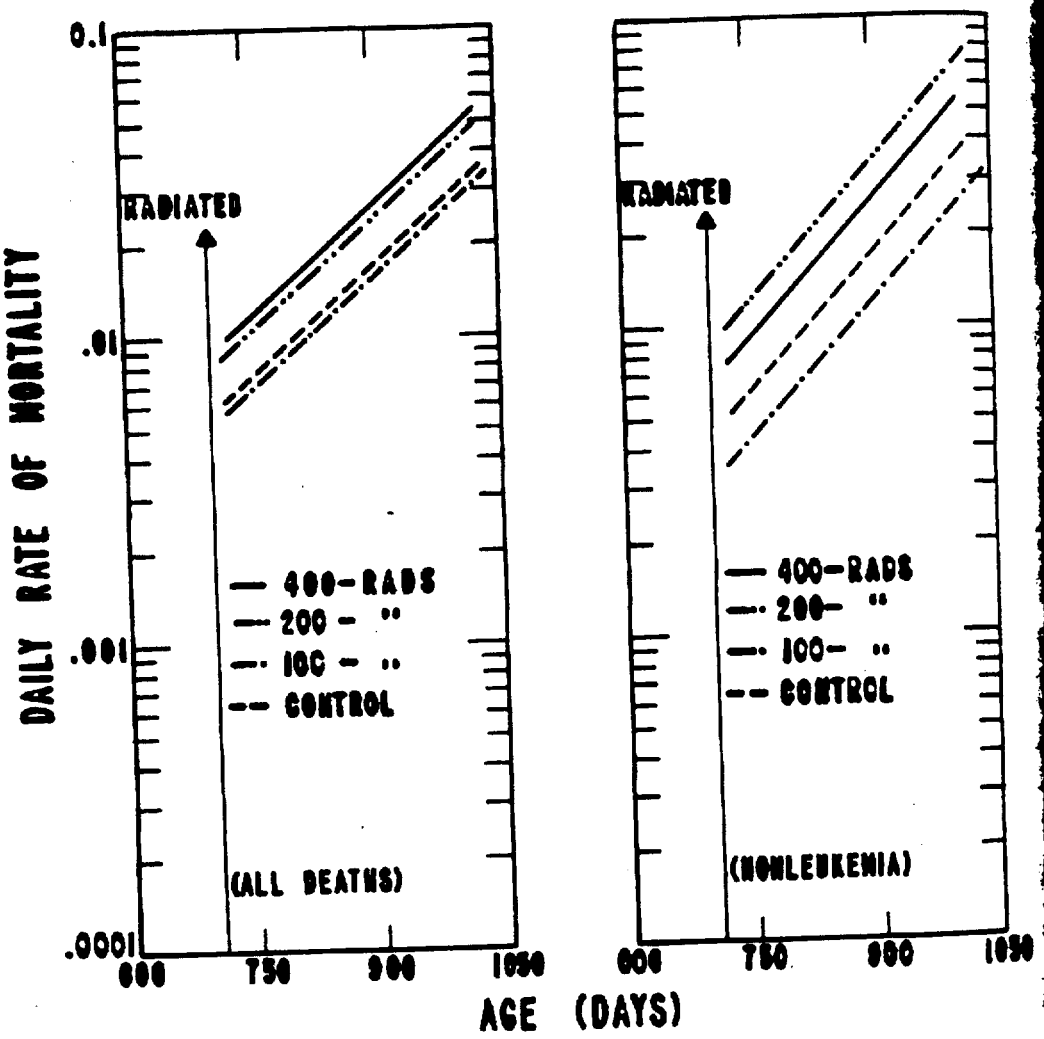

Fig. 3. Age specific rates of mortality for CF_1 mice irradia at 18 months of age.

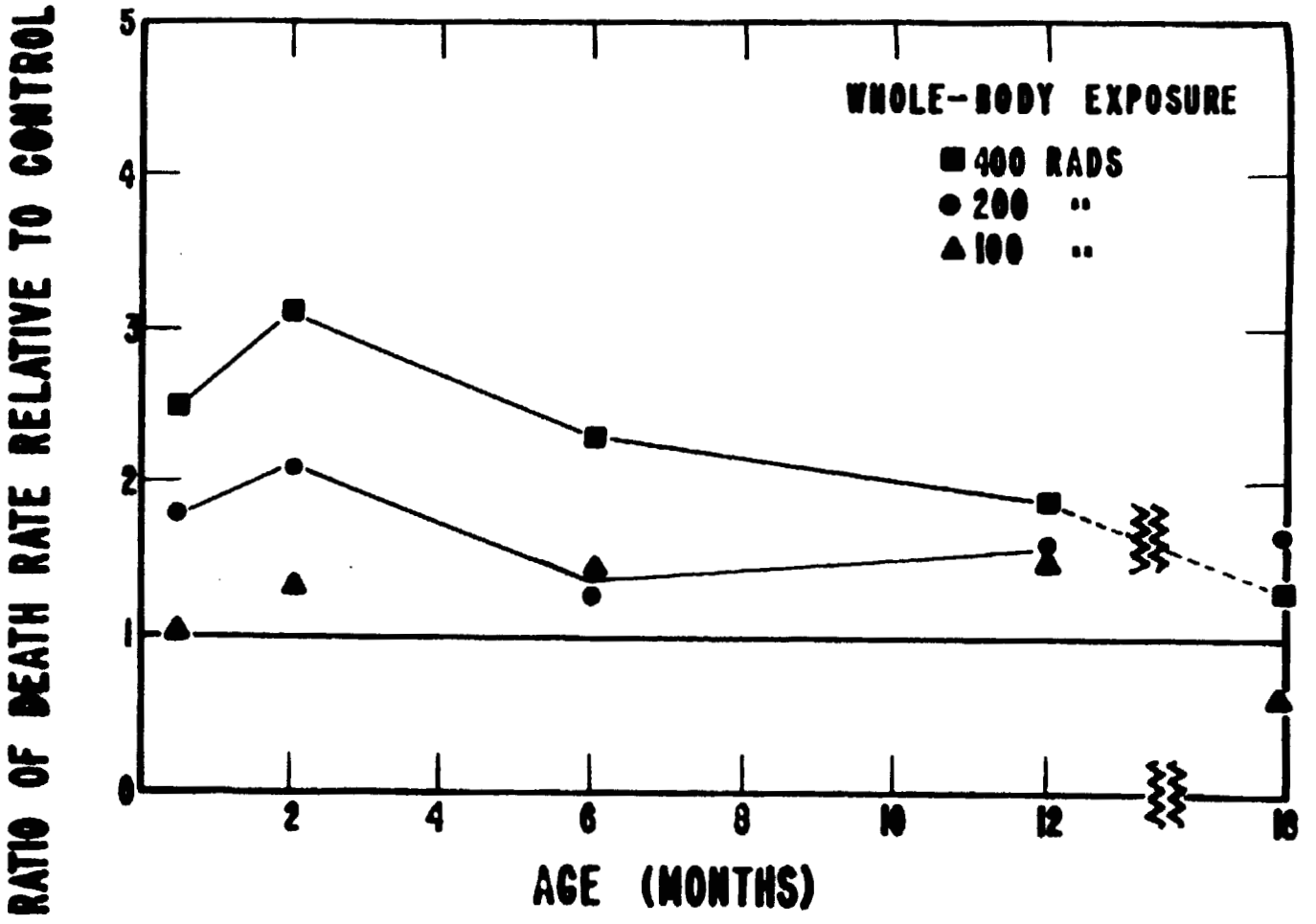

Fig. 4. Relation between Gompertzian displacement and age for nonleukemic deaths of irradiated CF_1 female mice.

REFERENCES

(1) Biological and Medical Research Group (H-4) of the Health Division - Semiannual Report July through December 1959, Los Alamos Scientific Laboratory Report LAMS-2445 (February 1960).

(2) I. U. Boone, Incidence of Tumors in Animals Exposed to Whole-Body Radiation, In: Proceedings of the Symposium on the Delayed Effects of Whole-Body Radiation, B. B. Watson (ed.), ORO-SP-127, pp. 19-37 (1960).

(3) I. U. Boone, Abstract No. 20, Rad. Res. 12, 424 (1960).

Effect of Single Sublethal Doses of Nitrogen Mustard (HN_2) on the Age Specific Log Rates of Mortality (Gompertz Function) as Compared to Whole Body X Irradiation (I. U. Boone, G. A. Trafton, and L. M. Conklin)

INTRODUCTION

It has been well established that certain drugs may mimic some of the observed effects of radiation, particularly the production of mutations. This experiment was based on the hypothesis that aging is a result of gradual accumulation of chromosomal aberrations or mutations in somatic tissue. If this theory is true, any agent which causes chromosomal damage should shorten life span in animals. Therefore, this study was designed to investigate the long-term and delayed effects of nitrogen mustard (HN_2), a known chemical mutagen, as compared to whole body X irradiation.

It has been reported previously that HN_2 administered as a single sublethal dose to CF_1 mice did not significantly affect their life span (1), while 400 rads of whole body X irradiation shortened mean life span 38 per cent (2). In the CFW Swiss strain of mice, mean life span was reduced 13.7 per cent following 400 rads of whole body irradiation and 9.2 per cent in mice receiving 3.5 mg/kg body weight of HN_2 intraperitoneally. These reduced mean life spans in CFW Swiss mice were significantly different from the mean life span of the control group of animals. The strain difference in life span

reduction following sublethal doses of HN_2 may be due to the variation in induced leukemia seen in the 2 strains of mice. CF_1 mice did not show an increased incidence of leukemia following HN_2, while CFW Swiss mice that received 3.5 mg/kg body weight of HN_2 showed an increase in incidence of leukemia similar to that group of animals which received 400 rads of whole body X irradiation (2,3).

The logarithm of daily rate of mortality (Gompertz function) has been widely used as a means of measuring the "aging" process following irradiation. Following irradiation, the Gompertz function is displaced upward from the control mortality rate. The present results compare the age specific log rates of mortality in the mice which received HN_2 to those that received whole body X irradiation.

METHODS

Nitrogen mustard was administered as single sublethal doses to CF_1 and CFW Swiss female mice. The doses administered were chosen on the basis of LD_{50} studies conducted on each strain. The radiation was delivered as a single whole body dose of 400 rads of 250 KVP X irradiation. The air dose rate was 52 r/min with a tissue dose rate of 50 rads/min. The CF_1 mice were irradiated or treated at about 4 months of age, and the CFW Swiss mice at about 3 months of age.

RESULTS AND DISCUSSION

Figures 1 and 2 illustrate the representative data of age specific rates of mortality for nonleukemia deaths following administration of HN_2 and whole body radiation in the CF_1 and CFW Swiss strains of mice, respectively. Leukemia deaths have been removed because of the characteristic phasic time pattern of appearance.

Least squares estimates of the linear regression of log mortality rate on age were obtained for all control and irradiated groups. In all instances, the regression coefficients (i.e., the slopes) did not differ significantly from that of the control lines, and the lines could be drawn parallel as shown. The log of the daily mortality rate was displaced upward in the irradiated groups for both strains of mice. In the CF_1 mice, HN_2 did not significantly displace the Gompertz line from the control group. In the CFW Swiss strain of mice, the displacement of the Gompertz line from the control line following administration of 3.5 mg/kg body weight of HN_2 was similar to the displacement following 400 rads of whole body X irradiation. The Gompertz line following 2.5 mg/kg body weight of HN_2, in this strain of mice, did not differ significantly from the control line.

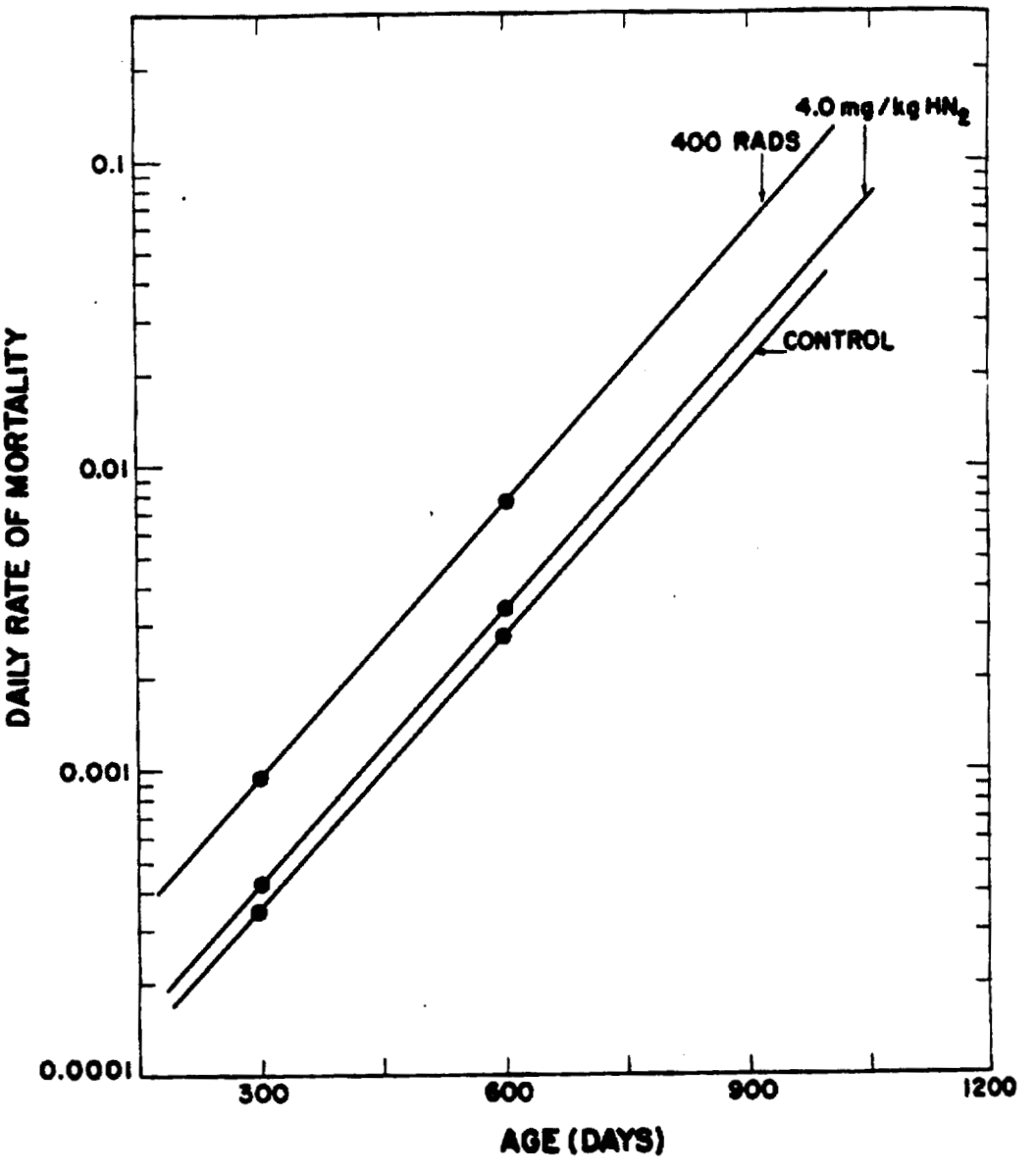

Fig. 1. Age specific rates of mortality in CF_1 mice following administration of a single dose of HN_2 or whole body X irradiation.

00131478.176

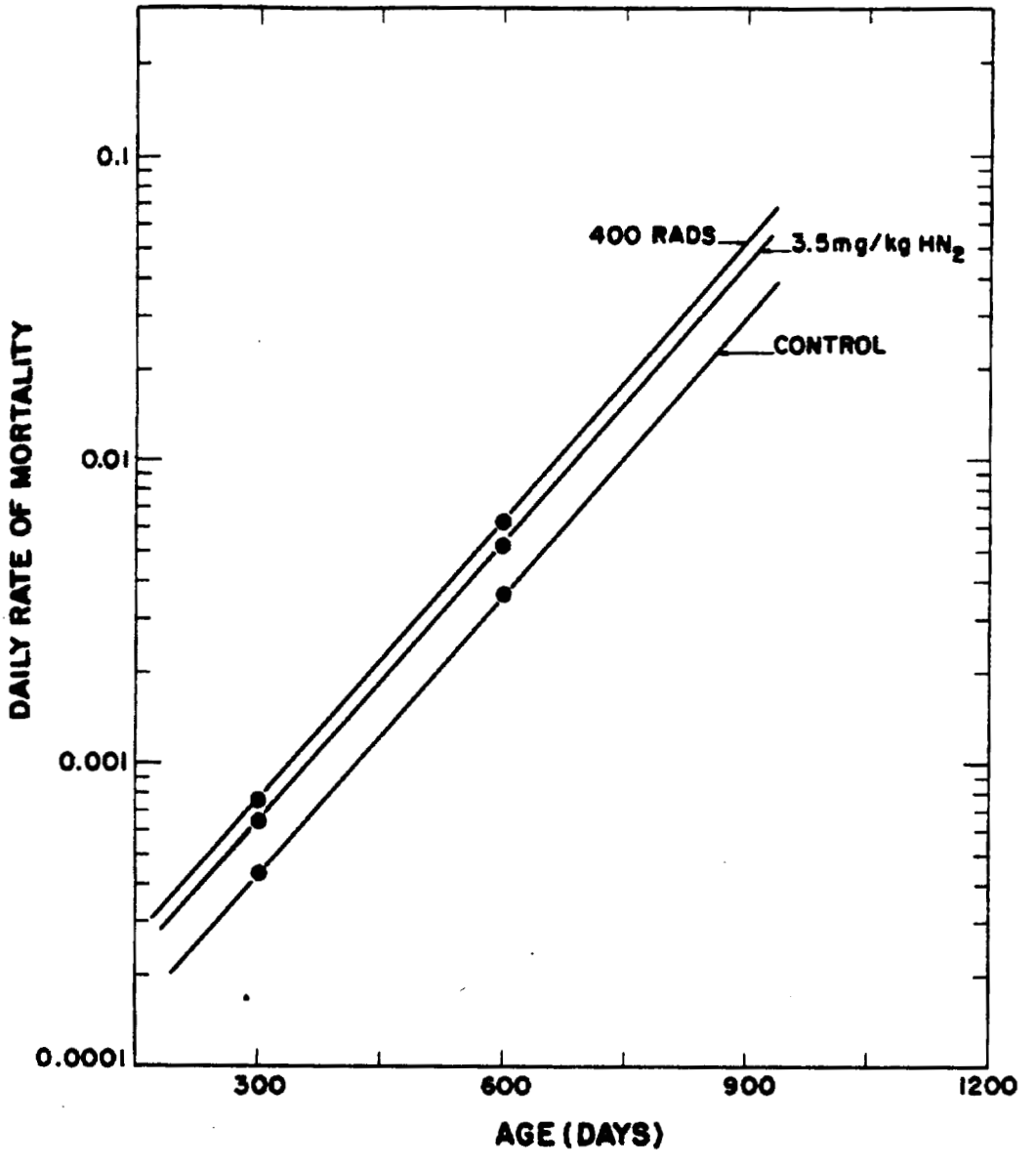

Fig. 2. Age specific rates of mortality for CFW mice following administration of a single dose of HN_2 or whole body X irradiation.

REFERENCES

(1) H. J. Curtis and R. Healey, Effects of Radiation on Aging, In: Advances in Radiobiology, Oliver and Boyd, Edinburgh (1957).

(2) Biological and Medical Research Group (H-4) of the Health Division - Semiannual Report July through December 1959, Los Alamos Scientific Laboratory Report LAMS-2445 (February 1960).

(3) I. U. Boone, Incidence of Tumors in Animals Exposed to Whole-Body Radiation, In: Proceedings of the Symposium on the Delayed Effects of Whole-Body Radiation, B. B. Watson (ed.), ORO-SP-127, pp. 19-37 (1960).

Relative Biological Effectiveness (RBE) of Various Ionizing Radiations on the Transforming Principle (DNA) of Hemophilus Influenzae (I. U. Boone and J. A. Sayeg)

INTRODUCTION

The transforming principle of Hemophilus influenzae represents a biologically active material whose chemical and physical properties are fairly well understood. It is of vital interest, relative to enzyme and other in vitro preparations, in that it represents chemically the essential constituent of the genetic factor of all cells, human as well as bacterial.

This report covers some preliminary investigations of the effects of various ionizing radiations on the activity of Hemophilus transforming principle when irradiated in solution.

METHODS

The techniques employed in transformation were those of Alexander et al. (1,2) as modified by Goodgal and Herriott. The irradiation of samples in all instances was a dilute (10^{-4}) citrate-saline solution of transforming deoxyribonucleic acid (DNA). This was equivalent to approximately 0.08 μg/ml of DNA. A dilute solution was irradiated in order to avoid the "excess" portion of the standard DNA-transformation curve.

The transforming DNA was extracted from H. influenzae (Sd) cells resistant to ~2000 μg/ml of streptomycin. It was deproteinized by chloroform-octonal and precipitated by 95 per cent ethanol. It was stored in citrate-saline at -15 to -20°C until used. A citrate-saline solution of DNA was irradiated with the following ionizing radiations: 250 KVP X rays (which was used as the base line), Co^{60} gamma rays (1.3 and 2.8 Mev), 14.1 Mev neutrons provided by the Cockcroft-Walton accelerator, and a fission neutron spectrum from the Los Alamos Godiva critical assembly.

RESULTS AND DISCUSSION

It has been shown previously by others that dry DNA, when irradiated, has an exponential type of inactivation response. In this study where DNA was irradiated in solution, the effect versus dose relationship was exponential down to approximately 2 per cent of residual DNA. Data showing the inactivation of transforming principle as a function of dose of 250 KVP X rays are presented in Fig. 1.

In the computation of relative biological effectiveness (RBE) values, only the simple exponential portion of the effect versus dose relation was considered. This was assumed to be a valid comparison because of the very low value of the resistant fraction (see Fig. 1). Table 1 lists the LD_{37}

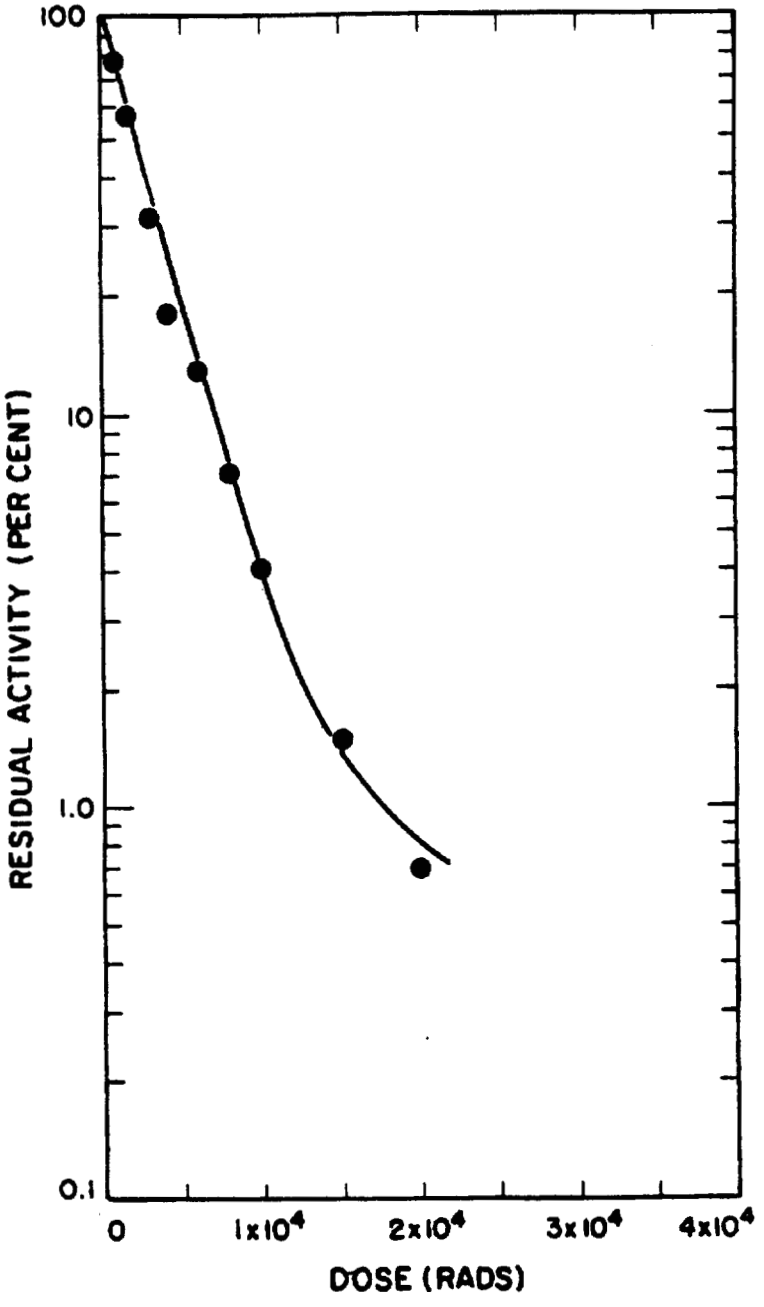

Fig. 1. Inactivation of Hemophilus transforming principle (DNA) as a function of dose of X irradiation.

TABLE 1. RELATIVE BIOLOGICAL EFFECTIVENESS (RBE) OF VARIOUS RADIATIONS WITH THE TRANSFORMING PRINCIPLE (DNA) OF HEMOPHILUS INFLUENZAE AS THE TEST SYSTEM

Radiation, R	Approximate LET (kev/μ water)	LD_{37} (rads)*	RBE $\frac{LD_{37}\ X\ rays}{LD_{37}\ Radiation,\ R}$
Cobalt^{60} gamma rays	~0.3	2000	1.5
250 KVP X rays	~2.5	3000	1.0
14 Mev neutrons	10-12**	5200	0.58
Godiva degraded fission neutrons	45**	7200	0.44

*In water.

**Recoil proton portion only.

(dose producing 37 per cent inactivation) and the preliminary RBE values obtained with the various radiations investigated, when compared with X irradiation as the base line. Most RBE studies are designed to test for differences in effectiveness as a function of linear energy transfer (LET). LET values for each radiation are also listed in Table 1 so that they can be compared with the RBE values. Although an interpretation of the results of RBE values obtained is not attempted at this time, with this particular system RBE appears to decrease with increasing LET as indicated by the fact that Co^{60} gamma rays were more effective than 250 KVP X rays, while fission neutrons were approximately half as effective.

REFERENCES

(1) H. E. Alexander and G. Leidy, J. Exp. Med. 93, 345 (1951).

(2) H. E. Alexander and G. Leidy, J. Exp. Med. 97, 17 (1953).

Intercomparison of Fast Neutron and Gamma Ray Dosimetry at AEC Installations (J. A. Sayeg and D. G. Ott)

INTRODUCTION

Because of the numerous biological experiments being conducted on the biological effects of neutron irradiation in a mixed field (neutrons plus gamma rays), it appeared to be important to make dosimetry intercomparisons at different AEC installations. These intercomparisons would, in principle, eliminate any biological effect versus dose discrepancies arising from dosimetric measurements. These intercomparisons were conducted at the Berkeley 60 in. cyclotron in cooperation with Mr. Gene Tochilin of the Radiological Physics Branch, U. S. Naval Radiological Defense Laboratory in San Francisco, California.

METHODS AND RESULTS

The Berkeley 60 in. cyclotron is able to produce a soft fast neutron spectrum by bombarding a thick beryllium target with 12 Mev protons. This spectrum has been measured by Tochilin and Kohler (1) and appears to be very similar to a fission spectrum.

The neutron and gamma dosimeters provided by the Biomedic Research Group (H-4) of the Los Alamos Scientific Laboratory included the following: threshold detectors of Pu^{239}, Np^{237},

U^{238}, and S^{32} (2), beryllium-shelled tissue-equivalent and graphite-CO_2 ionization chambers (3), Hurst proportional counter, and silver phosphate glass rods. The dosimeters used by the USNRDL included nuclear emulsions, sulfur foils, and film.

Data obtained with the threshold detectors have not been completely evaluated. However, in Table 1 are shown the preliminary results for the tissue-equivalent and graphite-CO_2 ionization chambers, Hurst proportional counter, silver phosphate glass rods, nuclear emulsions plus sulfur monitor, and film. The agreement between the different systems appears to be good. The estimated uncertainty in the LASL neutron measurements is approximately 10 to 15 per cent. The uncertainty in the silver phosphate glass rod gamma measurement is also approximately 10 per cent, whereas the uncertainty of gamma dose as measured by the graphite-CO_2 chambers may be as much as 50 per cent due to the low gamma-to-neutron dose ratio (3).

ACKNOWLEDGMENT

We are grateful to the personnel of the U. S. Naval Radiological Defense Laboratory at San Francisco, California, for their collaboration in this project.

REFERENCES

(1) E. Tochilin and G. D. Kohler, Health Phys. 1, 332 (1958).

(2) J. A. Sayeg, Los Alamos Scientific Laboratory Report LA-2432, in press (1960).

(3) J. A. Sayeg, J. H. Larkins, and P. S. Harris, Los Alamos Scientific Laboratory Report LA-2174 (January 1958).

TABLE 1. INTERCOMPARISON OF FAST NEUTRON AND GAMMA RAY DOSIMETERS AT THE BERKELEY 60 IN. CYCLOTRON
(preliminary data)

Location from Target (forward direction)	LASL Measurements					USNRDL Measurements	
	Neutrons, tissue rads/μamp hr			Gamma, roentgens/μamp hr		Neutrons, tissue rads/μamp hr	Gamma, roentgens/μamp hr
	Threshold Detectors	Hurst Proportional Counter	T-E Ionization Chamber	Graphite-CO_2 Ionization Chamber	Silver Phosphate Glass Rods	Nuclear Emulsions + Sulfur Monitor	Film
30 in.	Not evaluated to date	---	35.5	3.7	4.4	34.6	4.5
Outside cyclotron shield	---	0.48	---	---	---	0.47	---

Advances in the Threshold Detector Technique of Measuring Neutron Flux, Spectra, and Tissue Dose (J. A. Sayeg)

INTRODUCTION

Although the threshold detector technique as proposed by Hurst and his co-workers (1,2) was devised mainly for the

U^{238}, fabricated from Pu^{239} and U^{235}, were necessary for proper calibrations.

METHODS AND RESULTS

Equivalent foils as proposed by Hurst and his co-workers (7) were fabricated. The composition of each foil is shown in Table 1. These foils were exposed to approximately 3×10^{11} n/cm^2 (thermal) at the Los Alamos Water Boiler and were followed on a single tube gamma fission counter (4,8) for approximately 7 hours after irradiation. One-half mil Au^{197} foils were placed on the side of each foil to evaluate the flux depression and self-shielding (8).

The decay curves of the equivalent foils are shown in Fig. 1. Two threshold counting bias values were chosen, 0.51 and 1.1 Mev. The foils were irradiated with the same thermal flux. The difference in activity per unit mass between the Pu^{239} foil and equivalent Np^{237} foil was found to be approximately 30 per cent. This difference accounts for approximately 30 per cent of the 50 per cent discrepancy observed with the film track method (6).

A further investigation was made concerning the "best fit" cross sections to be used in the flux evaluations. The most recent Np^{237} and U^{238} cross sections (9) and the available Pu^{239} cross sections in the Brookhaven National Laboratory's report (10) were weighted by Godiva and undegraded

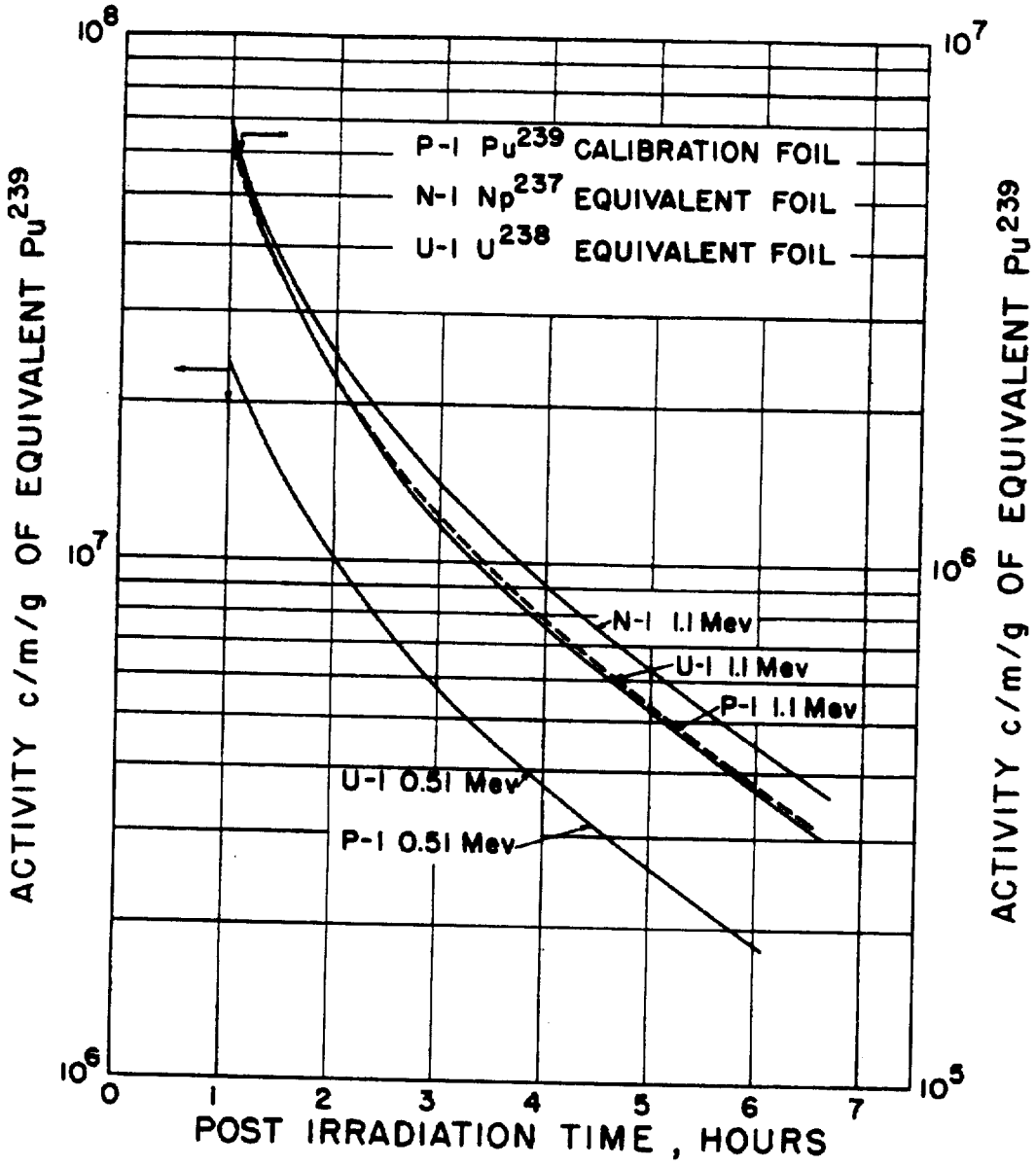

Fig. 1. Decay curves for Pu^{239} and equivalent foils of Np^{237} and U^{238}.

fission spectra (6) to obtain "best fit" values, which are shown in Table 2. Likewise, the first collision dose values were also weighted by these spectra and are shown in Table 3.

Using the equivalent foil method of calibration (7) and the best fit values for fast neutron cross sections and the first collision dose values (8), good agreement is obtained between the film track and the threshold detector methods. These comparisons are shown in Table 4. Computations are now under way to correct the Kiwi-A data.

REFERENCES

(1) G. S. Hurst, J. A. Harter, P. N. Hensley, W. A. Mills, M. Slater, and P. W. Reinhardt, Rev. Sci. Instr. 27, 153 (1956).

(2) P. W. Reinhardt and F. J. Davis, Health Phys. 1, 169 (1958).

(3) G. S. Hurst and R. H. Ritchie, personal communication (1958).

(4) J. A. Sayeg, E. R. Ballinger, and P. S. Harris, Los Alamos Scientific Laboratory Report LA-2310 (1959).

(5) L. Allen, personal communication (1956).

(6) G. M. Frye, J. H. Gammel, and L. Rosen, Los Alamos Scientific Laboratory Report LA-1670 (1954).

(7) G. S. Hurst and R. H. Ritchie, Oak Ridge National Laboratory Report ORNL-2748, Part A (November 1959).

(8) J. A. Sayeg, Los Alamos Scientific Laboratory Report LA-2432, in press (1960).

(9) H. W. Schmitt and R. B. Murray, Phys. Rev. 116, 1575 (1959).

(10) D. J. Hughes and R. B. Schwartz, Brookhaven National Laboratory Report BNL-325, Suppl. 1 (January 1, 1957).

TABLE 1. COMPOSITION OF EQUIVALENT FOILS

Foil Number	Weight Pu^{239} (mg)	Weight U^{235} (mg)	Equivalent Weight Pu^{239} (mg)
P-1 (Pu^{239})	9.88	--	9.88
N-1 (equivalent Np^{237})	5.29	7.13	10.6
U-1 (equivalent U^{238})	8.82	3.96	11.8

TABLE 2. WEIGHTED FISSION CROSS SECTIONS FOR FISSION SPECTRA*

Foil	σ (barns)	
	Previously Used Values	New Adopted Values
$Plutonium^{239}$	2.00	1.78
$Neptunium^{237}$	1.40	1.71
$Uranium^{238}$	0.54	0.54

*In 2 cm B^{10} balls.

TABLE 3. WEIGHTED FIRST COLLISION DOSE VALUES FOR FISSION SPECTRA

Energy Interval, Mev	tissue rad/n/cm^2 x 10^{-9}	
	Previously Used Values	New Adopted Values
0.004 - 0.75	0.93	1.30
0.75 - 1.5	2.33	2.46
1.5 - 2.5	2.98	2.97
>2.5	3.63	3.84

TABLE 4. COMPARATIVE NEUTRON FLUX AND TISSUE DOSE SPECTRA AT THE GODIVA II CRITICAL ASSEMBLY

Energy Interval, Mev	Per Cent Neutrons in Energy Interval		Per Cent Dose in Energy Interval	
	Threshold Detectors*	Track Plate Method (6)	Threshold Detectors*	Track Plate Method (6)
0.004 - 0.75	43	41	24	23
0.75 - 1.5	22	25	24	26
1.5 - 2.5	17	16	22	21
>2.5	18	18	30	30

*Average of data from 35 to 200 cm.

Neutron Flux, Spectra, and Neutron and Gamma Tissue Dose Evaluations at the Little Eva Critical Assembly (J. A. Sayeg, D. G. Ott, and P. S. Harris)

INTRODUCTION

Due to the demand for critical assembly time, it was necessary to calibrate existing critical assemblies that could be used for radiation effects tests by the Biomedical Research Group (H-4) of this Laboratory. The present report covers a study of the radiation characteristics of the Los Alamos Little Eva critical assembly.

METHODS AND RESULTS

The threshold detector technique (1,2) was used in this investigation for evaluation of neutron flux, spectra, and tissue dose. The data are shown in Tables 1, 2, and 3. The gamma dose was measured by tetrachloroethylene chemical dosimeters, and the method is discussed in detail in Ref. (3). These results are shown in Table 4. The gamma-to-neutron ratio is the lowest observed at any assembly tested thus far. The uncertainty of the neutron dose measurements is estimated to be approximately 15 per cent. The uncertainty of the gamma measurements is approximately 25 per cent due to the very low values obtained.

TABLE 1. NEUTRON FLUX VERSUS DISTANCE RELATIONS AT THE LITTLE EVA CRITICAL ASSEMBLY

Distance from Center of Assembly, cm	$n/cm^2 \times 10^{10}$/kw-min			
	F_{Pu} $E_n > 0.004$ Mev	F_{Np} $E_n > 0.75$ Mev	F_U $E_n > 1.5$ Mev	F_S $E_n > 2.5$ Me
50	13.3	4.45	2.28	0.905
75	5.07	2.10	0.959	0.409
100	2.74	1.01	0.452	0.179
150	1.81	0.716	0.226	0.101

TABLE 2. NEUTRON TISSUE DOSE VERSUS DISTANCE RELATIONS FOR THE LITTLE EVA CRITICAL ASSEMBLY

Distance from Center, cm	$\frac{\text{tissue rad}}{\text{kw-min}}$
50	234
75	98.1
100	50.3
150	33.0

TABLE 3. NEUTRON FLUX AND DOSE SPECTRA EVALUATIONS AT THE LITTLE EVA CRITICAL ASSEMBLY*

Energy Interval (Mev)	Neutrons (per cent)	Dose (per cent)
0.004 - 0.75	62.1	43
0.75 - 1.5	21.6	28
1.5 - 2.5	9.5	15
>2.5	6.8	14

*Average of the four distances measured.

TABLE 4. GAMMA DOSE VERSUS DISTANCE RELATIONS FOR THE LITTLE EVA CRITICAL ASSEMBLY

Distance from Center, cm	$\frac{\text{roentgens}}{\text{kw-min}}$
50	6.6
75	1.2
100	1.7
132	1.4
206	0.5

REFERENCES

(1) G. S. Hurst and R. H. Ritchie, Oak Ridge National Laboratory Report ORNL-2748, Part A (November 1959).

(2) J. A. Sayeg, Los Alamos Scientific Laboratory Report LA-2432, in press (1960).

(3) D. G. Ott, W. H. Schweitzer, S. B. Helmick, and P. S. Harris, Los Alamos Scientific Laboratory Report LA-2249 (1959).

Giant Cell Formation in HeLa Cells as a Function of Cobalt^{60} Gamma Rays and X Irradiation. II. Effect of Variable Dose Rates (D. C. White and P. C. Sanders)

INTRODUCTION

The purpose of this study was to correlate per cent of giant cells formed in HeLa cell cultures with total dose of irradiation given at varying dose rates. The first report of this series (1) gave results obtained with a dose rate of 5 r/min and gave a readily reproducible curve of giant cell production as a function of dose. More information was needed, however, to establish a satisfactory base line for further studies pertaining to the relative biological effectiveness (RBE) of other types of radiation and the effect of dose rate.

METHODS AND RESULTS

A series of experiments was performed with HeLa cells being exposed to Co^{60} gamma rays and X irradiation at total doses of 150, 450, and 750 r. The dose rates employed were 5, 20, 50, and 100 r/min. The cells were prepared, exposed, and examined for per cent giant cell formation as indicated in the previous semiannual report (1).

An analysis of the data revealed that irrespective of dose rate, the per cent of giant cells formed for any specific

total dose fell within statistical limits. All giant cell counts for each total dose were combined and plotted as per cent giant cells versus dose. The combined results are given in Table 1.

DISCUSSION

The results indicated that the per cent of giant cells formed is not dose rate dependent over the range studied, which was from 5 to 100 r/min. The number of giant cells formed is apparently a function of total dose only. Future studies using other types of irradiation would perhaps be of value, and this method may be an important adjunct to studies of RBE as the results appear to be very reproducible. Published results using much higher dose rates agree with the data presented in this report (2,3).

REFERENCES

(1) Biological and Medical Research Group (H-4) of the Health Division - Semiannual Report July through December 1959, Los Alamos Scientific Laboratory Report LAMS-2445 (February 1960).

(2) T. T. Puck and P. I. Marcus, J. Exp. Med. 103, 653 (1956).

(3) C. M. Pomerat, S. P. Kent, and L. C. Logie, Zeit. fur Zellforschung 47, 158 (1957).

TABLE 1. GIANT CELL FORMATION IN HeLa CELL CULTURES AS A FUNCTION OF RADIATION DOSE

Radiation and Dose (r)	Giant Cell Formation* (per cent)
Cobalt^{60} Gamma Radiation	
0	1.4
150	4.6
450	11.4
750	25.1
250 KVP X Rays	
0	1.1
150	3.7
450	10.6
750	23.5

*Combined data, all dose rates.

Effect of Cobalt^{60} Gamma Rays, X Rays, and Fast Neutrons on Total Cell Population of HeLa Cells in Tissue Culture (D. C. White and P. C. Sanders)

INTRODUCTION

The previous report indicated that HeLa cells grown in tissue culture appeared to be a promising system for studying the relative biological effectiveness of ionizing radiations. The present preliminary experiment was designed to compare the effects of gamma, X-ray, and fast neutron irradiations on total HeLa cell population and to relate total cell population to giant cell formation.

METHODS AND RESULTS

A method was devised such that cells grown in T-30 culture flasks and in Rose culture chambers were exposed simultaneously to the radiations. The flask cultures were used for total cell population determinations and the Rose chambers for determination of giant cell formation.

T-30 culture flasks were inoculated with a predetermined number of HeLa cells (in the range of 20,000 cells/ml) and Rose chambers with 5,000 cells/chamber. The cells were grown in Eagle's Basic Medium plus 10 per cent horse serum for 48 hours prior to irradiation. Cultures were exposed to total doses of 150, 450, and 750 r of Co^{60} gamma rays and

X irradiation. Since fast neutrons are more efficient, the doses employed were 85, 250, and 330 rads. Media were changed on all flasks and chambers immediately following irradiation and at 48-hour intervals until all were terminated.

Total cell populations in the culture flasks were determined immediately prior to irradiation and at intervals thereafter by utilizing the Coulter cell counter. The cultures were prepared for counting by removing the media, adding 2 ml of a 0.035 per cent trypsin solution, incubating until the cells were no longer attached to the glass, stopping the trypsin action with 3 ml N-saline, and agitating the cell suspension until the cells were completely separated. One ml of the cell suspension was diluted 1:50 with N-saline and this solution counted with the Coulter cell counter at the proper settings. Rose chambers were terminated at comparable time intervals and stained by the Jacobson method (1) for determination of giant cell counts and for the number of cells per colony. Flasks and chambers were terminated on days 1, 2, 3, 5, and 6 following irradiation. The results collected on the fifth day post exposure were chosen as optimum for comparison of per cent cell survival and per cent giant cell formation in relation to total radiation dose. The results are shown in Table 1.

TABLE 1. HeLa CELL GROWTH AND GIANT CELL FORMATION AS A FUNCTION OF RADIATION DOSE

Source	Dose (rads)	Cell Growth (per cent)	Giant Cells (per cent)
Cobalt^{60}	150	73	4.6
	450	57	11.4
	750	36	25.1
X Rays	150	87	3.7
	450	42	10.6
	750	15	23.4
Fast Neutrons	85	67	6.4
	250	30	34.0
	330	16	65.4
Controls	---	100	1.1

DISCUSSION

The results obtained thus far indicate a good method for following rate of cell growth after irradiation. By utilizing the Coulter cell counter, many accurate counts may be performed in a relatively short time. The data in Table 1 are strictly preliminary, and more studies are necessary before actual values of RBE can be established. The data do indicate, however, that both cell growth and giant cell formation provide a means of studying RBE. In both cases, the effect of fission neutrons is considerably greater than that of X and gamma rays.

REFERENCE

(1) W. Jacobson and M. Webb, Exp. Cell Res. 3, 164 (1952).

Neutron-Induced Activity in Humans as a Dosimetric Procedure

(E. R. Ballinger, P. S. Harris, and J. H. Larkins)

INTRODUCTION

The purpose of this study was to investigate the feasibility and techniques of using neutron-induced body activity as a measure of dose, and as a personnel monitoring and casualty assessment procedure.

Work completed during this reporting period concerns the design, construction, and calibration of a portable body sodium activity meter (SAM) for use as a casualty assessment device for personnel exposed to fast neutron fluxes in the range of 10 to 1000 rads. Work uncompleted to date will appear in the next semiannual report. This work will involve attempts to arrive at average neutron energy by means of body sodium to copper foil ratios in order to provide meter correction values which will permit estimates of absorbed dose from exposures to neutrons of unknown energies in the thermal and intermediate regions.

To the extent that dose effect information on humans may be obtained first-hand by observation of nuclear accident casualties, we have historically been hampered on two counts: it is more than likely that the individuals primarily involved will not be wearing the prescribed dosimetry at the time of exposure, and in the event prescribed dosimetry is worn it w

more than likely be the low-level monitoring type and hence of little value in determining the extent of casualty-level doses.

One of the oldest observations made on neutron exposure casualties is that activation of body constituents occurs and can be measured by certain detection techniques. On several occasions, these post exposure body activity measurements have played a role in estimating neutron exposure in the absence of any standard dosimetry. At the time of the last fatal LASL nuclear criticality accident, gamma spectroscopy was performed on the subject and the predominant induced activity was found to be Na^{24}. After-the-fact estimates of whole body neutron dose suggested that ~0.3 μc of Na^{24} activity was produced per rad of fast neutrons ($n + Na^{23} \longrightarrow Na^{24} \xrightarrow{14.8\ hr} Mg^{24} + 2\gamma$). These gamma spectroscopy measurements suggested the possibility of designing a portable monitoring instrument specifically for the purpose of measuring body sodium activity, which could be read in terms of the dose of neutrons required to produce the amount of sodium activity observed. Preferably, these measurements were to be made by placing a probe-type device against a body surface. The problem was divided into two major parts: the design and calibration of the instrument, and the determination of correction values to be applied to the readings in the

event that body sodium activity as a function of neutron energy did not parallel sufficiently clósely the absorbed dose calculations of Snyder (1). It was reasoned that such a device, having the decided advantage of using the body as its own neutron dosimeter, would be free of the continuing logistic, laboratory, and administrative support characteristic of the usual personnel monitoring procedures. The first part of the problem has been completed during this reporting period. The second portion is presently the subject of our attention and will be included in the next reporting period.

METHODS

Renal regulation normally serves to hold body sodium at the quite constant level of 1.5 g/kilo body weight. Although the sodium content of various body tissues and spaces differs, this difference is relatively constant with the greatest per cent of sodium per weight of tissue being found in the cerebrospinal fluid, bone, bile, and blood plasma (Table 1).

One would suspect, therefore, that the lumbar area of the back might overlie the area of richest sodium content in the body. A gamma detection device placed in this area would be expected to see the induced Na^{24} activity from the heavy lumbar vertebrae, the central nervous system fluid in the

TABLE 1. PER CENT SODIUM CONTENT PER GRAM OF TISSUE (2)

Man	0.150
Central nervous system fluid*	0.500
Bone*	0.440
Bile	0.400
Serum	0.330
Serous fluids	0.330
Plasma	0.330
Amniotic fluid	0.280
Skin*	0.230
Spinal cord*	0.200
Brain	0.200
Whole blood*	0.190
Kidneys	0.165
Liver	0.130
Heart	0.100
Muscle	0.080
Red blood cells	0.043

*Area seen by sodium activity probe.

spinal canal at this level, as well as from the renal arteriovenous plexis. As a test of this proposition, a 20 kilo polyethylene jug filled with a 1.5 g Na^{23}/kilo H_2O was exposed to fast neutron doses from 10 to 1000 rads using the Godiva II critical assembly. Various bench model devices were tested for ability to detect and reproducibly measure the activity present at the cylindrical surface of the jug. These devices included simplified versions of ion chambers, Geiger-Müller counters, and scintillation counting techniques. In terms of sensitivity, range, ease of operation, and portability, a photomultiplier-sodium iodide crystal assembly appeared to be the most satisfactory in the region of Na^{24} activities produced by 10 to 1000 rads of soft neutrons. Consequently, a detection system consisting of a probe and a reader was constructed as shown in Figs. 1 and 2. The probe is a 2 in. diameter photomultiplier tube, Model RCA No. 6655A, on the end of which is mounted a 2 x 2 in. sodium iodide crystal. These basic components are wrapped by 3/8 in. of lead to reduce normal background and by 7 to 8 turns of Co-netic magnetic shielding, which was found to be necessary to permit the probe to be held in any direction or orientation. Encased in an 1/8 in. thick aluminum cylinder with pistol grip the probe is connected to the reader by means of several feet of signal and high voltage cable. The reader unit consists

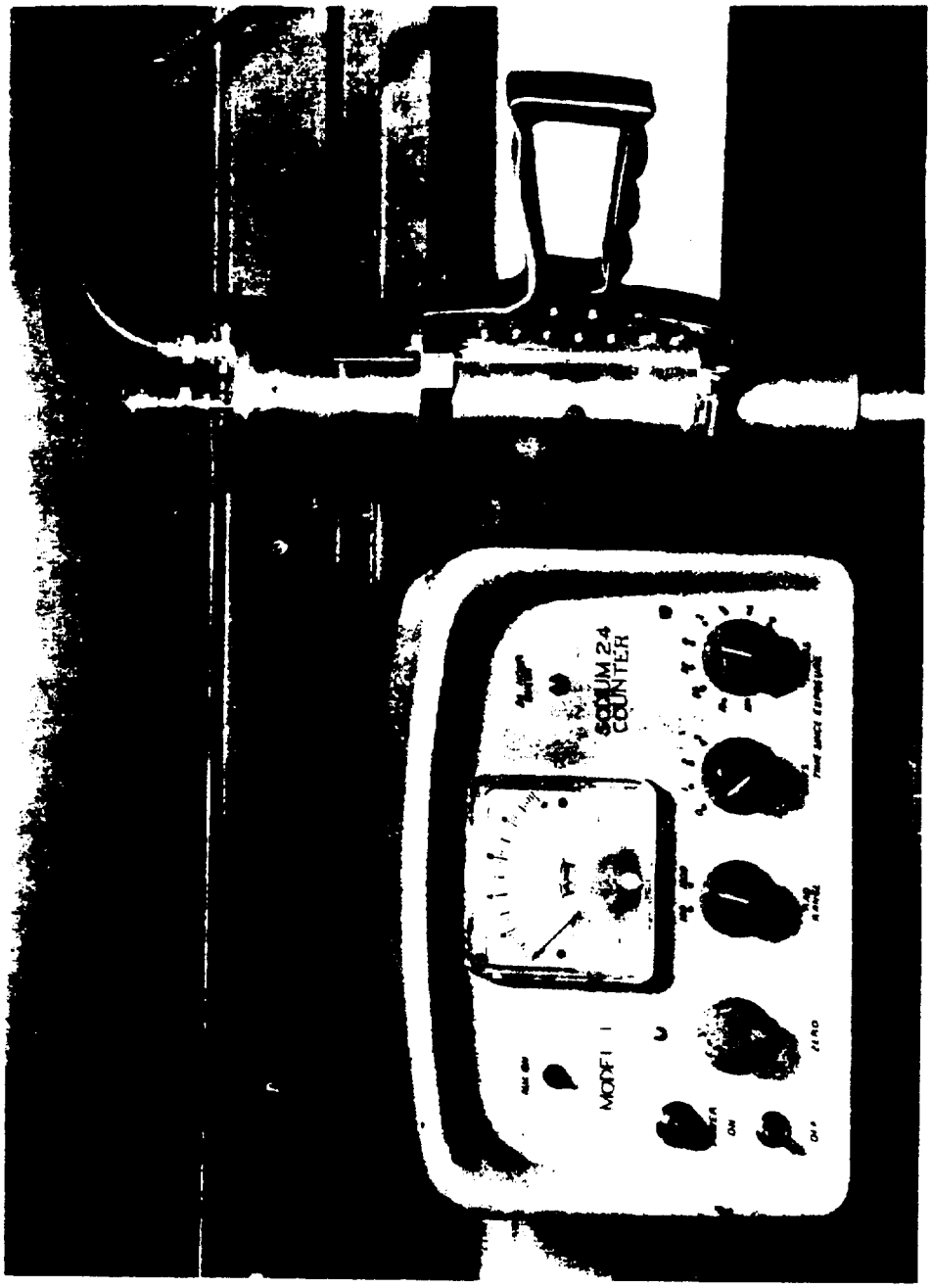

Fig. 1. Meter and probe unit.

00131478.210

1046812

LANL

of a power supply for 110 volt AC or self-contained batteries, an amplifier, and a rate meter circuit into which several helipots and resistor banks have been introduced to permit zero background adjustment, shift from 100 to 1000 rads range, and correction for decay of Na^{24} from the estimated time of exposure to time of reading.

Two complete units have been built to date, a 110 volt AC reader-probe unit weighing ~10 pounds each, and a self-contained battery operated reader-probe unit weighing ~ 8 and 5 pounds, respectively. Insofar as possible, both units are fabricated from transistorized components.

RESULTS AND DISCUSSION

The units were calibrated (using plastic mannequins exposed to fission neutrons from Godiva II, Figs. 3 and 4) to indicate the incident neutron rads corresponding to the levels of Na^{24} activity observed when the probe was placed over the small of the back. Plots of decaying activity from such exposures indicated that at times greater than 1-1/2 hours, the only remaining measurable activity was that of Na^{24}. A network of resistors introduced into the photomultiplier cathode high voltage supply enabled electrical half-life corrections at 2 hour intervals out to several days to be made. Thus, with the time interval between exposure and reading

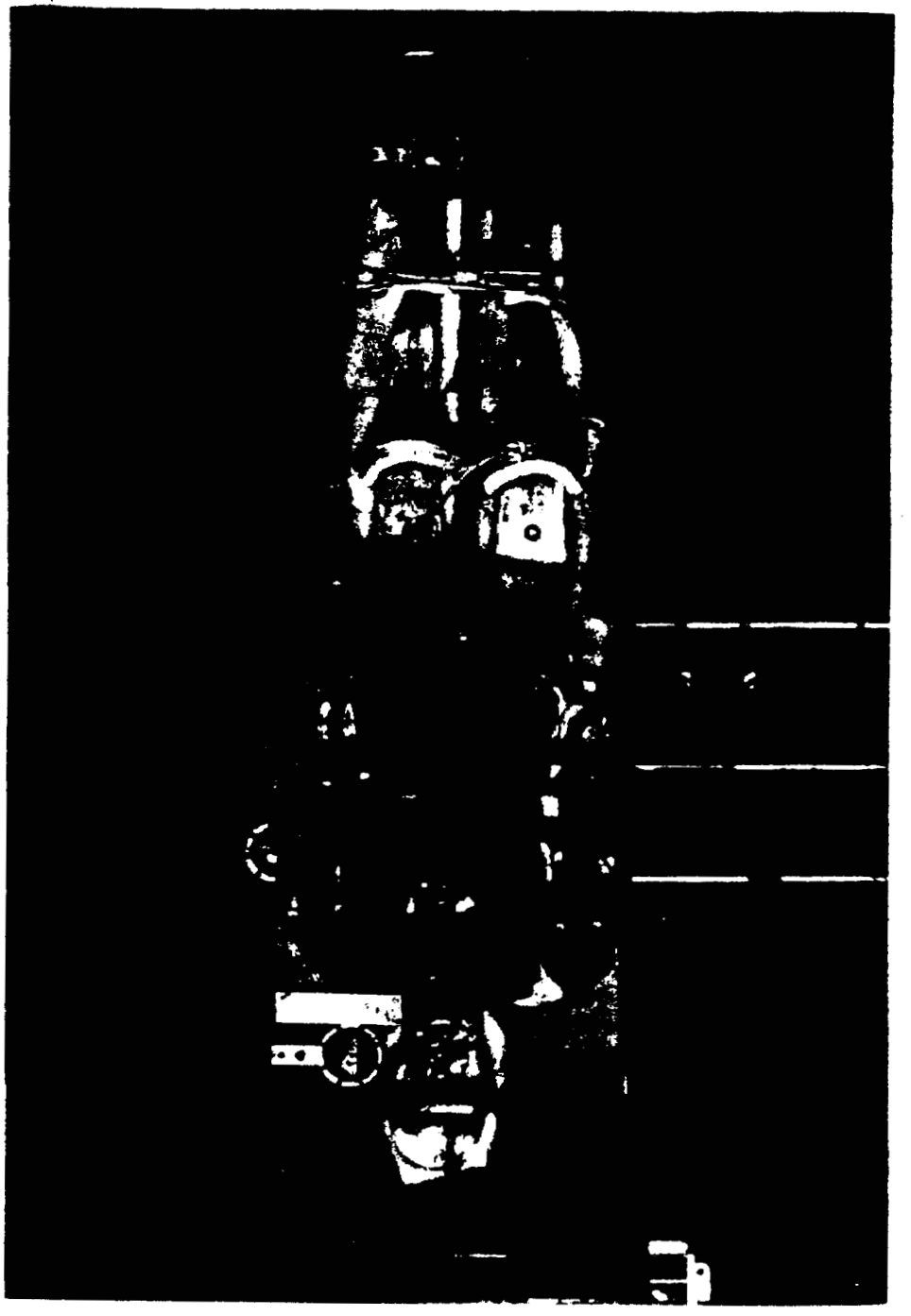

00131478.212

Fig. 4. Exposure of plastic mannequin to neutrons from the Godiva II critical assembly (back view).

dialed in, the meter read in terms of rads of Godiva neutrons delivered at time of exposure. The Godiva II critical assembly can be assumed to be a fast neutron source of 2 Mev average energy.

Exposures of the plastic phantoms were also made using the Omega West reactor as a thermal neutron source. Readings were made in the same manner as before and compared with the fast neutron exposures. On the basis of Na^{24} activity per incident neutron, it was determined that an approximate factor of 5 difference existed between the fast and thermal exposures. The meter calibrations as previously described were set to read 1 rad whenever the plastic mannequins were exposed to 4×10^8 Godiva neutrons per cm^2 (4×10^8 Godiva neutrons being the calculated equivalent of 1 rad). Without altering the meter calibration, it was found that an incident rad of thermal neutrons (2×10^{10} Omega West neutrons per cm^2) would produce a meter reading of 10 rads (or 2×10^9 thermal neutrons per rad reading). Thus, on a per neutron basis, the fast neutron source produced 5 times more Na^{24} activity than the thermal neutron source. However, on the same basis, the absorbed dose per fast neutron is ~50 times greater than per thermal neutron. Consequently, a factor of 10 reduction in meter dose is required if the incident neutron flux is of thermal energy. Between these extremes, the meter reading

dose is thought to vary from 1 to 10 times the actual dose, dependent upon the incident neutron spectra. Theoretical calculations of body sodium activity per energy group of incident neutrons have been accomplished by our Theoretics Division, and these are presently being checked against experimental exposures of the plastic mannequins to neutron sources of energies between 0.025 and 2×10^6 ev. These sources will, when completed, include Kiwi-A, Kiwi-A Prime, Kiwi-A III, Little Eva, and Hydro. Theoretical calculations also suggest the possibility of comparing the activities of body sodium with a simultaneously exposed metal foil of different apparent cross section* to give a rough index of the probable average incident neutron energy. At this time, the material under examination is copper. The theoretical activity of both body sodium and the externally worn copper foil as a function of neutron energy is given in Fig. 5. As can be seen, a comparison of these two activities will give a rough estimate of the average incident neutron energy involved, if the spectra is not bimodal.

*The cross section for Na^{24} production is higher for neutrons of thermal energies. However, when Na^{23} in solution is contained within 1/8 in. walled plastic material, the albedo of the thermal energy neutrons is so great and the moderating ability of the solution for fast neutrons so complete as to give an apparent high cross section to the fast and more penetrating neutrons.

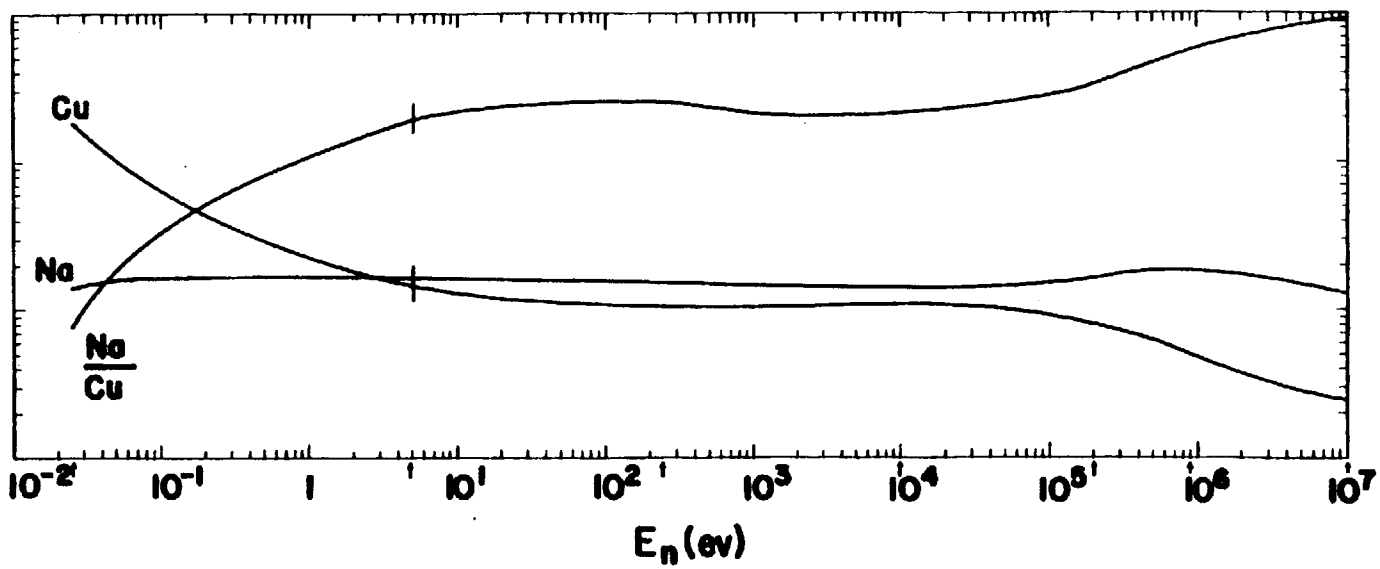

Fig. 5. Activity of body sodium and copper foil as a function of neutron energy.

Results to date indicate that a light-weight, portable, and self-contained personnel neutron monitoring device can be built to detect exposures to neutrons in excess of 10 rads whole body dose, based upon external measurements of body sodium activity. The absorbed dose may be read directly if the meter is calibrated to the incident spectra and may be estimated by correction values for known spectra other than those used for calibration of the meter. It is not known at this time how satisfactory the body sodium to copper foil ratio will be in terms of absorbed dose estimates from unknown neutron spectra. Incomplete evaluations of these ratios on such unknown sources as Kiwi-A Prime presently suggest that where fluxes of fast neutrons comprise 50 per cent or more of the total, the uncorrected meter reading may lie within 20 per cent of the calculated absorbed dose. As the practical value of such a device is closely associated to the above problem, we intend to pursue the project to this end. A complete evaluation of the body sodium to copper foil activities will be included in the next reporting period.

ACKNOWLEDGMENT

We are grateful to L. J. Carr and R. D. Hiebert of Group P-1 for their assistance with the transistorized equipment.

REFERENCES

(1) National Bureau of Standards Handbook No. 63, Appendix 1 (November 1957).

(2) Handbook of Biological Data, William S. Spector (ed.), W. B. Saunders Company, Philadelphia (1956).

RADIOBIOLOGY SECTION PUBLICATIONS

(1) I. U. Boone, Incidence of Tumors in Animals Exposed to Whole-Body Radiation, In: Proceedings of the Symposium on the Delayed Effects of Whole-Body Radiation, B. B. Watson (ed.), ORO-SP-127, pp. 19-37 (February 1960). Also in: The Delayed Effects of Whole-Body Radiation: A Symposium, Jointly sponsored by the Operations Research Office and the Walter Reed Army Institute of Research, The Johns Hopkins Press, Baltimore (1960).

(2) I. U. Boone, Chronic Effects of Sublethal Whole-Body Irradiation of CF_1 Mice at Different Age Levels, Abstract No. 20, Rad. Res. 12, 424 (1960).

(3) J. A. Sayeg, E. R. Ballinger, and P. S. Harris, The Godiva II Critical Assembly as an Irradiation Facility for Biological Research, Abstract No. 142, Rad. Res. 12, 469 (1960).

PUBLICATIONS SUBMITTED

(1) I. U. Boone, A. Murray, and R. Des Prez, Metabolism of C^{14}-Isoniazid in Humans, Los Alamos Scientific Laboratory Report LA-2420, in press (1960).

(2) M. J. Engelke, J. A. Sayeg, and B. Riebe, Neutron Tissue Dose Survey for the Little Eva Critical Assembly, Los Alamos Scientific Laboratory Report LA-2425, in press (1960).

(3) J. A. Sayeg, Revised Neutron Flux, Spectra, and Tissue Dose Measurements for the Godiva II Critical Assembly, Los Alamos Scientific Laboratory Report LA-2432, in press (1960).

(4) J. F. Spalding, V. G. Strang, and F. C. V. Worman, Effect of Graded Acute Exposures of Gamma Rays and Fission Neutrons on Recovery from Subsequent Protracted Gamma Ray Exposures, Rad. Res., in press (1960).

CHAPTER 6

RADIOPATHOLOGY SECTION

The Use of the Arm Counter to Determine the Degree of Hepatic Function (C. C. Lushbaugh, D. B. Hale, and R. McGill)

INTRODUCTION

The commonly used technique of determining the functional status of an organ by measuring its ability to clear the circulation of an injected dye has recently been replaced by radioassay of the accumulation of such dyes (now radioactively labeled) in the organ in question by means of a collimated sodium iodide crystal (1). This radioactive technique, in the case of hepatic function and the dye I^{131}-rose bengal, has not been accepted widely for the following reasons:

(a) The liver has a high blood background and a rapid excretion rate so that parenchymatous accumulation is difficult to measure.

(b) Accumulation of the radioactivity in the gallbladder causes a confusing rise in hepatic background unless collimation is precise.

(c) The test results can be reported to the physician only as exponential half-times, which are difficult to interpret.

(d) This rate of hepatic uptake is not altered significantly by serious hepatic parenchymatous disease.

The application of the Los Alamos Arm Counter (or Small-Animal Counter) to this technical problem appears to overcome these difficulties in the radioactive rose bengal test by affording a constant record of circulating blood-dye concentration so that blood clearance of the dye by the liver can be measured directly without the complicating problems caused by hepatic blood background, biliary excretion rate, gallbladder accumulation, and the unknown location in depth of the liver within the body. Since the original blood concentration of the dye (100 per cent) is determinable, the per cent of the dye retained in the blood after 20, 45, or any selected number of minutes can be reported as is commonly done clinically with the bromsulphalein dye test. The following results of a preliminary study show that blood retention is a better measurement of function than the clearance rate itself.

METHODS

In this study, 10 normal subjects and 18 persons

suffering from various but mostly inflammatory hepatic disease were used. The left arm of the person was placed in the Arm Counter (Fig. 1), and a collimated 2 x 2 in. NaI crystal was oriented to scan the liver. As precisely and rapidly as possible, 10 μc of radioactive rose bengal was injected intravenously in the other arm. Simultaneous Esterline-Angus recordings were made of the radioactivity measured by the two devices.

RESULTS

The curve of blood activity was found to be a composite of 2 exponential disappearance rates, the more rapid of which corresponded almost exactly with the hepatic uptake rate determined by the method of Lowenstein (2) from data obtained from a small crystal. The second, or slow, exponential corresponded to the hepatic excretion rate. The zero intercept of this second exponential line was considered as the "per cent retention" of the dye in the blood, although it would be more accurate to visualize it as the amount of dye in the blood when blood and intrahepatic cellular concentrations were equal. Figure 2 depicts the mean blood activity curves of the 2 groups of patients. The mean values obtained from this study are shown in Table 1.

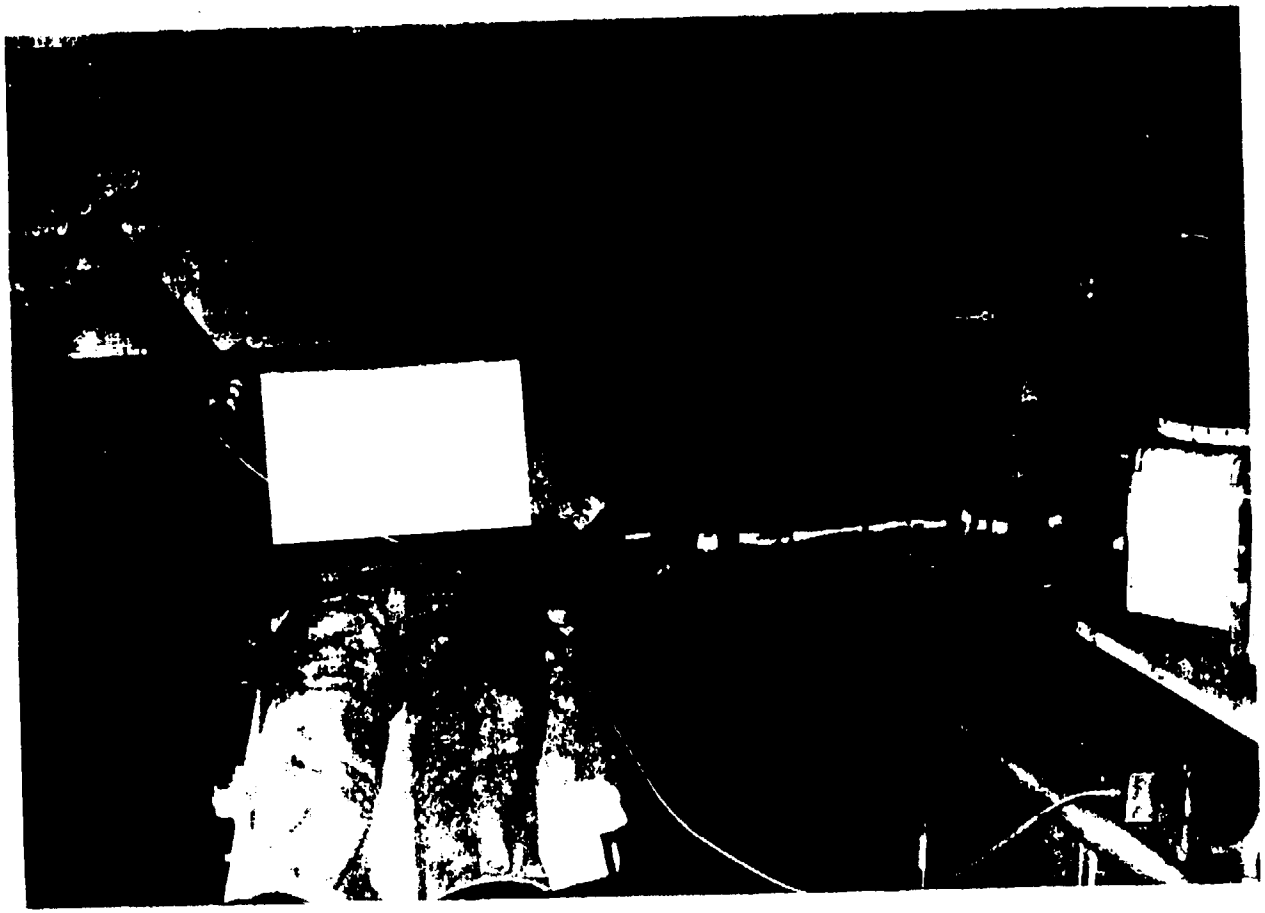

00131478.223

Fig. 1. Subject with his left arm in the Arm Counter and a collimated NaI crystal scanning his hepatic area during the rose bengal liver function test.

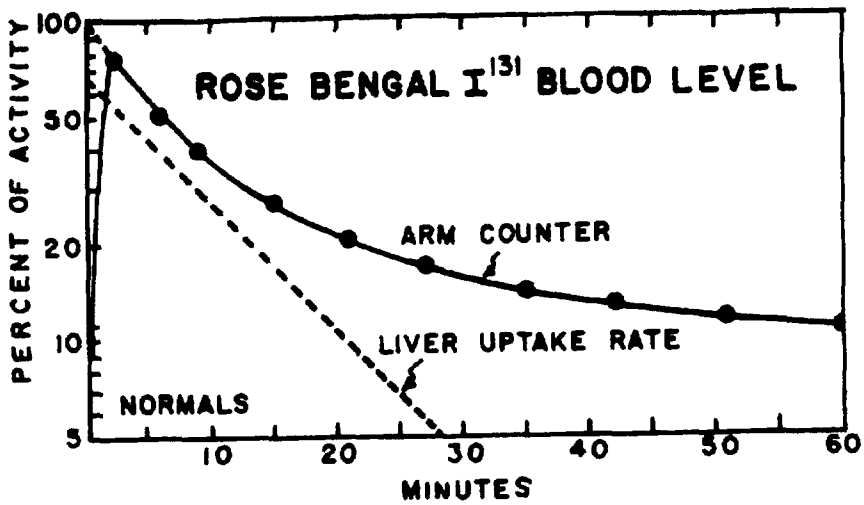

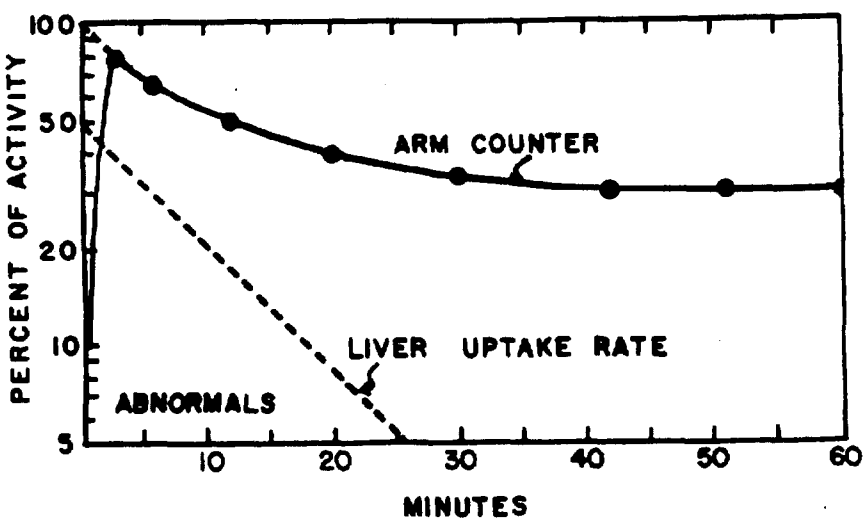

Fig. 2. Averaged curves for the rates of hepatic blood clearance of rose bengal by normal and diseased subjects as measured by the Arm Counter. The dotted line in each is the rate of hepatic clearance, computed from the solid curve which represents the total radioactive iodine in the blood.

TABLE 1. PARAMETERS OF BLOOD CLEARANCE CURVE FOR I^{131}-ROSE BENGAL

	Normals	Abnormals
Hepatic uptake (half-time)	7.5 ± 1.3 min	8.0 ± 1.2 min
Hepatic excretion (half-time)	284 ± 166 min	401 ± 249 min
Per cent retention (blood)	11.4 ± 6.0	33.6 ± 12.9
Range of blood retention values	8.3 - 14.3	19.3 - 76.7

DISCUSSION

The agreement of half-times of the hepatic blood clearance rate of 7.5 ± 1.3 minutes in the normal and 8.0 ± 1.2 minutes in the abnormal group demonstrates why this measurement has no clinical usefulness. While there was some detectable difference in half-times of hepatic excretion, the greatest difference was seen in the blood retention of the dye in the 2 groups. Examination of the ranges of such "retentions" shows that the 2 groups of persons did not overlap in this category.

From the analysis of the data, it appears that rose bengal is "cleared" just as rapidly by the diseased liver as by the normal one. Only in extremely severe hepatic disease, where fibrosis and endothelial thickening are extensive, does this clearance rate change. The data seem to indicate also that the volume of functioning liver in relation to total blood volume determines the amount of dye that will be cleared before "retention" becomes apparent.

This study is continuing as additional patients can be obtained in order to extend these observations and to correlate better the measurements with hepatic diseased states.

REFERENCES

(1) G. V. Taplin, O. M. Meredith, Jr., and H. Kade, J. Lab. Clin. Med. 45, 665 (1955).

(2) J. M. Lowenstein, Proc. Soc. Exptl. Biol. Med. 93, 377 (1956).

Whole Body Retention of Iodine^{131} from Various Labeled Organic Compounds in Starving and Irradiated Rats (C. C. Lushbaugh and D. B. Hale)

INTRODUCTION

Exposure to lethal amounts of ionizing radiation produces a syndrome which, in most respects, is quite similar to starvation. The larger the dose of radiation, the greater is the degree of anorexia until the lethally irradiated animal appears to avoid all food and to fast willfully and completely. Forced feeding of such an animal has been found to hasten, rather than to prevent, his death (1).

Although many of the physiologic effects of starvation are well known (2), few of these have been studied in irradiated animals. Significant but identical alterations in the whole body retention of sodium and potassium (1) and iodide ions (3) were recently demonstrated in animals that were starving, irradiated, or suffering from both stresses simultaneously, illustrating that altered retentions of electrolytes were secondary rather than primary effects of radiation damage. The primary effects of radiation damage upon in vivo cellular metabolism cannot, therefore, be differentiat from the secondary effects of the concomitant anorexia unless the latter are adequately understood.

The following experiments were done in order to expand

our previous observations upon electrolyte and thyroid metabolism by studying with radioisotopes the effects of starvation and irradiation upon hepatic and renal excretion rates and protein metabolism. Iodine^{131}-labeled rose bengal, commonly used clinically as a measure of hepatic function, was used here because its excretion from the body is determined first by its rate of blood clearance by the liver. Iodine^{131}-labeled sodium diprotrizoate (Miokan) was similarly chosen for study because its removal from the blood depends primarily upon renal function. Iodine^{131}-labeled human serum albumin was used in order to survey preliminarily the utilization rate of this protein in rats, although it was realized that the rat might not metabolize human albumin in the same manner as rat protein.

MATERIALS AND METHODS

In each experiment, the rats were divided into control and experimental groups. The experimental animals were starved throughout the course of the study, and the controls were allowed laboratory chow ad libitum. In the first experiment, rose bengal labeled with I^{131} was injected intraperitoneally (1.0 μc I^{131} in 0.125 ml of 1 per cent dye solution) into the animals of both groups and their per cent retention determined daily by whole body counting for the following 12 days. In the second experiment, the same procedure was

followed after intraperitoneal injection of I^{131}-Miokan. In the third experiment, radioiodinated human serum albumin was used similarly. This experiment was expanded to include 3 additional groups of 5 rats each that received on the day the labeled drug was administered 700 and 2100 rads of whole body X irradiation, respectively. One of the groups that received 700 rads and the one that received 2100 rads were deprived of food throughout the experiment.

RESULTS

The experimental results are shown in the accompanying graphs. Figure 1 shows the effect of starvation upon the retention of the I^{131}-labeled rose bengal. The intercepts and slopes of the second component (B) of the retention curves corresponded to the excretion rate of NaI^{131} after thyroid binding (3), and were used to derive the intercepts and slopes of the first component (A), which represented the hepato-biliary excretion of this dye.

Figure 2 shows the effect of starvation upon the retention of an I^{131}-labeled dye (Miokan) that is excreted solely by the kidney. The slopes of the B components of the retention curves again corresponded to those of thyroid-bound iodine in rats eating normally or deprived of food. The A components represented the rate of renal excretion of the I^{131}-labeled dye.

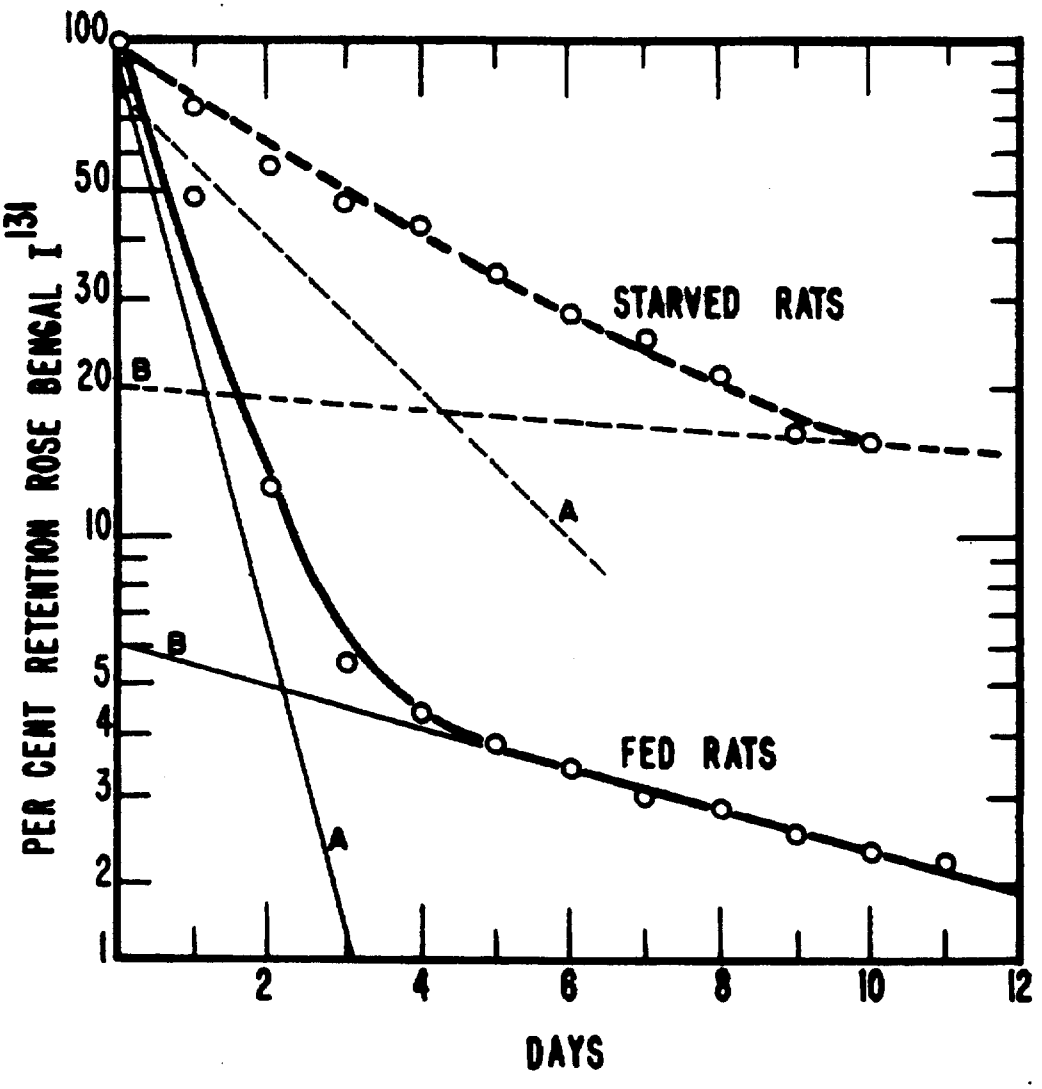

Fig. 1. The effect of starvation upon the retention of I^{131} administered as I^{131}-rose bengal (rats).

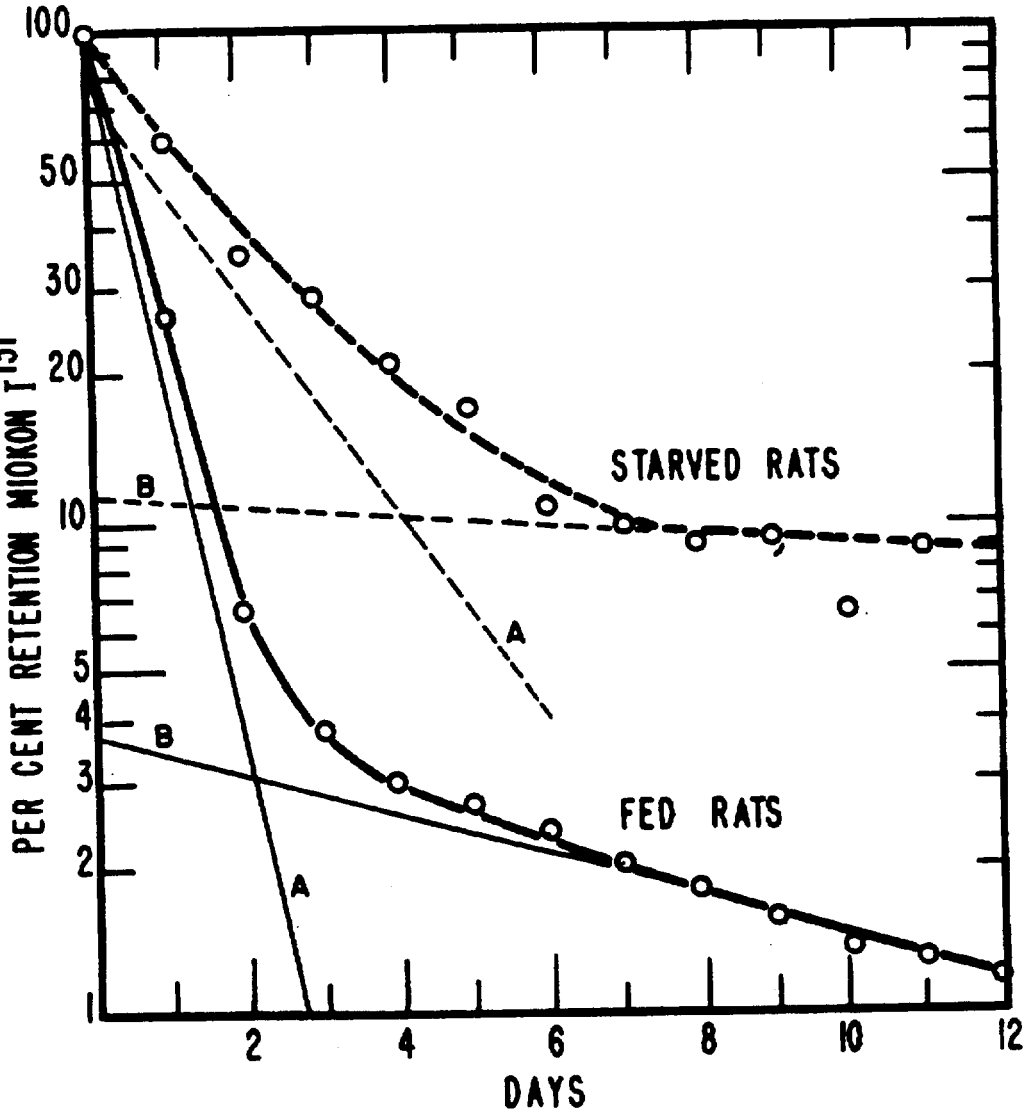

Fig. 2. Effect of starvation upon the retention of I^{131} administered as I^{131}-Miokan (rats).

Figure 3 shows the retention curves of I^{131}-labeled human serum albumin in rats being fed normally, starved, and irradiated with 700 and 2100 rads of X irradiation. The group that received 2100 rads and did not eat retained 55 per cent of the I^{131}; the group that was starved and the group that was irradiated with 700 rads each retained 30 per cent. The 2 groups that were fed ad libitum retained only 4.5 to 5.6 per cent of the I^{131}, even though 1 received 700 rads of X irradiation.

DISCUSSION

These results show that food deprivation reduces the rate of excretion of radioactive iodine bound to two dyes (one excreted largely via the liver and the other via the kidney) and a foreign protein. Regardless of the compound to which the iodine is chemically bound, it appears to enter the hormonal iodine pool. The proportion of iodine incorporated by the thyroid appears to be determined more by the nutritional status of the animal than by the character of the labeled chemical compound. The previously reported failure of X irradiation to modify the increased retention of Na^{22} and K^{42} in starving rats (1) was seen in these experiments in the case of the radioiodinated albumin. The apparent decrease in the rate of hepatic excretion of I^{131}-rose bengal

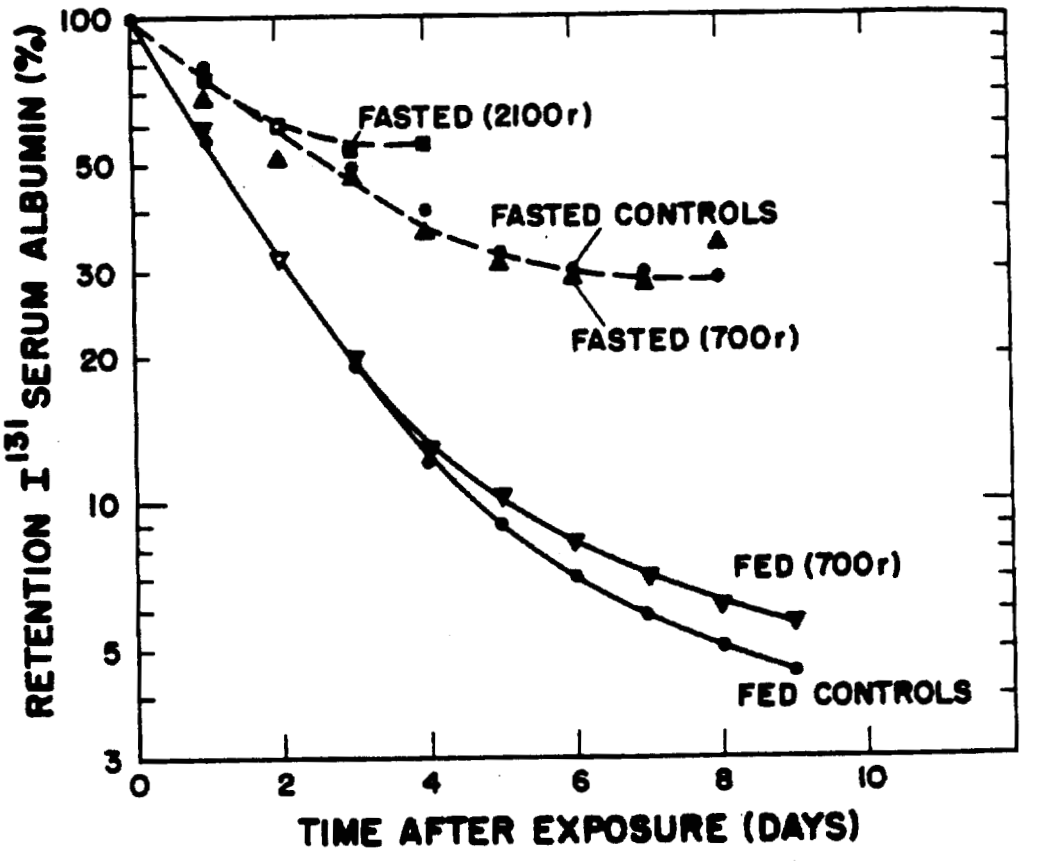

Fig. 3. Retention of I^{131} administered as I^{131}-human serum albumin, by normal, fasting, and irradiated rats.

and renal excretion of Miokan by starvation would seem to indicate that the function of these organs is altered by starvation. Sufficient X irradiation to cause anorexia should be accompanied, therefore, by decreased biliary and renal excretion rates and increased retention of these dyes. Should such changes occur, they would appear to be secondary to starvation rather than X irradiation. This conjecture is to be tested in the irradiated rat as an extension of these observations. The increased retention of the I^{131}-label on the human albumin in starving and irradiated rats would seem to have the same physiologic basis.

REFERENCES

(1) C. C. Lushbaugh, J. Sutton, and C. R. Richmond, The Question of Electrolyte Loss in the Intestinal Death Syndrome of Radiation Damage, Rad. Res. (in press).

(2) C. H. Best and N. B. Taylor, Chapt. II, pp. 1021-1023, The Metabolism in Starvation (Fasting), Obesity and Undernutrition, In: The Physiological Basis of Medical Practice. The Williams and Wilkins Company, Baltimore, Md. (1943).

(3) C. C. Lushbaugh and D. B. Hale, Iodine^{131} Retention in Normal and Starved Rats, Biological and Medical Research Group (H-4) of the Health Division - Semiannual Report July through December 1959, Los Alamos Scientific Laboratory Report LAMS-2445 (February 1960).

RADIOPATHOLOGY SECTION PUBLICATION SUBMITTED

(1) C. C. Lushbaugh, J. Sutton, and C. R. Richmond, The Question of Electrolyte Loss in the Intestinal Death Syndrome of Radiation Damage, Rad. Res. (in press, 1960).

CHAPTER 7

VETERINARY MEDICINE SECTION

INTRODUCTION

The Veterinary Section does no research but operates entirely as a service function for the research work of the other Sections of the Group. The responsibility and function of the Section were given in detail in the Semiannual Report covering the period July 1 to December 31, 1959 (1).

FACILITIES

In February of this year, the new animal quarters were occupied and give every indication of accomplishing the purpose for which they were designed. Figure 1 shows an architect's drawing of the new addition, which is the single story structure located on the southwest end of the laboratory structure (TA-43).

The new facility cost approximately $325,000.00 and includes 5 monkey pens with outside exercise areas (maximum

capacity 50 animals); 19 dog kennels with outside runs (maximum capacity 57 animals); 13 mouse rooms (maximum capacity 40,000 animals); mouse feeding room; dog and monkey feeding room; dog breeding room; dog metabolism room; monkey metabolism room; dog and monkey quarantine room; autopsy and treatment room; storage area; veterinary office; mouse cage cleaning room; mouse bedding and cage storage room; and locker room for the animal caretakers.

The mouse rooms are completely air conditioned with temperature control to $\pm$ 2°F. All cages are stainless steel mounted on racks suspended from the ceiling (Fig. 2). The other areas are not air conditioned but have forced air ventilation. Mouse cages are washed with a detergent, rinsed and dried in an automatic cage washer. As the cages emerge from the washer, they are automatically conveyed to the bedding and storage area, where they are filled with wood shavings and stored until used. Plans are underway to automatize the removal of used wood shavings from the dirty cages and also the hopper that dispenses new bedding into the clean cages. If this can be accomplished, the dumping, washing, and refilling of 1000 cages per day should be only a one-man job.

The inside monkey and dog quarters (Fig. 3) are glazed tile with adequate facilities for cleaning. The concrete floors of both the inside living area and the outside exercise

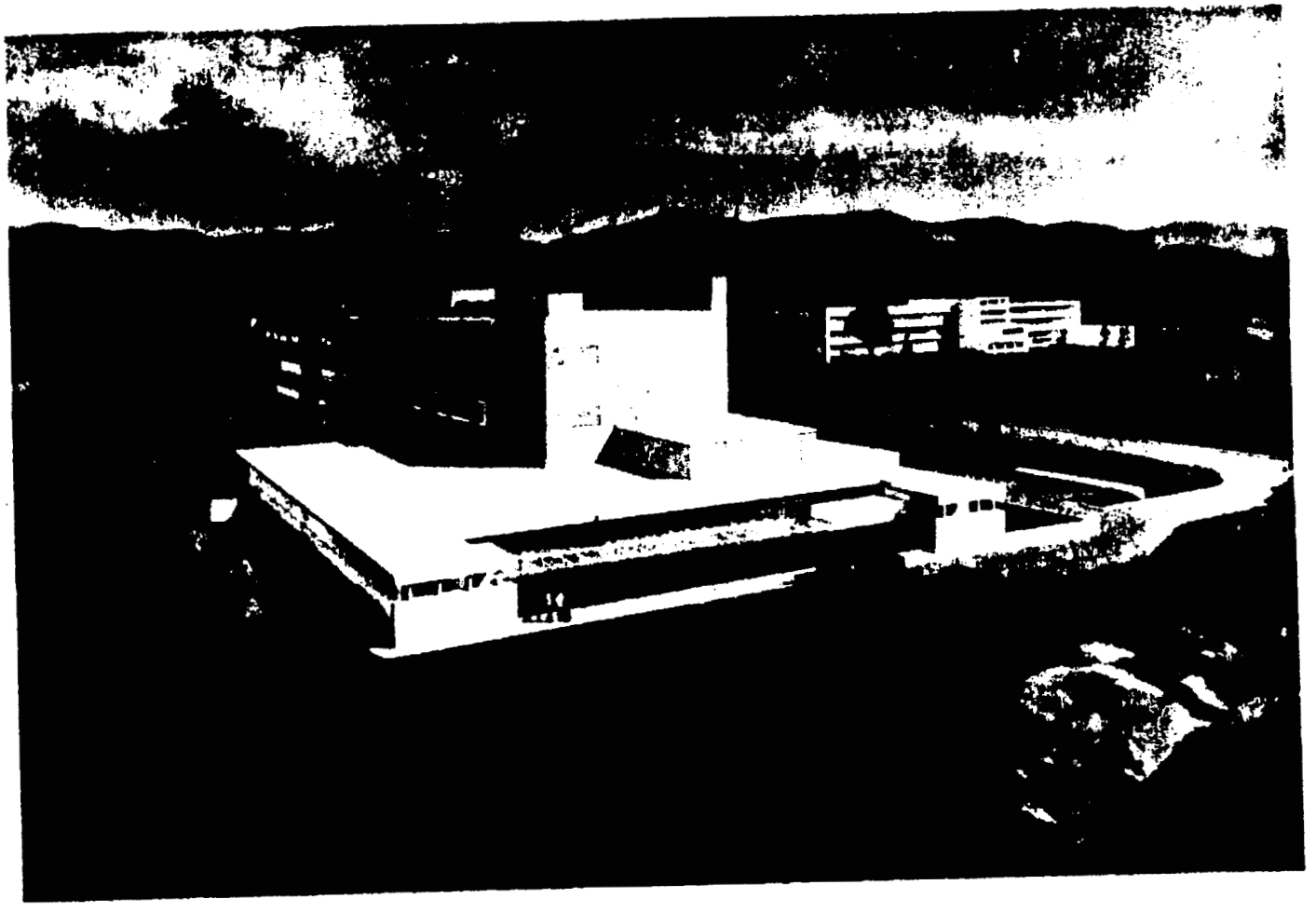

Fig. 1. Architect's sketch of new animal quarters added to the southwest end of the Health Research Laboratory (TA-43).

Fig. 2. Air conditioned mouse room showing caging arrangement.

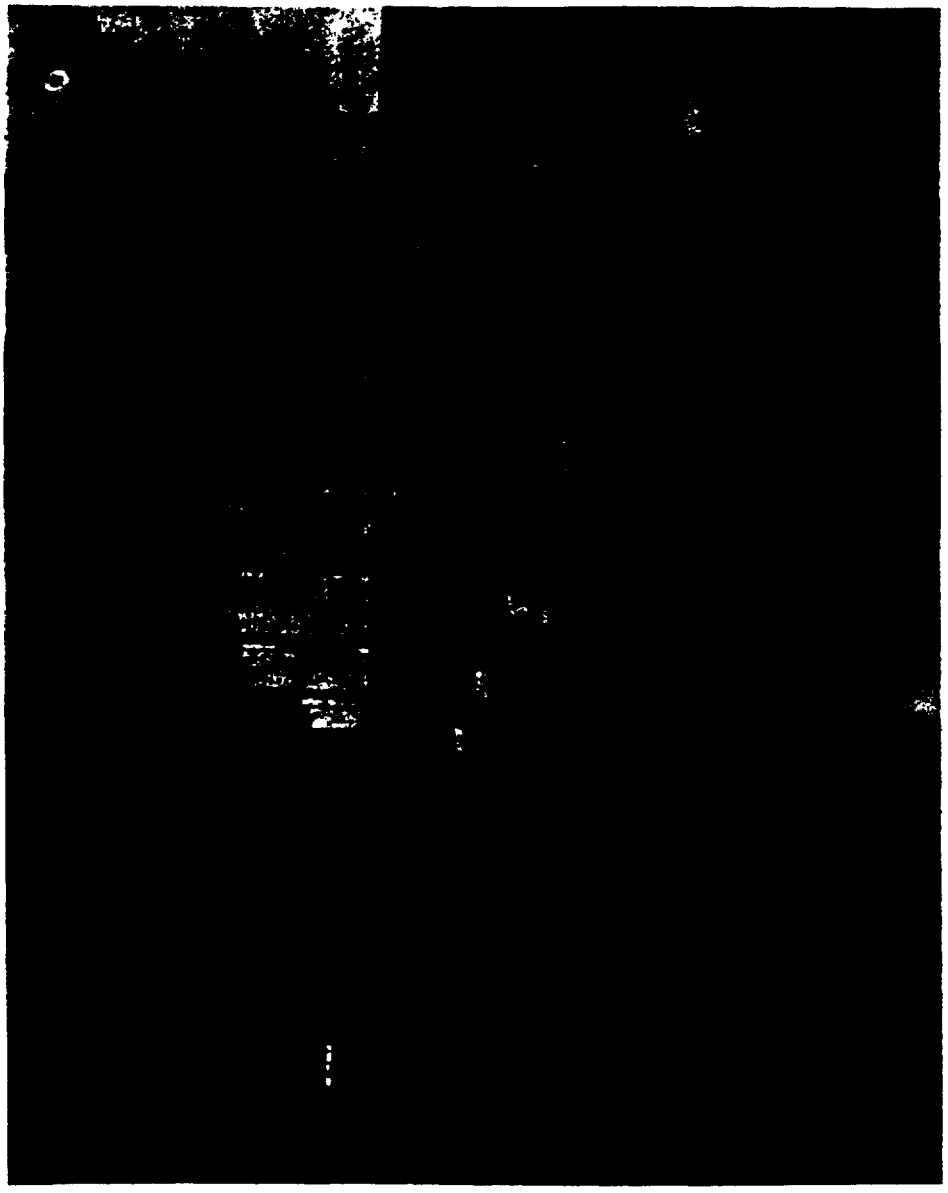

Fig. 3. Inside view of dog and monkey quarters.

runs are radiant heated with inside-outside temperature control. The outside heating provides a snow-melting arrangement during the winter. The outside areas are cleaned with a high pressure hose from a catwalk above the runs (Fig. 4).

ANIMAL PRODUCTION AND INVENTORY

Mice

RFM Strain

Total number of babies born	1503
Total number of weanlings	1329
Weaning percentage	88.4
Number of breeding females	189

RF Strain

Total number of female weanlings	5120
Number of females delivered for experimentation	2967
Number of females in stock	3703
Number of above being held for aging studies	1292
Number of breeding females	1249

AKR Strain

Total number of babies born	1687
Total number of weanlings	1635
Weaning percentage	96.9
Number of females delivered for experimentation	701
Number of breeding females	178

CFW Strain

Total number of female weanlings	241
Number of females delivered for experimentation	222
Number of breeding females	34

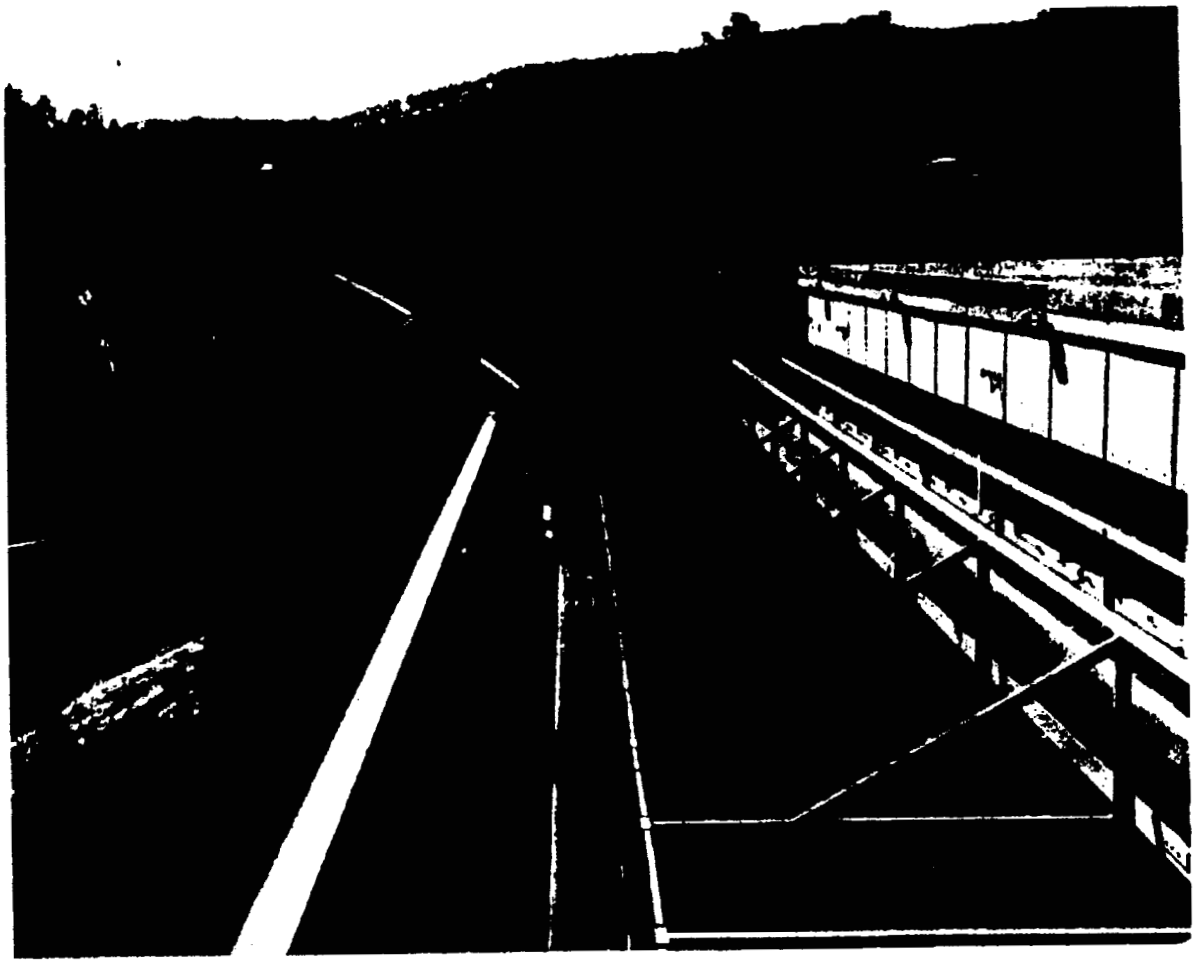

Fig. 4. View of outside exercise area for dogs and monkeys.

Sprague-Dawley Rats

Total number received	1361
Number delivered for experimentation	634
Number of male rats in stock	751
Number of above being held for aging studies	297

Beagles

Number of male beagles for breeding and stock	28
Number of female beagles for breeding and stock	8
Number of above females bred	1

Monkeys

Number in stock (males only)	3

Rabbits and Guinea Pigs

Number of rabbits received	0
Number in stock	13
Number of guinea pigs received	12
Number in stock	13

REFERENCE

(1) Biological and Medical Research Group (H-4) of the Health Division - Semiannual Report July through December 1959, Los Alamos Scientific Laboratory Report LAMS-2445 (February 1960).